Participant-Specific Modelling of the Proximal Femur during Lateral Falls: A Mechanistic Evaluation of Risk Factors

by

Steven P. Pretty

A thesis
presented to the University of Waterloo
in fulfillment of the
thesis requirement for the degree of
Master of Science
in
Kinesiology

Waterloo, Ontario, Canada, 2018

AUTHOR'S DECLARATION

This thesis consists of material all of which I authored or co-authored: see Statement of Contributions included in the thesis. This is a true copy of the thesis, including any required final revisions, as accepted by my examiners.

I understand that my thesis may be made electronically available to the public.

Statement of Contributions

I would like to acknowledge my co-author, Iris C. Levine, who contributed to the research design and collection of fall simulation data described in this thesis.

Abstract

Falls among older adults are a common occurrence with the potential to result in substantial injury. Hip fractures are among the most frequent and devastating fall induced injuries, resulting in increased morbidity and mortality, as well as significant socioeconomic costs. From a mechanistic perspective, the risk of a hip fracture during a fall is dictated by the ratio between the impact loading and the ability of the femur to withstand such loads. Investigations of clinical fracture risk factors have generally focused on the latter, neglecting the influence of these factors on impact dynamics. Experimental fall simulations provide a means to investigate factors modulating impact dynamics; however, these studies are limited to the skin surface with limited ability to draw conclusions on femoral loading and fracture risk. Investigations into the mechanical basis of clinical risk factors (sensitive to both loading and femur morphology) could provide insights to inform the development of protective devices and increase the accuracy of screening tools.

Therefore, the purpose of this thesis was to evaluate the influence of previously identified hip fracture risk factors on impact characteristics during lateral falls and how the application of these loading conditions influence femoral neck stresses and fracture risk. Specifically, the influence of fall simulation paradigm (FSP: a surrogate for fall type), sex, and trochanteric soft tissue thickness (TSTT) were evaluated through coupling of experimental impact dynamics with participant-specific proximal femur models. Healthy young males and females, encompassing a wide range of body compositions underwent a series of fall simulation paradigms. These paradigms varied in fall trajectory and impact configuration, ranging from highly controlled vertical drops (pelvis release) to releases more representative of falls observed in older adults (kneeling and squat releases). Peak impact force magnitude and localization over the proximal femur, as well as orientation and point of application with respect to the femur were extracted (Chapters 3 and 4). A subset of the participants subsequently underwent dual energy X-ray absorptiometry (DXA) imaging, enabling participant-specific modelling and tissue level analysis - driven by experimental loading conditions (reginal force magnitude, orientation, and point of application; Chapter 5).

FSP significantly influenced skin surface loading conditions, as well as femoral neck stresses and fracture risk. Compared to kneeling and squat, pelvis release elicited lower peak force magnitude; however, this force was applied closer to and was more concentrated over the greater trochanter. Despite the differences in force distribution, kneeling and squat release still elicited greater force directed over the proximal femur compared to pelvis release. Beyond force magnitude and distribution,

these FSP varied significantly in impact vector orientation with respect to the femur. Kneeling release was associated with the most perpendicular loading vector, while squat release elicited the most distally directed vector in the frontal plane. In the anterior-posterior plane, pelvis release was directed posteriorly, while kneeling and squat release were directed anteriorly. Observed difference in skin surface loading conditions across FSP interacted with underlying femoral geometry to influence stress generation and fracture risk. Compressive stress at the superior-lateral femoral neck was greatest in kneeling release, while tensile stress at the inferior-medial femoral neck was greatest in squat release (driven by proportion of force resulting in axial compression vs. bending stress). While no differences in femoral neck fracture risk were observed between kneeling and squat release, kneeling release may elicit a greater risk of local compressive failure in the superior femoral neck.

At the skin surface, sex and TSTT significantly influenced impact dynamics; however, underlying differences in femur morphology influenced the translation of these loading conditions to femoral neck stresses and fracture risk. Compared to females, males exhibited greater impact force magnitude, which was applied closer to and was more concentrated over the greater trochanter of the proximal femur. This increased loading in males was mitigated by differences in femur morphology (greater resistance to bending and shear stress generation, as well as strength), resulting in no differences in femoral neck stresses or fracture risk. The increased risk of hip fracture in females may be explained by age related changes in femur morphology, as well as sex-differences in the circumstances of falls. High-TSTT individuals exhibited greater impact force magnitude; however, these loads were applied further from and less focally over the greater trochanter compared to low-TSTT individuals. Combined, no differences were observed in the amount of force directed over the proximal femur across TSTT. Despite similar loading conditions, low-TSTT individuals elicited greater femoral neck stresses and fracture risk compared to their high-TSTT counterparts, driven by differences in underlying femur morphology (reduced resistance to bending and shear stress generation). The protective influence of TSTT to redistribute impact force peripherally away from the greater trochanter appears to play an important role in fracture risk. When global impact force was utilized instead of local force during modelling, no differences in femoral stresses or fracture risk were observed across TSTT.

In summary, this thesis combined two previously exclusive approaches (experimental fall simulations and tissue level modelling) to gain novel insights into the influence of FSP, sex, and TSTT on femoral neck stresses and fracture risk. Through a participant-specific multi-level approach, this analysis was sensitive to both impact dynamics and underlying femoral geometry. FSP influenced

fracture risk, as well as the location and magnitude of peak femoral stresses. Inclusion of muscle activation in future versions of the current approach may inform ‘safe-falling’ strategies, designed to reduce fracture risk. The current results support epidemiological findings suggesting TSTT is a protective factor against hip fracture; however, sex differences in fracture risk are likely driven by age related changes in femur morphology not included in this analysis. Based on the apparent importance to fracture risk, future work should aim to quantify the translation of skin surface pressure distributions to impact energy delivered to the proximal femur.

Acknowledgements

This work was made possible by countless individuals. I would first like to thank my supervisor Dr. Andrew Laing. Your door was always open when I thought the World was ending and needed a good talking down. You gave me the freedom to make this work my own, while also keeping my wandering mind in check. I look forward to my continued development under your invaluable mentorship.

My thesis committee, Drs. Jack Callaghan and Clark Dickerson, provided valuable insights that undoubtedly improved the quality of this thesis. You provided the foundational knowledge needed to undertake such work and subsequently challenged me with the hard questions. This project, and myself, benefited immensely from your contributions.

While tuition can cover resources and instruction, my experience over the last two years would be nothing without the individuals I shared it with. While too many to list, my IBAL lab mates and fellow Kinesiology graduate students provided encouragement, assistance, and friendship every step of the way. Special thanks to Iris Levine for her direct mentorship and guidance. You convinced me to pursue graduate studies, but I will hold off on thanking you for that until I submit a thicker document. I would also like to thank Tyler Weaver for padding my flag football stats with all those deep post routes (and Taylor Winberg for being open on check downs when Tyler decided to run half speed). While not everyone can have a personal shout out, I would like to acknowledge Dan Armstrong, Dan Martel, Dan Viggiani, Tom Hoshizaki, Jackie Alphabet, Dave Kingston, Laura Healey, Jeff Barrett, East Coast Merryl, Bhillie Luciani, Nick Patrick, Jerry Mangan, Graham Mayberry, Cheryl Kieswetter, Denise Hay, Jenny Crowley, Jeff Rice, Dr. Marina Mourtzakis and Janice Skafel. Each of you were either a valuable resource and instrumental to the completion of this project or simply fun to be around (I'll let you decide in which camp you fall). As I was fortunate enough to receive funding over the duration of my studies, I would like to thank NSERC and the province of Ontario for covering the aforementioned tuition, allowing me to focus on my studies.

My family and friends provided unwavering support and at times even faked an interest in my work. Thank you to my parents, who not only provided me every opportunity to succeed but also equipped me with the ability to handle adversity. Finally, I'd like to thank Emma Perego. Your constant encouragement and understanding during this process means more to me than you know.

Thank you.

Table of Contents

List of Figures

List of Tables

Chapter 1 Introduction & Thesis Overview

Hip fractures result in substantial socioeconomic impact in terms of both health care expenditure, as well as increased morbidity and mortality. Biomechanical modelling is a promising tool for fracture risk prediction and identification of individuals for clinical intervention. However, the utility of these models are sensitive to prediction and application of loading conditions during a fall.

1.1.1 Fall Related Injuries among Canadian Older Adults

Falls remain the leading cause of injury-related hospitalizations among Canadian seniors (Canadian Institute for Health Information, 2010) with between 20% and 30% of seniors falling each year (Statistics Canada, 2010). Self-reported injuries due to falls are steadily increasing, most notably the number of deaths due to falls increased by 65% from 2003 to 2008 (Public Health Agency of Canada, 2014). In 2011, an estimated 5 million Canadians, or 15% of the population, were 65 years of age or older, and this number is expected to double by 2036 (Statistics Canada, 2011). The high incidence of fall related injuries amongst older adults can be attributed to an increased propensity to fall, as well as increased susceptibility to fractures due to conditions such as osteoporosis with increasing age (Rubenstein, 2006).

In 2010, accidental falls in Canada resulted in 4071 deaths, 128,389 hospitalizations, 1,036,079 emergency room visits, 23,236 permanent partial disabilities and 1,969 permanent total disabilities. Falls on the same level accounted for 8 percent of fall deaths (n=327) and were the most common cause of hospitalized treatment (29% n=37,660), emergency room visits (32% n=330,199), permanent partial disability (31% n=6,721) and permanent total disability (27% n=492) (Parachute, 2015). Thirty-five percent (N=18,800) of seniors discharged from a fall-related hospitalization were discharged to continuing care despite the fact that only 18% (N=9,462) of falls leading to hospitalization occurred in continuing care settings. Of the discharges to continuing care, 68% were community dwelling prior to their fall (Scott, Wagar, & Elliott, 2010). The average acute length of stay for a fall-related injury was 70% longer (15.1 days) for Canada as a whole compared to the average length of stay for all other causes of hospitalization excluding falls (8.9 days) in 2008/09 (Scott, Wagar, & Elliott, 2010). This discrepancy highlights the disproportionate health care costs of fall-related injuries in comparison to other causes of hospitalization (Public Health Agency of Canada, 2014).

With an aging population, the economic cost of injury in Canada has increased by 35% since 2004 and is projected to reach $75 billion by 2035. Falls were the leading cause of injury costs in Canada

in 2010, accounting for $6.7 billion or 42% of direct costs (Parachute, 2015). Hip fractures alone are estimated to account for $1.1 billion in direct healthcare costs (Nikitovic, Wodchis, Krahn, & Cadarette, 2013) or $3.9 billion in total costs annually (R. B. Hopkins et al., 2016). With an annual incidence of approximately 30,000 (Leslie et al., 2009), which is expected to quadruple by 2030 (Papadimitropoulos, Coyte, Josse, & Greenwood, 1997), and a one-year mortality rate of 20% (Public Health Agency of Canada, 2014), hip fractures pose a large socioeconomic burden to the Canadian population.

1.1.2 Fall Induced Hip Fractures

In Canada, approximately 38% of all seniors who were hospitalized because of a fall sustained a hip fracture (Scott, Wagar, & Elliott, 2010) and research suggests 95% of all hip fractures result from falls (Grisso et al., 1991; Wolinsky et al., 2009). Approximately 1.6 million hip fractures occur worldwide each year and by 2050 this number could reach 6.3 million (Cooper, Campion, & Melton, 1992), equivalent to a fracture occurring every 5 seconds. An individual is at least 15 to 24% more likely to decease within the year of sustaining a hip fracture than someone of the same age and sex that did not sustain a hip fracture (Hannan et al., 2012; Omsland et al., 2014) and excess mortality persists up to 10 years (Haentjens et al., 2010; Omsland et al., 2014). Hip fractures are associated with chronic pain, reduced mobility, increased disability and dependence, as well as risk of institutionalization (Leslie et al., 2012). After sustaining a hip fracture 10-20% of formerly community dwelling patients require long term nursing care (Autier et al., 2000; Cree, Soskolne, Belseck, Mcelhaney, & Brant, 2000; Kiebzak et al., 2002), with the rate of nursing home admission rising with age (Cree et al., 2000; Reginster et al., 1999). Loss of function and independence among survivors is profound, with 40% unable to walk independently, and 60% requiring assistance a year later (Magaziner, Simonsick, Kashner, Hebel, & Kenzora, 1990; Wolinsky, Fitzgerald, & Stump, 1997). Because of these losses, 33% are totally dependent or in a nursing home in the year following a hip fracture (Kannus, Parkkari, Niemi, Palvanen, & States, 1996; Leibson, Tosteson, Gabriel, Ransom, & Melton, 2002; Riggs & Melton, 1995).

Due to the large societal burden and poor patient prognosis following a hip fracture, identification and treatment of high risk individuals is of paramount importance. A variety of interventions are available to high risk individuals including pharmacological intervention (Papapoulos, Quandt, Libeman, Hochberg, & Thompson, 2005), the use of hip protectors (Santesso, Carrasco-Labra, & Brignardello-Petersen, 2014) or compliant floors (Lachance et al., 2017), and exercise programs (Palvanen et al., 2014). Identification of high-risk individuals and appropriate intervention has been found to reduce the risk of hip fracture by at least 30-60% (Åstrand, Nilsson, & Thorngren, 2012;

Nguyen, Center, & Eisman, 2004; Palvanen et al., 2014; Papapoulos et al., 2005), yet 80% of patients do not receive screening or treatment post fracture (Nguyen et al., 2004). Accurate and widespread screening has the potential to dramatically reduce the hip fracture rates in the Canadian population.

1.1.3 Hip Fracture Risk Prediction

Historically, identification of individuals at high-risk for hip fracture has focused on the diagnosis of osteoporosis. Osteoporosis is 'a skeletal disorder characterized by compromised bone strength predisposing a person to an increased risk of fracture (National Institutes of Health, 2001). The World Health Organization has established diagnostic criteria for osteoporosis that are based on bone mineral density (BMD) measurements determined by dual-energy x-ray absorptiometry (DXA). The diagnosis of osteoporosis is made if a patient's bone density is 2.5 standard deviations or more below the mean value in a young reference population (World Health Organization, 1994). Implicit in this definition, is the existence of a relationship between BMD and bone strength. Bone strength is determined by a complex interplay of bone geometry, cortical thickness and porosity, trabecular bone morphology, and intrinsic properties of bony tissue (Bouxsein & Seeman, 2009). However strong correlations between BMD and bone strength have been found experimentally, with BMD explaining up to 80% of bone strength (Currey, 1986; C. H. Turner, 1989). While clinical studies have found that BMD is the most powerful single factor in predicting the risk of fracture (S. Cummings et al., 1993; Hui, Slemenda, & Johnston, 1989; Krege et al., 2013; McClung, 2005; Melton, Atkinson, O'Fallon, Wahner, & Riggs, 1993), the majority of fractures (up to 82%) occur among non-osteoporotic individuals (Siris et al., 2004).

In order to address the shortcomings of BMD screening, several statistical tools have been developed that consider multiple clinical risk factors. The most popular, FRAX ® (Fracture Risk Assessment Tool), predicts an individual's 10-year probability of hip fracture. In addition to BMD, factors including sex, age, body mass index, fracture history and drug use are incorporated into the fracture prediction (Kanis, Johnell, Oden, & Johansson, 2008). Inclusion of these clinical risk factors results in more reliable fracture prediction, especially among non-osteoporotic individuals (Hillier et al., 2011). FRAX is however not without limitations. Foremost, the loading conditions associated with a fall are not considered. Factors such as body composition can influence both the impact configuration and force (Nasiri & Luo, 2016) during a fall, which are important contributors to hip fracture risk (Nasiri Sarvi & Luo, 2017; Wei, Hu, Wang, & Hwang, 2001). Additionally, the included clinical risk factors are not exhaustive. Femur geometric parameters, such as hip axis length and neck shaft angle, have

previously been related to hip fracture risk (Lee et al., 2016). These factors, which can be extracted at the time of BMD assessment, are not currently included in FRAX. Statistical approaches such as FRAX have limitations in individual fracture risk assessment, primarily due to the variable nature of the clinical risk factors and specificity of the populations from which these relationships were generated (van Geel, van den Bergh, Dinant, & Geusens, 2010). Due to the limitations of statistical fracture prediction tools, a shift toward biomechanical approaches has occurred in recent years (Luo, 2017).

1.1.4 Advantage of Biomechanical Modelling

While biomechanical modelling of hip fracture risk is briefly introduced here, this topic is explored in-depth in Chapter 2. In contrast to statistical fracture tools, biomechanical models parallel the mechanical nature of a hip fracture and provide an 'exact' method of fracture prediction (Luo, 2017). The simplest biomechanical measurement of fracture risk is the ratio between the applied force to the bone strength, referred to as Factor of Risk (FoR). Theoretically, if the FoR exceeds one, a fracture is likely to occur (Dufour et al., 2012; Hayes et al., 1996). Thus, in biomechanical modelling both the bone strength and fall-induced impact force must be determined to predict fracture risk. While bone strength determination is complex due to the mechanical nature of bone, the estimation of loading conditions and impact force are especially difficult. In the literature, impact force is often predicted using empirical formulas and the loading conditions are oversimplified and inaccurate (Mourtada, Beck, Hauser, Ruff, & Bao, 1996; Yang, Peel, Clowes, McCloskey, & Eastell, 2009). A number of factors that influence impact force and loading conditions have been identified (Luo, 2016), but the complexity of real-life falls has prevented accurate estimations. Experimental fall simulation studies provide insight into impact dynamics during a fall and enable the identification of various modulators such as body composition, fall orientation and muscle activation state. However, these studies have limited ability to draw conclusions about tissue level loading as the impact dynamics are measured over the skin surface. A better understanding of factors that modulate loading conditions during a fall and the effect of these varying loading conditions on tissue level loading may inform the development of protective devices (designed to alter impact characteristics to minimize fracture risk) and increase the accuracy of fracture prediction models.

1.1.5 Thesis Rationale & Organization

This thesis will focus on the influence of fall simulation paradigm, sex, and body composition on impact characteristics during lateral falls on the hip and how the application of these loading

conditions influence femoral neck stresses and fracture risk. Coupling of experimental impact dynamics with participant-specific proximal femur models could provide more comprehensive insights (relative to either approach in isolation) into the mechanistic basis of clinical risk factors.

1.1.6 Framework

Analysis of a fall induced impact to the hip can be conducted at several levels, including whole body impact dynamics and tissue level structural-engineering analysis. While these approaches are often utilized in isolation, gross impact dynamics inform loading conditions (inputs) for tissue level analysis. As fracture risk could be modulated by both impact dynamics and underlying femur morphology, a comprehensive evaluation of clinical risk factors should be sensitive to differences at both levels (Figure 1.1). In this thesis simulated fall experiments will be utilized to determine participant-specific impact dynamics (Chapters 3 and 4). These skin-surface dynamics will subsequently be utilized to estimate femoral neck stresses and fracture risk, through participant-specific modeling (Chapter 5).

1.1.7 Chapter 3: The Influence of Fall Simulation Paradigm, Sex, and Soft Tissue Thickness on Femoral Loading Conditions during Lateral Falls on the Hip

Differences in skin surface loading during lateral falls may provide insight into the differences in fracture risk across fall orientations, sex and body composition values. In this study, participants were recruited to generate a cohort with a large range of body compositions and were stratified by sex and trochanteric soft tissue thickness (TSTT). Participants completed a series of three fall simulation paradigms (FSP). The most controlled paradigm, the lateral pelvis release, most closely resembles the simplified loading conditions utilized in the modelling literature. In contrast, the squat and kneeling release paradigms more closely resemble ‘real-life’ falls, incorporating lateral and rotational components. The average magnitude, point of application and orientation of the net impact force were extracted for each FSP. This study provides insights into the effect of FSP, sex, and TSTT on 3D skin surface loading. Additionally, this study provides participant-specific input parameters for femoral neck stress and fracture risk analysis (Chapter 5).

1.1.8 Chapter 4: Pressure Distribution during Lateral Falls on the Hip: Implications of Participant Characteristics and Methodology

While factors influencing peak net impact forces were addressed in Chapter 3, this study aimed to evaluate factors influencing the spatial distribution of these forces over the hip. As anatomical exposure to loads is a key determinant of injury risk (Cummings & Nevitt, 1989), enhanced knowledge

of pressure distribution over the hip could provide insights into injury mechanics and be incorporated as inputs to computational impact models. In this analysis, the proportions of total impact force overlying the proximal femur were quantified during the experimental session outlined in Chapter 3. The influence of FSP, sex, and TSTT on force localization were evaluated to supplement insights into skin surface loading gained in Chapter 3. Additionally, participant-specific force proportions were subsequently utilized in conjunction with global impact characteristics (Chapter 3) as input parameters for femoral neck stress and fracture risk analysis (Chapter 5).

1.1.9 Chapter 5: Participant-Specific Beam Modelling of the Proximal Femur: The Influence of Fall Simulation Paradigm, Sex, and Trochanteric Soft Tissue Thickness on Femoral Neck Stresses and Fracture Risk during Lateral Falls on the Hip

Skin-surface impact characteristics (Chapters 3 and 4) provide valuable insight into factors influencing fall severity. In isolation however, these impact characteristics offer limited insight into tissue level loading and fracture risk, which are dependent on underlying bone morphology. In this study, a subset of the participants recruited in Chapter 3 underwent dual-energy X-ray absorptiometry (DXA) scans, enabling the development of participant-specific proximal femur models. Utilizing experimental impact dynamics as inputs (Chapters 3 and 4), these models enabled calculation of femoral neck stresses and fracture risk. The adopted multi-level approach enabled a comprehensive evaluation of the influence of FSP, sex, and TSTT on femoral neck stresses and fracture risk.

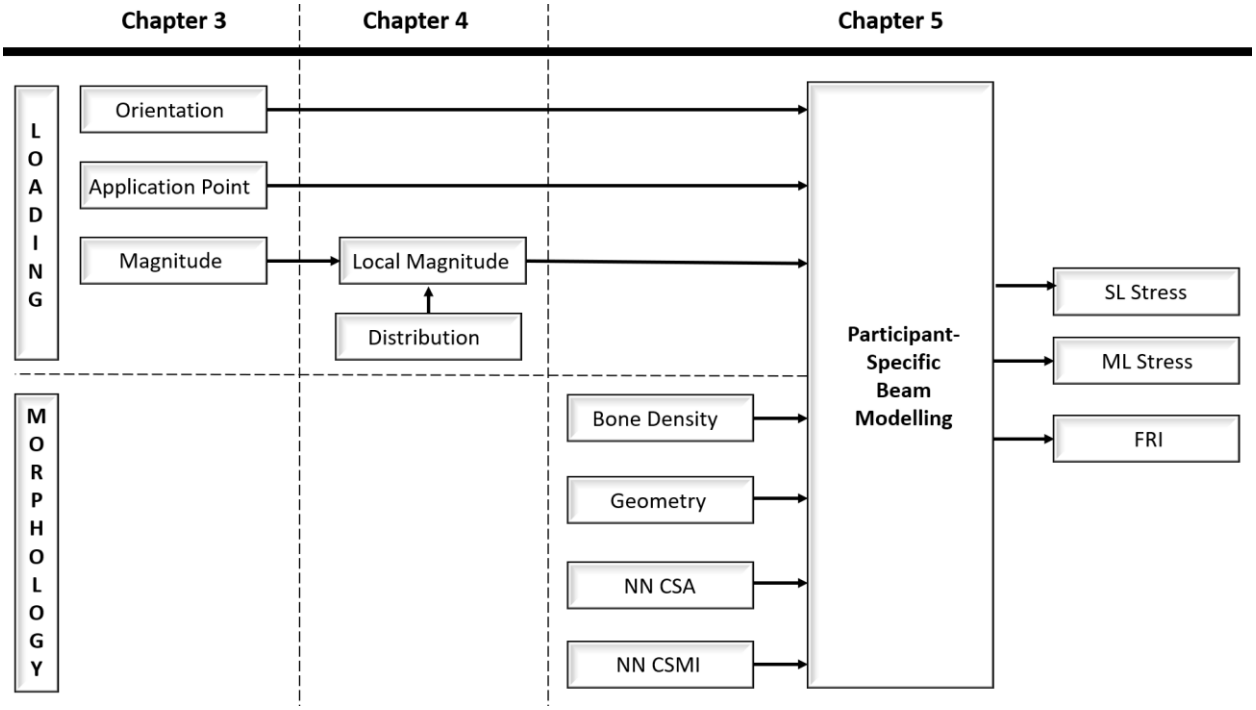

Figure 1.1: Thesis framework. The effects of FSP, sex, and TSTT will be evaluated on global impact vector characteristics (Chapter 3) and force localization over the proximal femur (Chapter 4). A subset of participants underwent DXA imaging enabling the development of participant-specific proximal femur models (Chapter 5). These models were utilized to investigate the influence of FSP, sex, and TSTT on superior-lateral (SL) and inferior-medial (IM) femoral neck stresses, as well as fracture risk index (FRI). The adopted approach is sensitive to potential FSP, sex, and TSTT effects on loading parameters, as well as sex and TSTT effects on femur morphology (bone density, geometry, narrow neck cross sectional area (NN CSA), and narrow neck cross sectional moment of inertia (NN CSMI)).

Chapter 2 Literature Review

In this chapter, the utility of a mechanistic approach to fracture risk prediction will be highlighted. While this approach provides a deterministic method of prediction, several gaps exist in the literature which must be explored to better our understanding of fracture mechanics and increase the accuracy of biomechanical screening tools.

Experimental fall simulations aim to address one such gap by increasing our understanding of impact characteristics during a fall. The insights gained from these studies are however limited to skin surface characteristics, which may contribute to their underutilization in fracture risk models.

2.1.1 Bone Composition, Architecture and Aging in the Proximal Femur

Bone is a living material that is in a constant dynamic state of remodeling, adapting to the mechanical stimuli of daily living. Bone composition and geometry are integral to the strength of the bone and by extension its resistance to fracture. Various disease states and the aging process affect bone composition and geometry resulting in reduced strength. The bone arrangement/distribution in the proximal femur is 'optimized' to resist physiological loading – supporting the body weight during gait and other activities. In response to age-related declines in bone mass, compensatory architectural changes occur to maintain sufficient bone strength during physiological loading.

2.1.1 Bone Composition and Proximal Femur Architecture

Bone is a living composite biomaterial, consisting of 60-70 % inorganic minerals (ex. hydroxyapatite) and 20-30% organic proteins (predominantly type 1 collagen) in their dry weight (Wu, Yu, Chen, & Wang, 2017). The inorganic and organic constituents in bone play different roles in regulating bone stiffness, flexibility and strength; the inorganic mineral content mainly regulates bone stiffness and compressive strength and the organic collagen proteins control bone flexibility and tensile strength (Luo, 2017). Bone combines the mechanical properties of these two constituents to provide sufficient rigidity and strength, as demonstrated by the distribution of cortical and cancellous bones at the femoral neck. Under the action of body weight, the normal physiological loading condition for the femur, the superior side of the femoral neck has tensile stress and the inferior side has compressive stress. The femur adapts to this loading condition by optimally distributing bone mass and most efficiently using the strengths of mineral and organic composition in the bone. More cancellous bones are 'allocated' on the superior side, and more cortical bones are 'assigned' on the inferior side, as cancellous bone has more organic content and higher tensile strength; cortical bone has more mineral content and higher compressive strength.

Based on Wolff's law, bones are continuously formed and removed throughout life in a dynamic metabolic process to adapt to the loads under which they are subject to. This bone remodelling process is regulated and executed by three bone cell types. Osteocytes embedded within the bone act as mechanosensors to receive information of physical strains and micro damage, and to initiate the remodeling process (Bonewald, 2007). If the osteocytes detect increased loading in a region, new bone will be formed or rearranged to enable support of the increased loads in an efficient manner, and vice-versa for mechanical unloading. The balance between osteoblast and osteoclast activity dictate bone remodeling as they are responsible for bone formation and resorption respectively (Pagani, Veronesi, Salamanna, Cepollaro, & Fini, 2018). The architectural arrangement of the trabecular bone as well as bone distribution in the proximal femur is optimized to handle the bending stresses of daily activity (Koch, 1917).

2.1.2 Age Related Changes in the Proximal Femur

The exponential increase in hip fracture incidence among older adults can be attributed to an increased rate of falls and reduced bone strength (Jordan & Cooper, 2002). With ageing, several factors cause a shift toward net bone resorption and bone mass is decreased in older adults (Luo, 2017). The diagnosis of osteoporosis is made based on BMD measures with respect to reference population (World Health Organization, 1994). Although BMD decreases with age and femoral BMD explains up to 80% of bone strength (Currey, 1986; C. H. Turner, 1989), femoral strength has been found to decrease more than 40% faster than BMD on average (Rezaei & Dragomir-Daescu, 2015). The age-related decrease in femur strength cannot be explained by quantity of bone alone and is regulated by hierarchical processes ranging from reduced nano-level toughening mechanisms to whole bone architecture (Milovanovic et al., 2015; Reeve & Loveridge, 2014).

During aging, osteoblast and osteoclast activity on the periosteal and endosteal surfaces are unbalanced resulting in changes in external size and shape, internal architecture and bone mass (Seeman, 2009). A gradual widening of the femoral neck has been observed with age (Kaptoge et al., 2003) which is driven by periosteal apposition (Power et al., 2003). Periosteal apposition, which acts to counteract cortical thinning due to endosteal resorption is greater in men than women (Thomas J Beck, Ruff, & Bissessur, 1993; Duan, Beck, Wang, & Seeman, 2003; Ruff & Hayes, 1988) (Figure 2.1).

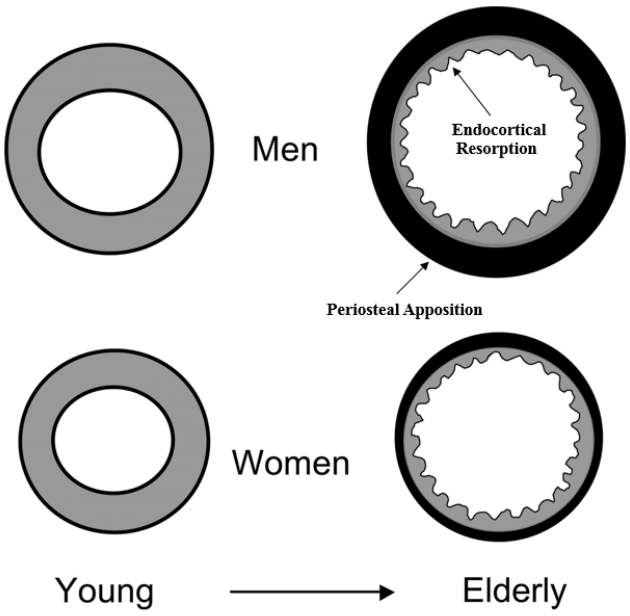

Figure 2.1: Periosteal apposition, which acts to counteract the cortical thinning of endocortical resorption with age, is greater in males than females. Modified from Seeman (2003).

The reduced activity of this compensation mechanism may in part explain the reduced bone strength (Rezaei & Dragomir-Daescu, 2015) and increased fracture rates among women (R. Hopkins et al., 2016). Despite this compensation mechanism, asymmetrical thinning of the femoral neck cortex is observed with ageing, resulting in older adults having much thinner super-lateral cortices than young adults (Mayhew et al., 2005). This process is thought to result due to a reduction in physical activities that sufficiently load the superior cortex to maintain bone mass among older adults (Turner, 2006).

2.1.3 Femoral Loading during a Fall and Fracture Mechanics

The loading vectors on the proximal femur during a fall vary greatly compared to the loading produced during activities of daily living such as walking. While the aforementioned arrangement of the proximal femur and age related architectural changes are well suited to maintain bone strength during daily living, the bone is susceptible to fracture under a fall loading condition in which the stress distributions are reversed compared to normal loading. During a fall the superior cortex of the neck and intertrochanteric region undergo compressive stresses and these regions are susceptible to buckling failure due to asymmetrical cortical thinning. Some experimental and epidemiological evidence exists in the literature to support this injury mechanism theory. This highlights the mechanical nature of hip fracture and points toward a mechanistic fracture risk approach.

2.1.4 Femoral Loading During a Fall

More than 95% of hip fractures are the result of a fall (Parkkari et al., 1999), with sideways fall onto the hip being implicated in the majority of cases (Hayes et al., 1993).While the morphology of the proximal femur is optimized to handle the loads of daily living, it is vulnerable to fracture during a fall event.

In normal weight bearing activities, bending stresses on the supero-lateral cortices are in tension and the majority of the load is borne by the thicker infero-medial cortices, which are in compression (Rudman, Aspden, & Meakin, 2006) (Figure 2.2a). During normal ambulatory activity, the lateral neck is relatively unloaded due to summation of physiological compressive loads (muscle forces) (Lovejoy, 1988), leading to bone adaptation and cortical thinning. The thick infero-medial cortex is retained with age due to this habitual loading, resulting in asymmetrical cortical thinning observed with aging (Mayhew et al., 2005) and a medial shift of cross-sectional center of masses (Beck, Looker, Mourtada, Daphtary, & Ruff, 2006).

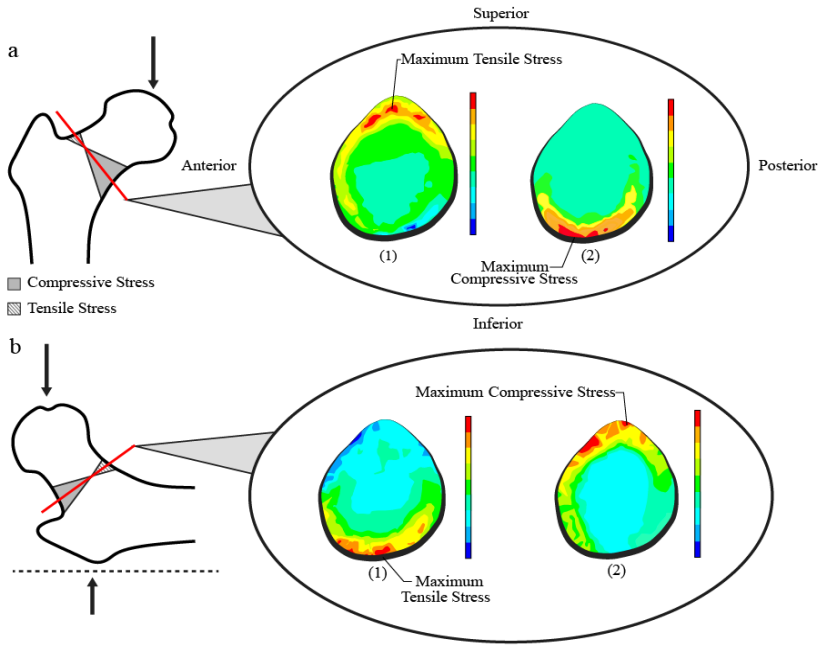

Figure 2.2: Comparison of tensile (1) and compressive (2) stresses in the femoral neck between weight bearing activities (a) and a fall onto the greater trochanter (b). In the fall loading configuration the stress distributions are effectively reversed compared to weight bearing activities. The morphology of the femur is well suited for ambulatory loading but is susceptible to fracture. Modified from deBakker et al., (2009)

The reverse is true in fall loading condition. Bending stresses on the inferior medial cortices are in tension and the majority of the load is borne by the thin superior lateral cortices which are now in compression (Figure 2.2b). Axial forces on the femoral neck during a fall further increase the compressive load on the superior lateral cortices. Thus, during a fall, the femur is susceptible to fracture due to the reversal of stress distributions compared to ambulatory loading, resulting in the thin superior lateral cortices bearing the majority of the load. This is confounded by geometric changes with age in response to ambulatory loading, which increase the compressive stresses on the superior lateral cortices, particularly in women (Beck et al., 2006) (Figure 2.3).

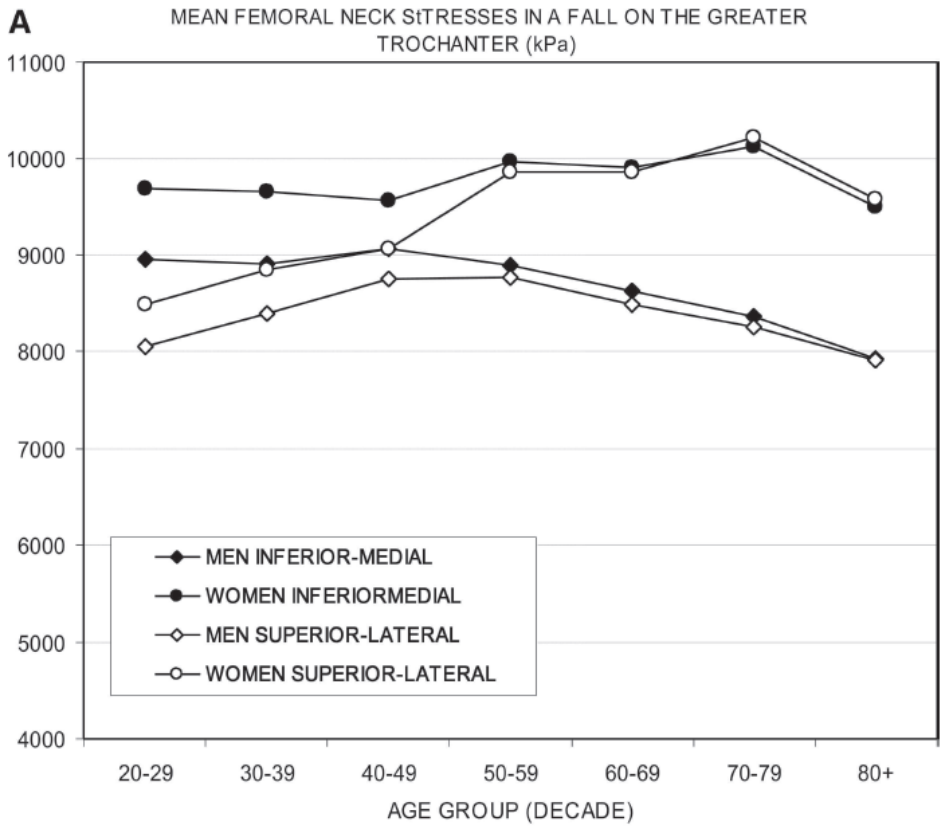

Figure 2.3: Femoral neck stresses during a fall onto the greater trochanter. A medial shift of cross-sectional center of masses with age result in increased superior lateral stresses. This effect is greater in women, whom have greater hip fracture rates than men (Beck et al., 2006).

2.1.5 Fracture Mechanics

Due to the relatively high stresses experienced by the thin superior lateral cortex, it has been suggested that this is a likely location of proximal femur fracture initiation (Yoshikawa, Turner, Peacock, Slemenda, & Weaver, 1994; Mayhew et al., 2005). In support of this theory, it has previously been shown that BMD in the superior but not inferior femoral neck is predictive of femoral neck fractures (Duboeuf et al., 1997; Long, Leslie, & Luo, 2015) and that fractures are associated with a thinner superior cortex (Johannesdottir et al., 2013). More recently experimental fracture testing of the proximal femur with high speed video indicates that fall induced fractures are a result of a two-stage failure process, with fracture initiation in the superior cortex followed by failure in the inferior neck (de Bakker et al., 2009). It has been mathematically demonstrated that following a macro-scopic crack in the superior cortex, the section modulus of the femoral neck collapses suddenly with the inferior medial cortex failing in bending due to the lack of bracing by the damaged superior cortex (Mayhew et al., 2005). A better understanding of the failure type in the superior cortex (crushing vs. buckling) has implications to clinical screening as well as the generation of bone failure models (Reeve & Loveridge, 2014). The mechanical nature of both bone loading and failure allows for the generation biomechanical and structural engineering models to predict fracture loads and relative individual fracture risk.

2.1.6 A Mechanistic Approach to Fracture Risk

Statistical methods of fracture prediction are clinically prevalent but have limitations in individual fracture risk assessment, primarily due to the variable nature of the clinical risk factors and specificity from which these relationships were generated. Biomechanical models integrating patient specific structural models and loading conditions can offer a more accurate, 'exact' method of fracture risk assessment. Various frameworks for assessing hip fracture risk exist including the Cummings and Nevitt Hypothesis and more recent frameworks encompassing clinical risk factors. Fundamentally, a mechanistic approach requires consideration of both the fall induced femoral loading as well as the bones strength or ability withstand loading.

2.1.7 Cummings and Nevitt Hypothesis: The Cause of Hip Fractures

Adopting a mechanistic view of hip fracture Cummings and Nevitt (1989) present a hypothesis for the cause of fall induced hip fractures. This hypothesis states that for a given fall to result in a hip fracture a sequence of four conditions must be satisfied: 1) the faller must be oriented as to impact the hip; 2) the protective responses to reduce the energy of a fall must be insufficient; 3) the local shock absorbers such as soft tissues must be insufficient in reducing the impact energy; and 4) the strength of the bone must be less than the residual energy of the fall (Figure 2.4).

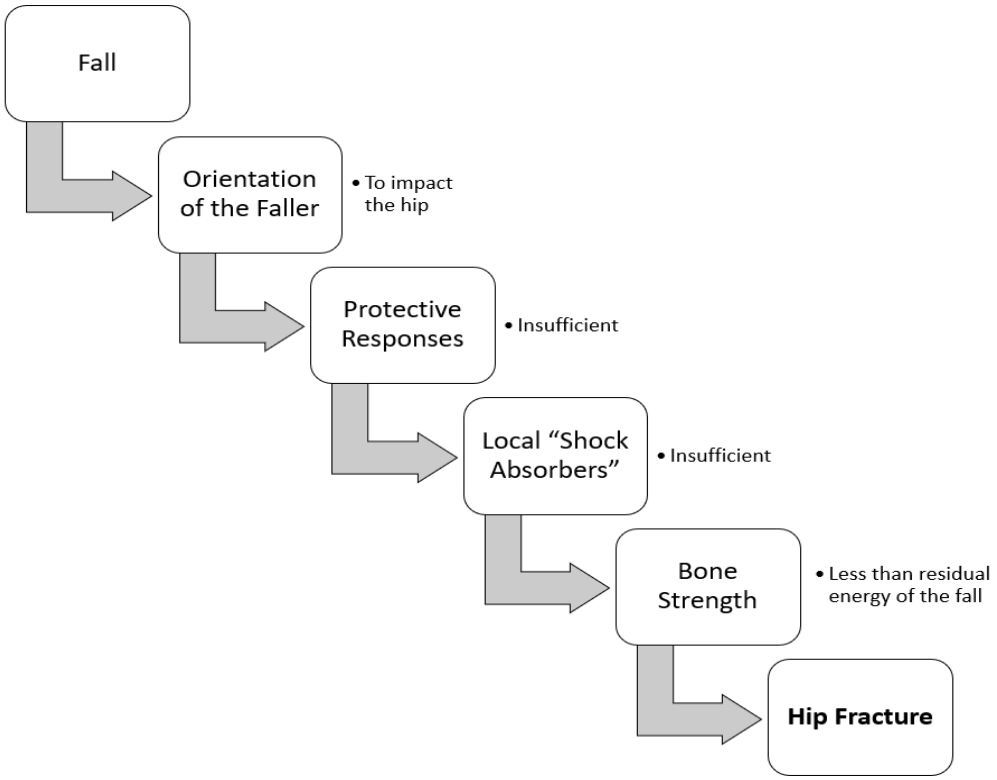

Figure 2.4: Cummings and Nevitt (1989) hypothesis of fall induced hip fractures.

While this approach neglects the initiation of a fall (a fall must occur and therefore the individual must also have insufficient balance responses), it provides a systematic framework and identifies key points for intervention and screening. In this framework, a hip fracture can be prevented at multiple points in the sequence and failure at one point does not guarantee a fracture will occur. This hypothesis has been supported by research of actual falls in long-term care (Grisso et al., 1991; Yang, Schonnop, Feldman, & Robinovitch, 2013) and serve as the basis for fall modeling efforts and more recent frameworks (Luo, 2017).

2.1.8 Biomechanical Sorting of Clinical Risk Factors

Factor of risk (FoR) is a biomechanical approach to predict the likelihood of tissue damage, such as a hip fracture, and is calculated as the ratio of applied load to tissue tolerance (the force that can be sustained by the structure prior to damage). Theoretically, if the FoR exceeds one, a fracture is likely to occur (Dufour et al., 2012; Hayes et al., 1996). This framework parallels the final stage of the Cumming and Nevitt Hypothesis is which the residual energy of the fall is either dissipated by the bone or exceeds the bone strength resulting in fracture. Thus, when adopting this framework, both the applied load on

the bone and bone strength must be determined to calculate fracture risk. Luo (2016) adopted a similar framework referred to as Load-Strength Ratio and generated a biomechanical sorting of clinical risk factors for hip fracture (Figure 2.5).

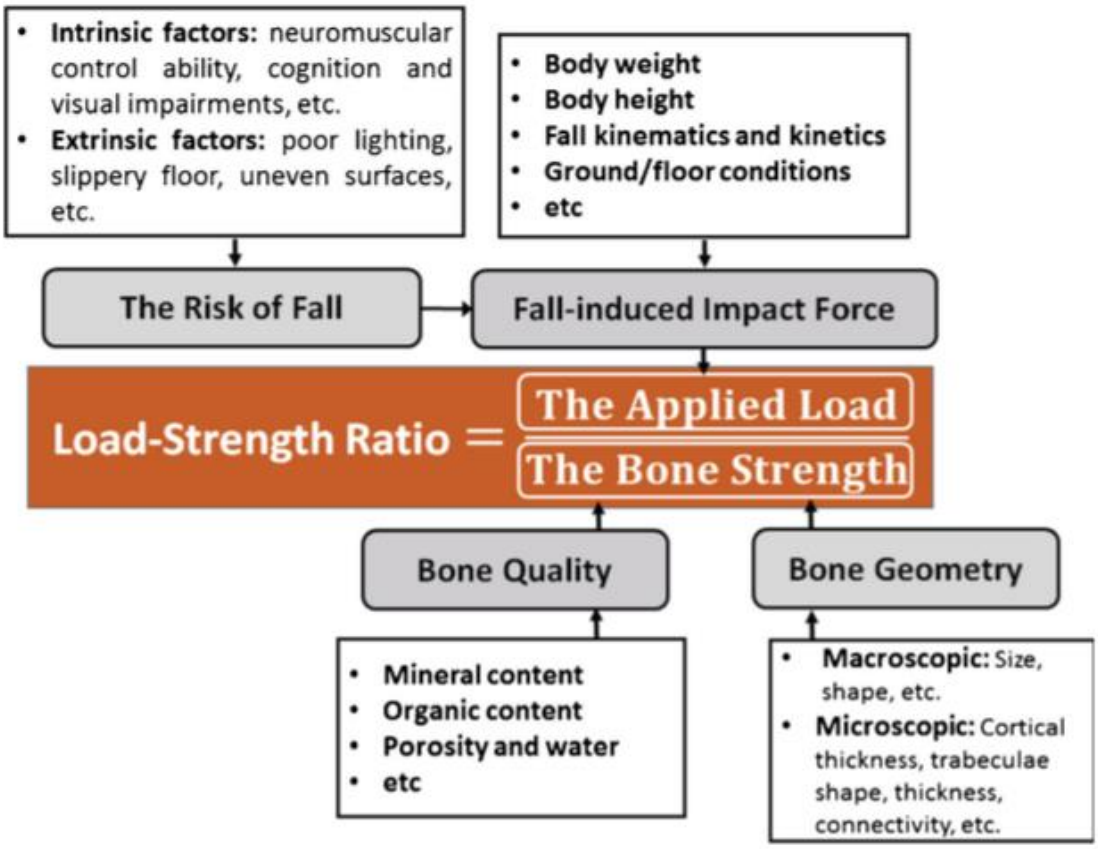

Figure 2.5: Major and minor biomechanical variables contributing to hip fracture risk (Luo, 2016).

With this framework more complete framework, it is clear that several biomechanical variables contribute to fracture risk and points towards the value of mechanistic fracture risk assessment. Models integrating BMD distribution, femoral geometry, and patient-specific loading conditions can offer more accurate hip fracture risk assessment than statistical methods (Dufour et al., 2012; Luo, 2017; Orwoll et al., 2009), which have limitations in individual fracture risk assessment, primarily due to the variable nature of the clinical risk factors and specificity from which these relationships were generated (van Geel et al., 2010). The accuracy of such a biomechanical approach would be sensitive to accurate determination of subject specific loading conditions and bone strength.

2.1.9 Biomechanical Models of the Proximal Femur

A complete fracture risk assessment would require a multi-level biomechanical model including sub models of fall risk, whole-body dynamics, impact, tissue-level stress/strain, and failure mechanism. With exception of a few research groups, the focus has been put on the tissue-level models of the proximal femur. These models allow the input of femur geometry and material information, in addition to impact force and constraint conditions to compute metrics of fracture risk. The primary difficulty with such models are the accurate determination of real-life fall loading and constraint conditions as well as establishing relationships between mechanical properties of the femur and information contained in medical images. While finite element models are prevalent in the literature, beam models may offer a simpler alternative with clinical appeal.

2.1.10 Impact Force and Constraint Conditions

Determination of the fall induced impact force is an important step in fracture risk assessment that is complicated by individual anthropometry, fall kinematics and the compliance of the impact surface (Sarvi & Luo, 2017). Despite the complexity of real life falls, the impact force is commonly predicted using mathematical modelling of human body falling or simpler empirical functions (Sarvi & Luo, 2017).

Mathematical human body dynamic models are utilized to predict falling kinematics and impact velocity in conjunction with an impact model to simulate the interaction between the hip and the ground. These dynamic models range from simple point-mass or one-link single-degree of freedom models based on conservation of energy (van den Kroonenberg, Hayes, & Mcmahon, 1995) to more complex 11-link models (Lo & Ashton-Miller, 2008) utilizing body segment anthropometric parameters derived from DXA images (Sarvi & Luo, 2015). Once the impact velocity and energy are estimated impact models (Figure 2.6) enable the estimation of peak impact force.

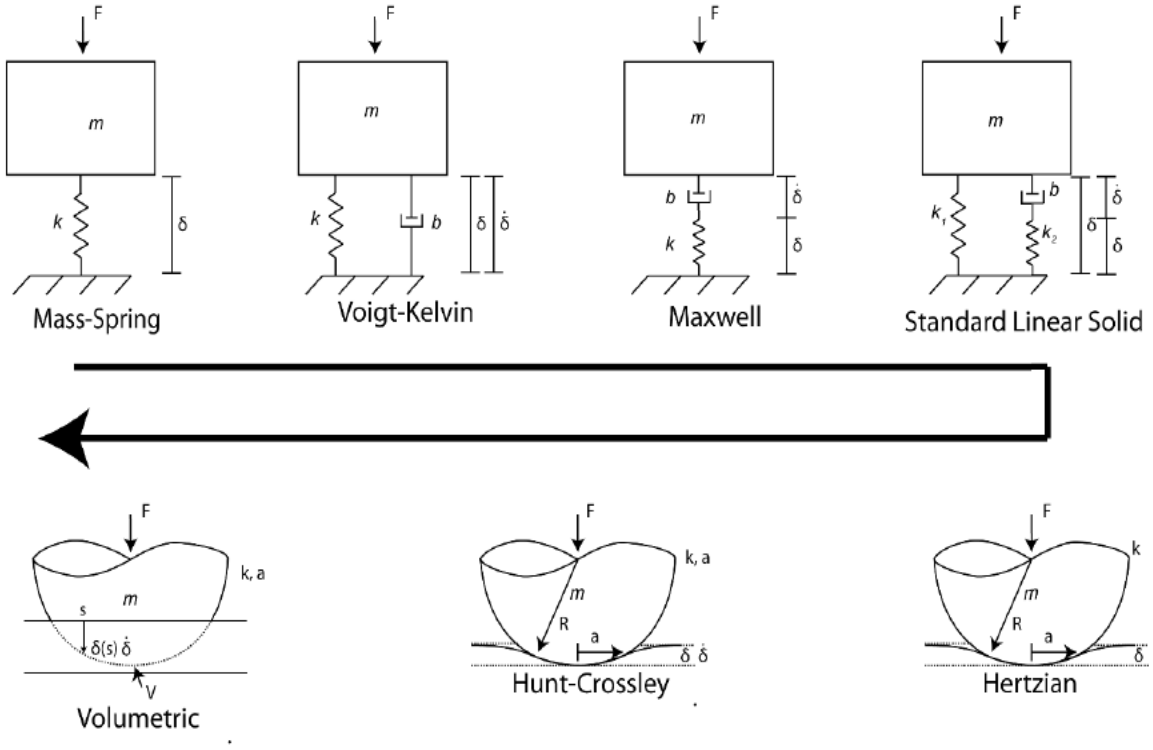

Figure 2.6: Impact models for estimating impact force (complexity increases along the black arrow). The top-row models follow Hookean-spring mechanics, while the second row expands on these models to follow Hertzian spring theory. The Volumetric contact model, simulates uneven stress distribution across a deformable body according to Winkler elastic foundation theory (Levine, 2017).

The above impact models may provide the most accurate impact force estimations but several individual parameters must be known such as tissue stiffness and dampening properties, and the complexity of some of these models limit their clinical applicability. Empirical equations offer a simpler alternative which are more commonly employed even in the tissue level modelling literature.

Kroonenberg et al. (1995) and Yoshiwaka et al. (1994) proposed empirical functions, which are widely used in the literature to estimate impact force based on an individual's height and mass. These functions notably do not account for the effect of trochanteric soft tissue to reduce the impact force during a fall (Robinovitch, Hayes, & McMahon, 1991). Robinovitch et al. (1995) suggested that for each millimeter increase of soft tissue thickness, peak force magnitude over the greater trochanter is decreased by 71 N. A combination of the original empirical functions and the soft tissue attenuation have been utilized to estimate peak impact force magnitude. As anatomical exposure to loads is a key determinant

of injury risk (Cummings & Nevitt, 1989), the distribution of impact force over the hip is likely an important consideration in fracture risk. In biomechanical models however, the spatial distribution of impact force is neglected and represented as a point load. Enhanced knowledge of pressure distribution over the hip could provide insights into injury mechanics, and potentially be incorporated as inputs into computational models of pelvic impacts. While impact force magnitude and distribution have obvious implications on tissue level loading, the direction in which it is applied to the femur and the constraint conditions during a fall also influence fracture risk.

Falling is an unpredictable event and the directions of the impact vector can vary between individuals and falls, influencing the strength of the femur. Femoral strength testing and biomechanical modelling are commonly performed based on a single sideways fall loading configuration dating back to the first fall simulation tests by Backman (1957). Loading conditions in the literature commonly simplify a fall into its vertical component, neglecting shear forces associated with arresting the forward momentum of the body. Zani et al. (2015) performed invitro femur testing systematically across a variety of loading configurations and assessed how the magnitude and direction of principal strains varied. The largest strains occurred in the neck region and these strains increased as internal rotation was increased from 0 to 30 degrees and as adduction angle was increased from 0 to 30 degrees. Such a loading direction can be associated with a posterior lateral fall, with the lower limb adducted and flexed (Majumder, Roychowdhury, & Pal, 2009; Nankaku, Kanzaki, Tsuboyama, & Nakamura, 2005; A. van den Kroonenberg et al., 1995; A. J. Van Den Kroonenberg, Hayes, & McMahon, 1996). Keyak et al. (2001) utilized finite element (FE) models to determine that a posterolateral impact with the force directed through the greater trochanter at an angle of 60-70% generated the lowest predicted fracture loads (load at which a fracture is likely to occur). Pinilla et al., (1996) also performed mechanical testing of femurs and found that failure load decreased by 24% when loaded in a posterolateral configuration equivalent to the decrease associated with 25 years of bone loss after the age of 65. Similar results were found by Ford et al., (1996) utilizing FE modelling techniques and more recently by Bessho et al. (2009) and Carpenter et al. (2005), who also found differences in predicted fracture type and location across fall configurations. Experimental fall simulation studies have also shown the magnitude of the skin-surface impact force of a fall changes with impact orientation. Choi et al. (2010) found external peak force was 12% greater in posterolateral and 17% lower in anterolateral compared to lateral falls. Together these studies demonstrate that load direction is likely a critical determinant of hip fracture risk that is independent of bone composition and should be incorporated into biomechanical models and screening tools.

A limited number of studies exist evaluating the effect of loading conditions on clinical fracture predictions. Falcinelli et al. (2014) performed a case-control study using FE models simulating a variety of fall impact orientations. The occurrence of minimum FE-strength (angle at which hip fracture was most likely) was widespread across loading conditions for individuals, with a general trend toward decreasing strength with increased internal rotation. Interestingly, the minimum strength across fall loading conditions was the strongest predictor of fracture, supporting the value of considering multiple loading conditions. Keyak et al. (2013) also evaluated the effect of loading condition of fracture risk and found posterolateral and posterior loading of the greater trochanter were most strongly associated with fracture risk in men and women respectively.

The final consideration related to the coupling between skin-surface impact force and tissue level loading is the point of application on the femur. In the literature, the impact force is often distributed with the net force acting through the greater trochanter (Keyak et al., 2001, 2013 etc.). Experimental studies have found that the impact load during a fall does not necessarily correspond with the greater trochanter and can be influenced by a number of factors. Choi et al. (2010) found that in pelvis-release experiments the location of peak pressure was on average 52 mm distal to the greater trochanter and was significantly associated with body composition and impact angle.

Factors that influence the loading conditions (peak force magnitude, distribution, direction and point of application) during a fall require additional research and inclusion of these considerations may improve the accuracy of fracture risk models. Another important factor that may influence the accuracy of tissue level models such as FE is the boundary conditions during an impact (Enns-bray et al., 2018). Haider et al. (2013) investigated the effect of using different boundary conditions prevalent in the literature on strain outputs of an FE model (Figure 2.7). The boundary conditions tested did not alter the prediction of fracture location or strain pattern. However, in the boundary condition in which the femoral head was loaded instead of the greater trochanter peak strain increased by 22% and fracture strength decreased by approximately the same amount (18%).

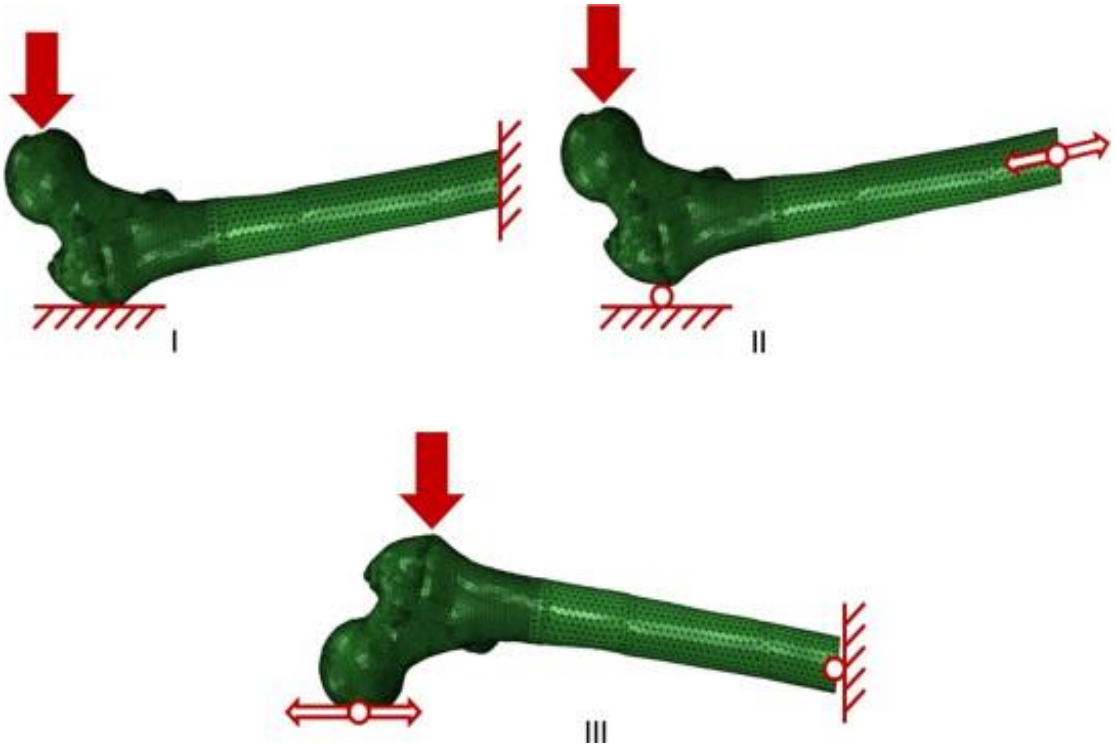

Figure 2.7: Three boundary conditions investigated by Haider et al. (2013). (I) the femoral shaft (FS) and GT were fully constrained to rotation and translation, while the femoral head (FH) was loaded; (II) the FS was only free to rotate in the coronal plane and translate along the shaft axis in the coronal plane. The GT was constrained in translation but free to rotate in all directions; (III) the FS was only free to rotate and translate in a cranio-caudal direction in the coronal plane. The FH was only free to rotate in the coronal plane. Load was applied to the GT.

More recently Rossman et al. (2016) evaluated six boundary conditions utilized in the literature to determine their effect on femora stiffness predictions (Figure 2.8). Average stiffness varied by 280% across boundary conditions, with the boundary conditions most closely matching the expected test conditions (Figure 2.8: DSS, MPC and Contact 1) producing the best agreement with experimentally determined stiffness. It is difficult to determine which of the investigated boundary conditions best represents a femur during a fall but it is clear that model predictions are sensitive to boundary condition assignment. Additional research is required to determine the boundary conditions during real falls for inclusion in tissue-level models.

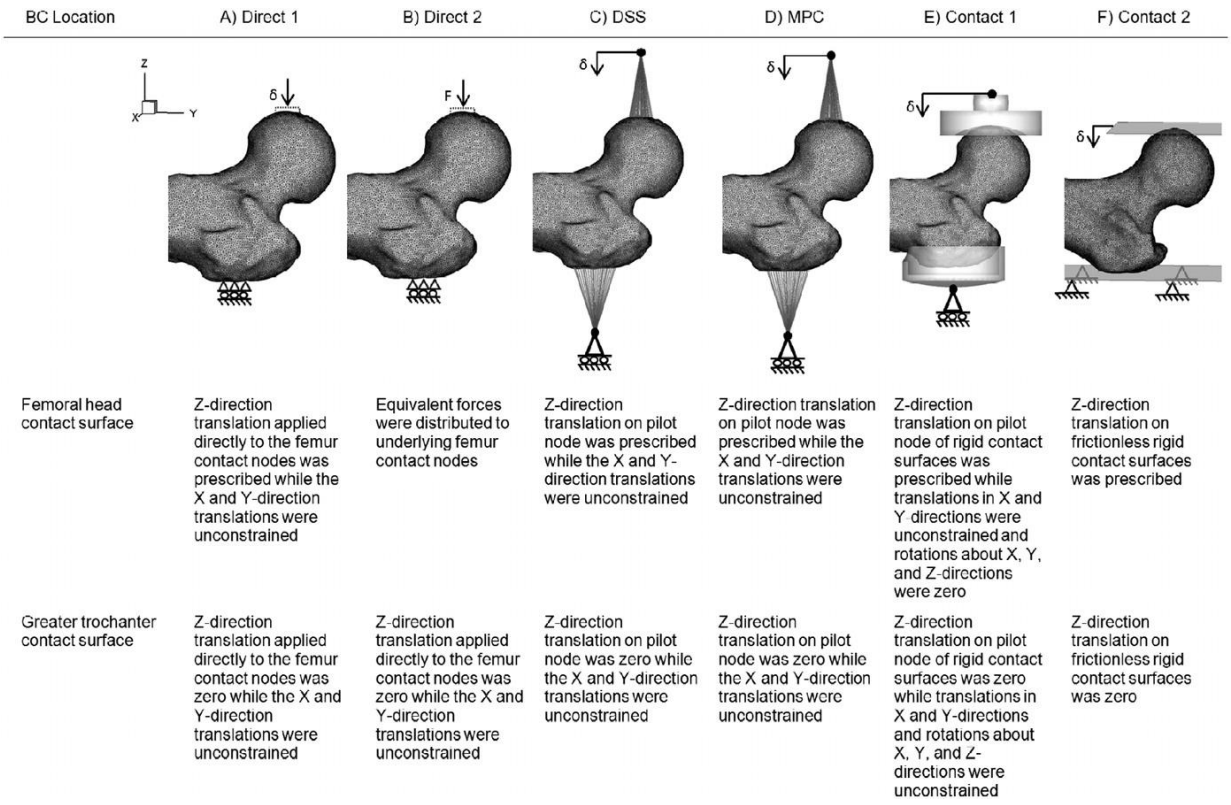

Figure 2.8: Femoral boundary conditions utilized by Rossman et al. (2016).

The effect of the impact dynamics during a fall on tissue level stress/strain and fracture prediction appear to be profound and require additional research. Multiple approaches can be employed and a number of factors influencing impact dynamics have been identified, which will be reviewed in Section 2.6. This thesis will aim to determine the effect of fall simulation paradigm (a surrogate for different fall types/impact configurations), sex, and local body composition (trochanteric soft tissue thickness) on skin surface impact dynamics (Chapters 3 and 4) and tissue level stresses and fracture risk (Chapter 5).

2.1.11 Relationship between Bone Density and Mechanical Properties

The strength of a bone in a sideways fall can be determined experimentally by destructive testing but this method is inappropriate for fracture risk prediction among living individuals. For this reason, researchers have sought to generate mechanical models of the femur to estimate failure loads and femoral strength. In order to extract subject specific bone geometry and material distributions, medical imaging such as dual energy X-ray absorptiometry (DXA) and quantitative computed topography (QCT) are commonly employed. The utilization of the information contained in these images to assign material

properties to structural models is dependent on establishing relationships between measures of bone density, elasticity, and yield properties (Luo, 2017). A large number of elasticity-density relationships have been proposed and subsequently utilized in the literature with no explicit considerations on the suitability and accuracy of the chosen relationship (Helgason et al., 2008). In a review of several relationships in the literature, Helgason et al. (2008) found substantial inter-study discrepancies. While the lack of agreement between studies can in part be attributed to differences in testing methodology, specimen geometry, anatomical location, and strain rate, a standardized testing protocol would likely still produce discrepancies due to the complexity of the elasticity-density relationship (Luo, 2017). Bone has complicated material properties including inhomogeneity, anisotropy, and viscosity as well as variable architecture at several hierarchical levels that preclude the determination of an elasticity-density relationship that is appropriate across bones and loading conditions.

Helgason et al. (2016) systematically evaluated the effect of modulus-density relationship selection on the outputs of finite element (FE) models of simulated sideways falls. Several modulus density relationships utilized in fall simulation FE models were sourced from the literature (Figure 2.9). Selection of elasticity-density relationship was found to have a substantial effect on model accuracy with r^2 ranging from 0.79 to 0.91 for experimental compared to FE predicted superior neck strain, dependent on the selected relationship. These authors concluded that future work in establishing the optimal modelling method and elasticity-density relationship for sideways fall simulations is required. Similar results under different loading conditions have been found (Eberle, Göttlinger, & Augat, 2013) highlighting the importance of research in elasticity-density relationships for application in tissue level models.

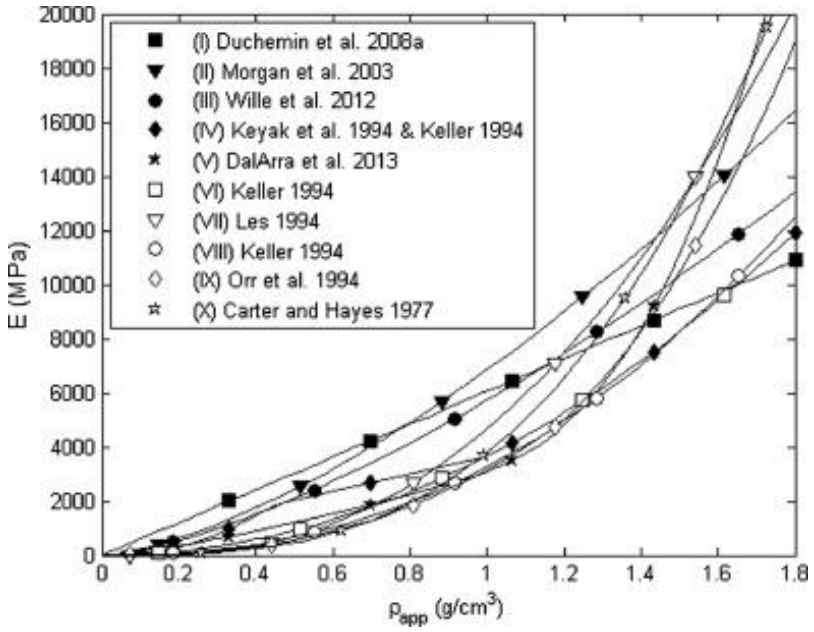

Figure 2.9: Modulus of elasticity (E) as a function of apparent bone density (Papp) relationships utilized in the literature (Helgason et al., 2016).

Relationships between bone density and mechanical properties have been found to have site dependency (Morgan and Keaveny, 2001). In Chapter 5, femoral neck and proximal femur material properties will be assigned based on the site-specific density relationships established by Morgan and Keaveny (2001). As these relationships were established through in vitro mechanical testing, side-artifacts (a result of disrupting the trabecular network during sample extraction) further complicate prediction of in situ behavior. In order to reconcile the side-artifact error in these relationships, a site-specific correction factor of 1.20 (Bevill, Easley, & Keaveny, 2008; Un, Bevill, & Keaveny, 2006) will be applied in Chapter 5.

2.1.12 Finite Element Models

The most promising biomechanical model for bone stress analysis is finite element analysis, which can account for the irregular geometry and heterogeneous bone of the proximal femur (Huiskes & Chao, 1983). FE models were introduced to the field of orthopedic biomechanics in 1972 (Brekelmans, Poort, & Slooff, 1972) and have seen a rise in prevalence particularly in modelling of the proximal femur. Both two- (Luo, Ferdous, & Leslie, 2011; Den Buijs & Dragomir-Daescu, 2011) and three- (Enns-bray et al., 2018; Keyak et al., 2013) dimensional FE models of the femur are present in the literature, dependent on the imaging modality utilized (DXA scans preclude 3D analysis unless a

statistical shape and appearance model is employed (Grassi, Väänänen, Ristinmaa, Jurvelin, & Isaksson, 2017)). These models vary in complexity from quasi-static to dynamic models, with the latter more accurately representing the femur's response to fall-induced impacts (Ariza et al., 2015; Enns-bray et al., 2018; Varga et al., 2016). QCT based FE models have been found to be the best predictor of femoral strength ex vivo (Johannesdottir et al., 2017) and DXA based 2D FE models have been found to better predict failure load compared to aBMD alone (Den Buijs & Dragomir-Daescu, 2011). The added predictive value of FE analysis points towards the importance of bone geometry to femoral strength compared to bone quality alone (BMD). Despite their accuracy in failure prediction ex vivo (Grassi et al., 2012), FE models have been reported to only marginally increase fracture predictive capabilities in clinical populations (Kopperdahl et al., 2015), in some cases offering no statistical improvement compared to measures of BMD alone (Yang et al., 2009). These conflicting reports may suggest that while FE models accurately predict failure load during mechanical testing ex-vivo, the predictive capacity (ability to identify high fracture risk individuals in a population) of these models is limited due to a lack of important information about real life falls. Factors that influence the impact force and constraint conditions during a fall are not fully captured by the current models, and the mechanical testing on which these models are based/validated may not be representative of real falls (Ariza et al., 2015; Enns-bray et al., 2018). The short-comings of these models must be addressed to increase predictive capabilities if researchers are to advocate for their wide-spread use over far less computationally intense and time-consuming methods (Bessho, 2009).

2.1.13 Beam Models

The overall complexity and cost (economic, computational and time) of QCT based FE models limits their clinical applicability (Danielson et al., 2014). Beam models offer an alternate approach which are comparatively simple and computationally cheap, with reasonable accuracy in stress predictions (Mourtada et al., 1996). The clinical application of such an approach is illustrated by Hip Structure Analysis (Beck, 2007), a software package commercially available for use with DXA imaging. While this software does not estimate loading/stresses resulting from a fall, it outputs femoral geometry and strength parameters such as cross-sectional area, moment of inertia and section modulus which are relevant to beam mechanics and associated with fracture risk (Kaptoge et al., 2008). Despite the commercial availability of Hip Structure Analysis, the International Society of Clinical Densitometry does not recommend its use in hip fracture screening citing a lack of established thresholds for risk and low precision (Broy et al., 2015). Beam models offering computation of a risk index, accounting for

loading during a fall may offer a deterministic method of fracture prediction while still being clinically applicable (Yang, 2017).

Mourtada et al. (1996) proposed a DXA based 2-D curved beam (CB) model of the proximal femur for calculating stresses during one-legged stance and a fall onto the greater trochanter. This model represents the femur as two straight beams in the femoral shaft and neck connected by a curved beam through the trochanteric region. Utilizing external loading conditions and femoral geometry, this model allows the computation of stresses using well established equations from the linear theory of elasticity. The stress outputs of this model were validated against a more complex FE model. Despite the vast differences in complexity and computational cost, the beam model performed well, with good agreement with the FE computations of internal stresses (Figure 2.10; The fitted model was CB = 0.99 FE + 1.05 (r^2 = 0.97)). This model was later utilized to predict failure load in cadaveric specimens by Beck et al. (1998), with an r value of 0.91. Combined, these studies suggest that beam models, although simple, offer a means to calculate internal stresses that reasonably agree with historical FE computations and can accurately predict ultimate failure loads. While recent advances in FE modelling (non-linearity and dynamic simulations) more accurately characterize the mechanical response of the femur, simple beam models still offer valuable insight into mechanics with greater clinical applicability.

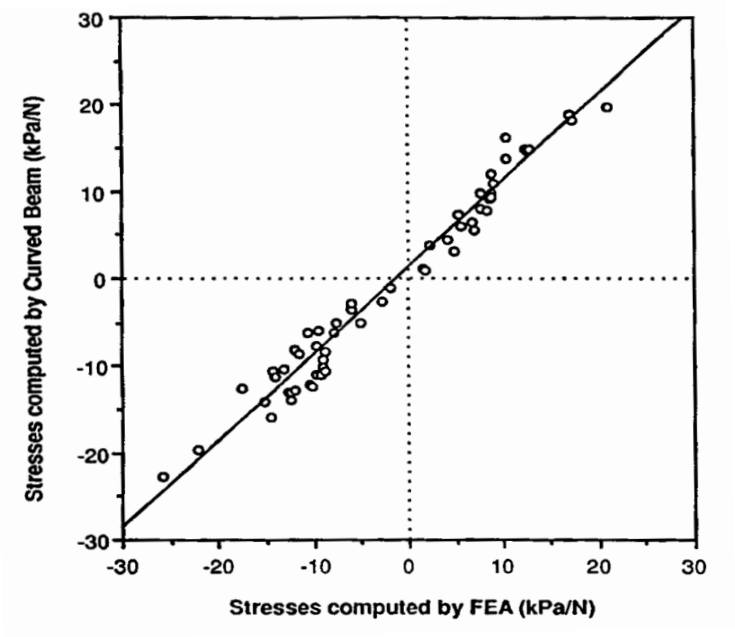

Figure 2.10: Comparison of curved beam (CB) and finite element analysis (FE) stress prediction. The fitted model was CB = 0.99 FE + 1.05 (r^2 = 0.97) (Mourtada et al., 1996).

Beam models have been utilized to predict fracture in clinical populations (Yang et al., 2009), with some studies reporting model outputs as significant fracture predictors independent of bone density (Faulkner et al., 2006). These comparatively simple yet mechanistic beam models may provide a good tradeoff between FE models and simple measures of BMD for clinical screening. Similar to FE models, the accuracy of such an approach would likely be dependent on the application of realistic loading conditions, which account for individual variability during a fall related impact. While current beam models simulate a single simplified loading configuration, a beam modelling approach will be introduced in Chapter 5, which is novel in that it utilizes participant specific experimental data to more accurately estimate tissue level stresses during simulated impacts.

2.1.14 Biomechanical Variables of Fracture Risk

Several metrics are utilized in the literature to assess the ability of the femur to withstand loading during a fall. These measures of fracture risk can be classified based on site specificity and theoretical bases with regards to bone failure mechanism. Selection of an appropriate fracture risk criterion is dependent on the purpose of the model and the available input variables. While simple whole bone metrics are attractive for clinical application, more complex anatomical-site-specific metrics could offer more accurate fracture prediction (although their wide spread clinical application is not presently feasible). In their present form, the more advanced hip fracture metrics are a valuable tool to researchers aiming to identify the effect of various clinical risk factors on tissue level risk.

2.1.15 Load-Strength Ratio (Factor of Risk)

The most commonly used and simplest fracture risk criterion is the load-strength ratio commonly referred to as factor of risk (FoR):

$$FoR = \frac{F_{Impact}}{F_{Max}}$$

where F_{Impact} is the magnitude of the load placed on the femur and F_{Max} is the magnitude of the maximum force the femur can withstand before fracture (bone strength). This criterion considers the integrity of the whole femur with a ratio greater than 1 indicating a fracture will occur. For this reason the specific location of fracture cannot be predicted. Implicit in this criterion is that the impact and maximum load vectors are in the same direction (Luo, 2017). This simplification is likely inappropriate as the fall induced loading vector could be applied at various points on the femur in any direction, and the strength of a bone is dependent on the location and direction of loading (Section 2.4.1). Additionally, this criterion is based on structural engineering ultimate strength methods in which partial failure of a material is allowed, which is likely too risky for hip fracture risk prediction (Luo, 2017).

Despite the drawbacks of this approach, FoR is appealing from a clinical perspective due to its simplicity. Empirical functions can be utilized to estimate both the impact force and bone strength of an individual based on clinically available factors such as height, weight and aBMD. Bouxsein et al. (2007) provides an example of the utility of this approach in their assessment of the contribution of trochanteric soft tissues to fracture risk. FoR was estimated and found to be 50% greater in hip fracture cases than aged matched controls using simple empirical functions. This approach does not require computationally intensive models and therefore may have value in clinical screening of fracture risk.

2.1.16 Fracture Risk Index (FRI)

Clinical studies have demonstrated that the proximal femur fractures in three primary regions: the femoral neck, intertrochanteric and subtrochanteric regions (in decreasing order of prevalence) (Pasi Pulkkinen, Eckstein, Lochmüller, Kuhn, & Jämsä, 2006). For this reason, site specific hip fracture risk assessment based on these regions has been introduced. Compared to whole bone approaches, these anatomical-site-specific risk assessment tools enable fracture type/location predictions at the expense of increased complexity and the need for additional input variables.

Various fracture risk indexes exist and vary primarily in the theoretical bases of fracture mechanics. In the literature strain-based criteria (Keyak & Rossi, 2000), stress-based criterion (Yoshikawa, Turner, Peacock, Slemenda, Weaver, et al., 1994) and energy-based criterions (Kheirollahi & Luo, 2015) are utilized. There is evidence that bone failure is likely governed by a combination of both stress and strain (Keyak & Rossi, 2000). Cancellous bone failure is primarily attributed to buckling and deformation (strain-based) and cortical bone failure is linked to local cracking (stress-based) due to their respective material properties (Luo, 2017) - cortical bone is brittle and cancellous bone is ductile (Cordey & Gautier, 1999). In the proximal femur, where load is shared between these two bone types, a fracture risk index combining both distortion energy and volume change energy is theoretically more accurate than stress or strain-based approaches in isolation. Such an approach was introduced by Kheirollahi and Luo (2015) in which the fracture risk index is taken as the ratio of the strain energy to the yield strain energy for a bone cross-section. Cross-sectional strain energy is the potential energy produced by both stress and deformation of a material resulting from axial, bending, shear and torsional loading. While this method offers a more detailed and mechanically reasonable approach to fracture risk prediction, its implementation is more complex and requires experimental and clinical validation. In Chapter 5, a beam model utilizing a stress-based criterion will be introduced.

2.1.17 Impact Dynamics during Falls

As demonstrated in Section 2.4.1, loading and constraint conditions can have large effects on tissue level loading and fracture predictions. Due to the complexity of real-life falls, the loading conditions are not well understood and often simplified using empirical equations and idealized loading directions and points of application. Additional insight into these factors, and their inclusion in biomechanical models, may improve fracture risk prediction through more realistic mechanistic analysis. Several approaches exist (in-silico, in-vitro and in-vivo) to investigate impact dynamics during a fall and a number of potential factors that influence these dynamics have been identified.

2.1.18 In-silico, In-vitro and In-vivo Approaches

Studying the dynamics of real life falls is a challenging task for a number of reasons. First, the environment in which the falls occur (such as a long-term care (LTC) facility) is large and is not optimal for the collection of kinematic or kinetic information. Successfully-captured real-life falls are typically limited to two-dimensional, low-quality surveillance video with low sampling rates, limiting the information that can be extracted from this data (Robinovitch et al., 2013a). There are also ethical concerns by LTC residents, family members, visitors and staff regarding privacy and compliance with instrumentation or intervention use (Chan, Estève, Fourniols, Escriba, & Campo, 2012). While improvements in wearable sensors represents a potential future direction for analysis of dynamics of actual falls, impact dynamics are currently studied experimentally through a combination of in-silico, in-vitro and in-vivo approaches. These approaches will briefly be reviewed here and a framework for a combined approach will be introduced.

In-silico approaches (computational modelling) can be utilized to study impact dynamics at multiple points during the fall process. Falling dynamics models have been utilized to demonstrate the effect of parameters such as height and mass on impact velocity and impact energy (Lo and Ashton-Miller, 2008). FE models have been utilized to demonstrate the effect of various external loading conditions (Keyak et al., 2001, 2013) and body composition metrics (Majumder, Roychowdhury, & Pal, 2008, 2013) on tissue level stresses/strains or failure loads. Utilizing a multi-level model Nasiri and Luo (2016) investigated the relationships between body parameters and hip fracture risk. This approach allows for the investigation individual fall impact dynamics and tissue level loading but the conclusions that can be drawn are subject to the validity of the models and accuracy of the input parameters (simple predicted loading conditions). Despite recent advances in modelling efforts, a greater understanding of impact events are required to improve the accuracy of model inputs (and subsequent outputs).

Due the high energy and catastrophic injuries that can result from falls, it is not possible to simulate fall related impacts from standing height in living older adults. One approach is to utilize cadaveric tissues in in-vitro testing. Isolated femur testing has been used to validate FE models (Enns-bray et al., 2018) as well as investigate the influence of aBMD and loading condition on failure loads (Keyak et al., 2001). While these tests provide valuable insight into mechanical failure and are not subject to the same pit-falls as computational approaches (Section 2.4.2), the ability of these simulations to represent realistic fall conditions is questionable. Mechanical testing may not simulate realistic impact characteristics or loading rates (Enns-bray et al., 2018) and are subject to a high dependency on boundary conditions (Choi, Cripton, & Robinovitch, 2014). These tests can often result in non-physiological fracture patterns suggesting the testing methods may not accurately simulate loading in-vivo (Levine, 2017). Cadaveric testing is also limited in its ability to account for active-responses such as muscle tension and the tissue properties may vary due to post-mortem treatment (Goh, Ang, & Bose, 1989).

The final approach to impact dynamic investigations are low-energy simulated falls, which utilize healthy young adults. The most common fall simulation is the pelvis release experiment introduced by Robinovitch et al. (1991) but a number of simulation methods exist such as the squat and pelvis release (Levine, 2017) (Figure 2.11). These approaches have been utilized to test the efficacy of protective devices (Laing & Robinovitch, 2008), characterize mechanical properties of the pelvis system (Laing & Robinovitch, 2010), and investigate the effect of body composition (Levine, Bhan, & Laing, 2013; Pretty, Martel, & Laing, 2017), muscle activation (Martel, Levine, Pretty, & Laing, 2017; Pretty, Martel, & Laing, 2017), and impact orientation (Choi et al., 2010) on skin surface impact dynamics during falls. Low energy fall simulations can be utilized to provide valuable inputs to computational models such as stiffness and dampening parameters of the impacting pelvis. These studies may also be used to identify factors that are observed to influence impact dynamics (Chapter 3: impact force magnitude, orientation, and point of application; Chapter 4: pressure distribution over the hip) for inclusion in computational models (Chapter 5). The obvious limitation of this method is the applicability of low-energy falls in young adults to higher energy impacts in older adults due to the non-linearity of the mechanical responses of biological tissues and the differences in tissue properties with aging. These studies are also limited to skin-surface impact characteristics, limiting the conclusions that can be drawn regarding tissue loading and fracture risk.

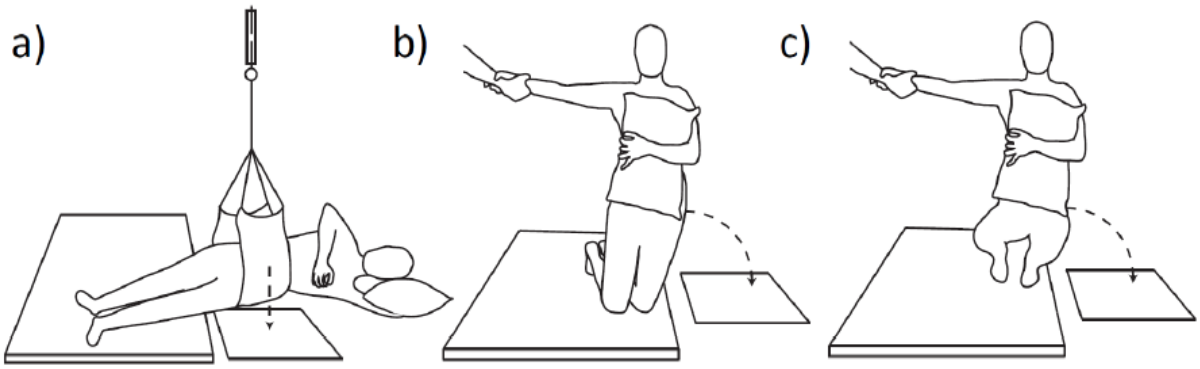

Figure 2.11: Low energy fall simulation paradigms include: a) pelvis release; b) kneeling release; and c) squat release. These paradigms vary in the trajectory of the pelvis and may be utilized to investigate different fall types (Levine, 2017).

While each method has advantages and disadvantages, a better understanding of impact dynamics will likely come from a combination and integration of these approaches. For instance, the identification of factors influencing impact dynamics during a fall could be identified through in-vitro fall simulation, tested in terms of tissue level loading and failure in in-vitro testing and subsequently included in in-silico computational models for fracture risk assessment. Under such a framework it would be important for fall simulation studies to publish data enabling the utilization of realistic loading conditions for both in-vitro testing and computational models. In this thesis a combination of in-vitro fall simulations (Chapters 3 and 4) and in-silico beam models (Chapter 5) will be utilized to assess the effect of fall simulation paradigm (a surrogate for impact configuration/ fall type), sex, and local body composition on femoral neck stresses and fracture risk. While a number of potential factors exist (Luo, 2016), these three were selected due to their epidemiological relationships with fracture risk.

2.1.19 Impact Configuration

Impact configuration has been identified as a key determinant of injury risk (Cummings & Nevitt, 1989), with characteristics such loading direction, distribution, and anatomical exposure to loading key to predicting how falling patterns influence injury mechanics. However, falls to the hip are more commonly simplified to a one-dimensional model in fall simulations and biomechanical models, where the vertical elements are the primary components of interest (Dufour et al., 2012; Robinovitch, Hayes, & McMahon, 1997; Sarvi & Luo, 2015). In a comparison of fall simulation paradigms, Levine

(2017) found that vertical and shear forces, pressure distributions and impact configuration varied significantly. These paradigms vary in the path and the orientation of the body during a fall (Levine, 2017). It is unclear however, how these skin surface impact characteristics, which vary across fall simulation paradigms (FSP), translate to femoral stresses and fracture risk. Such analysis requires tissue level computational models, in addition to detailed loading parameter inputs with respect to the femur. The net impact force magnitude, line of action and point of application may influence fracture risk (Keyak, Skinner, & Fleming, 2001), but it is currently unknown how fall simulation paradigms influence these variables.

Posterolateral falls appear to reduce the strength of the femur (Pinilla et al., 1995), increase femoral loading (Keyak et al., 2001), and skin surface impact force (Choi et al., 2010) independently. These individual effects likely combine to influence femoral loading and fracture risk across fall orientations. Among fall simulation paradigms, the squat release results in a posterolateral impact orientation and increased shear forces, suggesting this fall type may simulate a worst case scenario (Levine, 2017). A greater understanding of how various fall types (and orientations) influence femoral loading, utilizing experimentally derived loading conditions, may inform 'safe fall' training aimed to reduce the energy of a fall and high-risk impact orientations.

2.1.20 Sex

Compared to males, females have significantly higher rates of hip fracture (Bjørgul & Reikerås, 2007; Chevalley et al., 2007). Beyond fracture risk, sex-based differences have been identified in fracture location and prognosis. When males do suffer a fracture they experience excess mortality compared to females (Kannegaard, van der Mark, Eiken, & Abrahamsen, 2010) and are less likely to fracture the femoral neck (Pulkkinen et al., 2008; Pulkkinen et al., 2006). The observed differences could potentially be attributed to differences in fall rates/ circumstances, impact dynamics, and femoral strength; however, fracture screening literature has focused on the latter.

Femoral geometry and strength differ across sex and age (Keaveny et al., 2010; Nissen et al., 2005). Consistent with epidemiological findings, female cadaveric femurs have lower femoral strength during mechanical testing (Lochmüller, Groll, Kuhn, & Eckstein, 2002), and clinical metrics of femoral strength are lower among females in living populations (Nieves et al., 2005; Looker, Beck, & Orwoll, 2001). Compared to males, females lose an additional 16% of their femur strength over the life cycle and substantial declines in strength start a decade earlier than in males (Keaveny et al., 2010). Differential loss of bone in the superior-lateral cortex with advancing age has been shown to increase

superior-lateral femoral neck stresses through an inferior-medial centroid shift, and this effect is greater in females than males (Beck et al., 2006). Thus, literature examining sex-based differences in femur morphology (in isolation) suggest females are at a greater risk of fracture than males.

Studies assessing sex-based differences in fracture risk often neglect sex differences in impact dynamics, which may overestimate the increased risk observed in females (Cummings et al., 2006; Keyak et al., 2011). While several studies have found no differences in peak total impact force between males and females (Pretty et al., 2017, Levine et al., 2013), males have been found to exhibit more focal loading over the proximal femur (Pretty et al., 2017). Compared to males, females have significantly less lean tissue mass, increased fat mass, and a greater proportion of their fat mass located in the lower body (Ley, Lees, & Stevenson, 1992). More local to the proximal femur, females have significantly more soft tissue overlying the greater trochanter (TSTT) than males (Lafleur, 2016). The observed differences in impact dynamics suggest males experience greater loading during a fall than females. In addition to sex-based anthropometric differences, differences in falling strategy/conditions between males and females may influence impact dynamics. While no differences in fall rates have been observed across sex (Yang et al., 2018), the circumstances of falls in females (ex. tripping during gait) are associated with greater hip fracture risk (Yang, Feldman, & Robinovitch, 2018; Yang et al., 2018). It is currently unclear how the previously reported differences in fracture tolerance and impact dynamics (both greater in males) combine to influence femoral stresses and fracture risk.

2.1.21 Body Composition

Increased BMI is a protective factor against hip fracture in older adults, (Stolee, Poss, Cook, Byrne, & Hirdes, 2009) but its specific influence on impact dynamics during lateral falls is unclear. Body composition factors related to BMI might influence impact dynamics during falls on the hip through several mechanisms. Previous research has shown a positive correlation between BMI and soft tissue thickness over the greater trochanter (Maitland, Myers, Hipp, Hayes, & Greenspan, 1993). The additional soft tissue of high BMI individuals could serve to reduce total in-series stiffness of the trochanteric soft tissue/proximal femur/pelvis system and subsequently reduce the force transmitted to the greater trochanter (Laing & Robinovitch, 2008; Robinovitch et al., 1995). However, BMI is directly related to the kinetic energy of an impact as mass is an input parameter for both (BMI = body mass/body height^2). Therefore, the increased mass associated with higher BMI individuals could serve to increase impact force. These conflicting mechanisms may in part explain some inconsistencies in the literature—while some studies have found no effect of BMI on peak force (Choi et al., 2010), others have found an

increase in peak force for high BMI individuals (noting that this relationship reverses when force is normalized to effective mass of the pelvic region) (Levine, Bhan, & Laing, 2013). The distribution of force also seems to be influenced by body composition, with low BMI individuals exhibiting more localized loading over the greater trochanter compared to high BMI individuals (Pretty et al., 2017). While these studies provide insight into a potential mechanism explaining the increased risk of hip fracture among low BMI individuals, additional computational analyses including tissue specific models are required to predict how these changes in skin-surface loading may influence femoral loading.

The majority of tissue-level models do not account for the effect of body composition on impact dynamics or utilize simple empirical equations to account for the effect of soft tissue. Majumder et al. (2007) developed a 3D FE model of pelvis–femur complex having 14-mm-thick trochanteric soft tissue to more accurately simulate the interplay between tissues during a fall. Majumder et al. (2008) subsequently varied the soft tissue thickness in this model and evaluated its effect on impact force and tissue strains. It was found that under constant impact energy, for 81% decrease in soft tissue thickness (26–5mm), impact force and peak strain increased by 38% and 97%, respectively. While this model demonstrates the effect of soft tissue on femoral strains, the loading conditions were simplified compared to real-life falls and the effect of varying body composition on bone health were not accounted for. Different studies have shown a protective role of obesity against osteoporosis but recent evidence suggests that obesity, and thus fat mass, may prove to be risk factors for decreased bone density and fractures (Palermo, Tuccinardi, Defeudis, Watanabe, & Manfrini, 2016). Therefore, a particpant-specific model of an impact event, utilizing data from simulated falls, may address these limitations and provide a more comprehensive understanding of the effect of body composition on femoral loading.

2.1.22 Literature Review Summary and Thesis Objectives

2.1.23 Identification of Literature Gaps to be Addressed

Statistical methods of fracture prediction are clinically prevalent but have limitations in individual fracture risk assessment, primarily due to the variable nature of the clinical risk factors and specificity from which these relationships were generated. Biomechanical models integrating patient specific structural models and loading conditions can offer a more accurate, ‘exact’ method of fracture risk assessment. These models range in complexity from simple static beam models to dynamic non-linear FE models, with a general tradeoff between accurate representation of the femur (FE) and clinical applicability (beam models). These models have common limitations including determination of mechanical properties from radiographic images and the application of loading conditions representative

of real life falls. The dramatic effect of loading conditions on bone strength and model predictions has been demonstrated (Section 2.4.1) and may in part explain the discrepancy between model performance in experimental studies (good prediction of bone failure under known loading conditions) and clinical studies (mild improvement in fracture risk assessment compared to BMD alone). There is very little data available in the literature on real-life fall dynamics that can be utilized as loading conditions for these models. Simulated fall studies may provide an approach to provide more realistic loading conditions for these models but the data reported in these studies are often insufficient to describe the anatomical point of application, magnitude, distribution, and line of action relative to the femur of the impact force.

- *Literature Gap #1: Lack of detailed loading conditions during real falls (or simulated falls as a surrogate) for application in biomechanical models*

It is also unknown how the variation between loading conditions of different fall types, sex, and individual body compositions may influence tissue level loading and fracture risk.

- *Literature Gap #2: The effect of loading condition variation between fall types, sex, and individual body compositions on femoral neck stresses and fracture risk is unknown*

Simulated fall studies have been utilized to investigate the effect of various factors (ex. Muscle activation, body composition, floor type, etc.) on impact dynamics but the measures are limited to the skin-impact surface interface. These studies therefore cannot be used to draw conclusions on tissue level loading (particularly relevant for fracture risk).

- *Literature Gap #3: The effect of various factors on tissue level loading during a fall are not investigated during simulated fall studies due to their restriction to skin surface impact characteristics*

2.1.24 Thesis Objectives

The overall object of this thesis is to increase our understanding of the effect of fall type, sex, and local body composition on loading conditions during a fall and how these loading conditions influence femoral neck stresses and fracture risk.

The first literature gap will be addressed in Chapters 3 and 4. Utilizing previously collected fall simulation data, relevant loading conditions for application to tissue level biomechanical models will be extracted across three fall simulation types in males and females encompassing a variety of body compositions. In Chapter 5 this data will be applied in participant-specific beam models to evaluate the

effect of these loading conditions on femoral neck stresses and fracture risk (Literature Gap #2). The framework utilized in this thesis will allow for the application of experimental fall simulation data in tissue level models, enabling translation from skin surface metrics to more relevant tissue stresses and fracture risk (Literature Gap #3).

Chapter 3

The Influence of Fall Simulation Paradigm, Sex, and Trochanteric Soft Tissue Thickness on Femoral Loading Conditions during Lateral Falls on the Hip

3.1.1 Introduction

Hip fractures are a prevalent and severe health concern in older adults (Cummings & Melton, 2002), with sideways falls onto the hip being implicated in the majority of cases (Hayes et al., 1993). From a mechanistic perspective, the simplest measure of hip fracture risk during a fall is the ratio between the fall induced impact force and proximal femur tolerance (maximum force prior to failure), commonly referred to as Factor of Risk (FoR). Theoretically, if this ratio exceeds one, a fracture is likely to occur (Dufour et al., 2012; Hayes et al., 1996). Implicit in this definition, is that these vectors are acting in the same direction (i.e. the fracture tolerance must be defined in the same direction as the impact force). Fracture tolerance has previously been found to be sensitive to loading direction across a range of feasible values during a fall (Keyak et al., 2001), with differences in ultimate load of up to 24%, equivalent to 25 years of bone loss after the age of 65 (Pinilla et al., 1996). While the importance of loading direction on fracture tolerance (FoR denominator) has been established, limited information is available on the loading conditions during real falls (FoR numerator). Insights into fall induced loading conditions could serve to inform the development of protective equipment and 'safe-fall' strategies, as well as increase the accuracy of biomechanical screening tools (ex. FoR) through reductions in directional sensitivity error.

Impact configuration has been identified as a key determinant of injury risk (Cummings & Nevitt, 1989), with characteristics such loading direction and anatomical exposure key to predicting how falling patterns influence injury mechanics. Falcinelli et al. (2014) performed a case-control study using finite element models (FEM) simulating a variety of fall impact orientations. The occurrence of minimum FEM-strength (angle at which hip fracture was most likely) was widespread across loading conditions for individuals, with a general trend toward decreasing strength with increased internal rotation. Interestingly, the minimum strength across fall loading conditions was the strongest predictor of fracture, supporting the value of considering multiple loading conditions during clinical screening. In biomechanical models however, lateral falls onto the hip are commonly simplified and represented as point loads applied over the greater trochanter (GT), directed perpendicular to the femoral shaft. (Dufour et al., 2012; Robinovitch, Hayes, & McMahon, 1997; Sarvi & Luo, 2015). While video recordings in long-term care settings (Robinovitch et al., 2013b) are a promising strategy to gain insights into the conditions of real falls, experimental fall simulations enable collection of detailed kinematics and kinetics. In an evaluation of fall techniques in judokas, van der Zijden and colleagues (2012) found that the anatomical point of force application was consistently posterior and distal to the GT and the net impact vector was directed distally and anteriorly. While this study highlights the discrepancy between

simulated and experimental loading conditions, it remains unclear how these loading conditions may differ across additional fall patterns and individual characteristics. Beyond impact force magnitude, differences in these loading conditions could mechanistically influence fracture risk, which is currently not addressed in the literature.

In order to encompass some of the variability observed in fall patterns (Choi, Wakeling, & Robinovitch, 2015; Kangas et al., 2012; Robinovitch et al., 2013b), multiple fall simulation paradigms (FSP) are utilized in the literature. These paradigms vary in the path and the orientation of the body during a fall. The pelvis release paradigm is highly controlled and represents a scenario where the faller rotates into a horizontal position before impacting the hip directly laterally. In this paradigm, the fall is simplified into a one-dimensional motion, focusing on the vertical component. Kneeling and squat release paradigms incorporate a lateral motion component, which is more representative of falls observed in older adults (Choi et al., 2015; Kangas et al., 2012; Robinovitch et al., 2013b). Kneeling release reflects a scenario where the faller impacts the knee prior to rotating to impact the hip laterally, like a pendulum. Squat release reflects a scenario where the faller flexes the knee, hip and ankle during the descent phase prior to rotating laterally to impact the hip. In a comparison of these paradigms, Levine (2017) found that vertical and shear forces, pressure distributions and impact configuration varied significantly. It is unclear however, which paradigm represents a 'worst case' fall (i.e. how these skin surface impact characteristics translate to femoral stresses and fracture risk). Such analysis requires tissue level computational models, in addition to detailed loading parameter inputs with respect to the femur. The net impact force magnitude, line of action and point of application may influence fracture risk (Keyak, Skinner, & Fleming, 2001), but it is currently unknown how fall simulation paradigms influence these variables.

Due to significantly higher rates of hip fracture (Bjørgul & Reikerås, 2007; Chevalley et al., 2007), females have been the focus of studies investigating impact dynamics during falls. However, when males do suffer a fracture they experience excess mortality compared to females (Kannegaard et al., 2010). Fracture site has been found to vary between sexes, with females more likely to suffer cervical fractures than males (Pulkkinen et al., 2008; Pulkkinen et al., 2006). While sex related differences in bone strength have been well researched (Looker, Beck, & Orwoll, 2001), differences in impact dynamics during a fall may provide additional insight into epidemiological findings. While several studies have found no differences in peak total impact force between males and females (Pretty et al., 2017, Levine et al., 2013), males have been found to exhibit more focal loading over the GT (Pretty et al., 2017). Compared to males, females have significantly less lean tissue mass, increased fat mass, and

a greater proportion of their fat mass located in the lower body (Ley et al., 1992). More local to the proximal femur, females have significantly more soft tissue overlying the greater trochanter (TSTT) than males (Lafleur, 2016). In addition to sex-based anthropometric differences, differences in falling strategy/conditions between males and females may influence impact dynamics (Yang et al., 2018). It is currently unclear how these sex-based differences may influence 3-dimensional loading parameters at the proximal femur during a fall.

Increased thickness of trochanteric soft tissues (TSTT) has been linked to lower epidemiological risk of fracture (Johansson et al., 2014), primarily attributed to energy absorption during an impact (Etheridge et al., 2005). While increased TSTT could serve to reduce the total in-series stiffness of the of the hip, increases in TSTT are associated with increases in body mass (Maitland, 1993), and thus impact energy during a fall (Bhan, Levine, & Laing, 2014). The mechanistic pathway through which TSTT reduces fracture risk may be more complex than simple one-dimensional compression and reduction of vertical impact force. Pretty et al. (2017) found high-BMI individuals exhibited a redistribution of force radially away from the GT compared to low-BMI individuals. Utilizing fall simulation paradigms incorporating lateral motions, Levine (2017) did not find significant reductions of peak vertical force but did observe significant decreases in net and shear impact force with increasing TSTT. It is unclear how the redistribution of loads and reduction of shear forces previously attributed to TSTT may influence 3-dimensional loading parameters at the proximal femur during a fall.

To address these gaps in the literature, the purpose of this study was to evaluate the influence of FSP, sex, and TSTT on femoral loading conditions during lateral falls on the hip. Our first hypothesis was that pelvis release would be associated with: a) lower net impact force and b) a more localized point of force application (with respect to GT) than kneeling and squat release. Additionally, it was hypothesized that c) direction of loading would be significantly different across all FSP. Our second hypothesis was that no differences in a) net impact force or b) direction of loading would be observed across sex; however, it was hypothesized that c) females would exhibit a more distal point of force application compared to males. Similarly, our third hypothesis was that no differences in a) net impact force or b) direction of loading would be observed across TSTT groups; however, it was hypothesized that c) increasing TSTT would be associated with a more distal point of force application.

3.1.2 Materials and Methods

3.1.3 Participants

Forty-one healthy young-adults (<35 years old) consented to participate in this study, covering a wide range of body compositions (Table 3.1). Exclusion criteria included any history of pelvis, femur or spine fractures, history of easily invoked bruising, or any other health conditions that may have been aggravated by the experimental protocol. Transverse-plane TSTT was measured via ultrasound (C60x, 2-5 MHz transducer, M-Turbo Ultrasound, SonoSite, Inc., Bothell, WA) in a side-lying position, similar to that expected during the impact phase of the fall simulations. Participants were grouped into low-, mid- and high-STT groups based the following criteria: males low <3 cm, mid 3.1-4 cm, high >4.1 cm; females low <3.5, mid 3.6-5, high >5 cm (Levine, 2017). All participants provided written informed consent. This study was approved by the Office of Research Ethics at the University of Waterloo.

Table 3.1: Mean (SD) participant anthropometric characteristics.

Sex	STT	N	Height (m)	Mass (kg)	BMI (kg/m^2)	TSTT (cm)
Females						
	Low	7	1.62 (0.04)	54.0 (6.1)	20.4 (1.7)	3.0 (0.4)
	Mid	8	1.67 (0.06)	68.3 (10.0)	24.5 (2.7)	4.3 (0.3)
	High	7	1.65 (0.07)	81.2 (25.0)	29.7 (9.2)	6.6 (1.7)
Males						
	Low	7	1.80 (0.07)	73.0 (12.4)	22.4 (2.5)	2.4 (0.4)
	Mid	6	1.81 (0.05)	83.3 (5.9)	25.5 (2.3)	3.5 (0.3)
	High	6	1.79 (0.07)	92.1 (8.4)	28.8 (1.9)	4.9 (1.1)

3.1.4 Instrumentation

A three-dimensional motion capture system (Optotrak Certus, NDI, Waterloo, ON, Canada) and a force platform (OR6-7, Advanced Mechanical Technology Incorporated, Watertown, MA, USA) were utilized to acquire lower body kinematics (300 Hz) and impact kinetics (3500 Hz) respectively. Rigid body clusters placed on the sacrum and impacting (left) thigh were utilized to track the position of the GT, as well as lateral and medial epicondyles of the impacting femur

3.1.5 Experimental Protocol

Each participant completed six blocks of trials, each consisting of one pelvis, kneeling, and squat release, in randomized order (Figure 3.1). These paradigms were selected to represent different fall scenarios observed in older adults (Choi et al., 2015; Kangas et al., 2012; Robinovitch et al., 2013b), with good experimental repeatability (Levine, 2017). In all trials, participants impacted their left hip on the force platform.

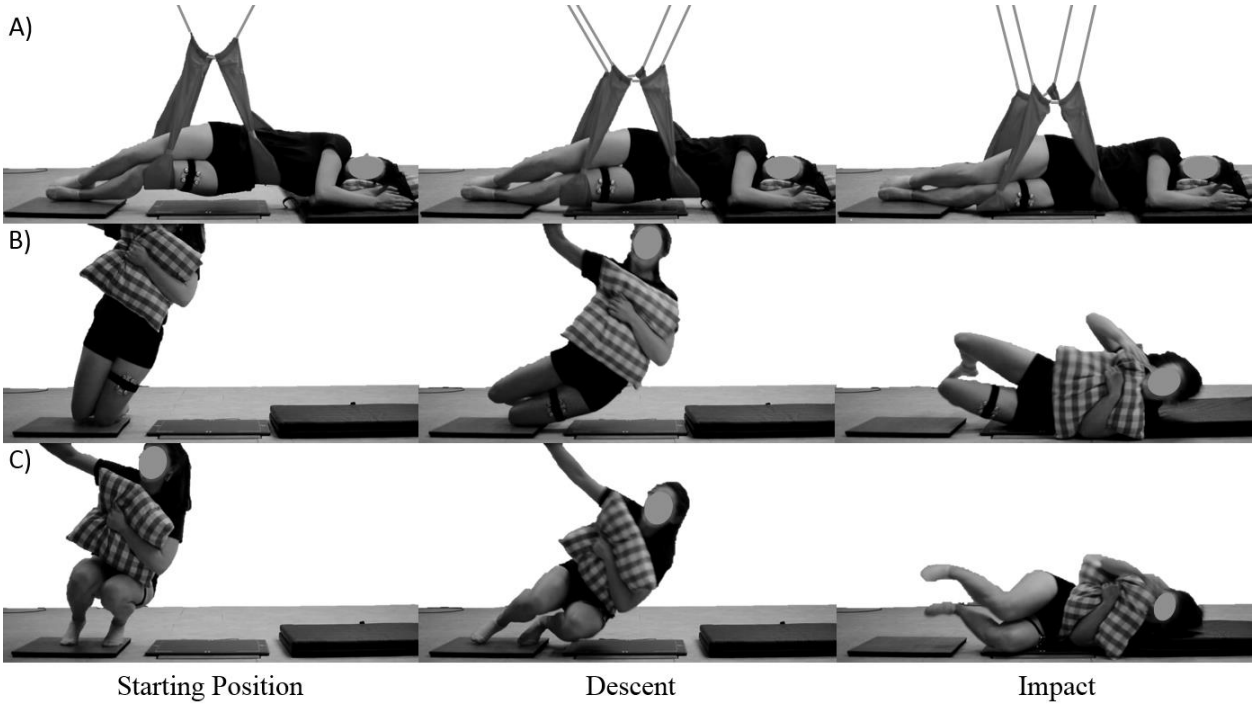

Figure 3.1: Phases of a) pelvis, b) kneeling, and c) squat release fall simulations.

During pelvis release, the participant's pelvis was raised in a thin nylon sling until the soft tissues overlying the hip were 5 cm above the force plate. The participant's hips and knees were initially flexed to 45 and 90° respectively. The participant was instructed to relax in the sling and at a random time interval the electromagnet supporting the sling was released, allowing the lateral hip of the participant to impact the force plate. For kneeling and squat release, the participant was supported by the researcher and instructed to lean until their weight was supported by their left lower limb. Participants self-released and grasped a pillow (to prevent upper arm bracing during impact), allowing their lateral hip to impact the force plate. During kneeling release, participants adopted an initial position with their hips flexed to 0° and their knees flexed to 90° (the lower leg was in contact with the starting mat). During squat release,

participants adopted an initial heel-lifted squat, with maximal thigh-calf contact and an upright torso. Following each fall simulation, a minimum of one minute of rest was provided.

3.1.6 Data Analysis

All data processing was performed using customized software routines (MATLAB version 7.10, Mathworks, Natick, MA, USA). To conserve magnitude, peak net force (F_{max}) was determined from un-filtered kinetic data (both vertical and shear components). All dependent variables were extracted at the time of F_{max}. Time-varying kinetic and kinematic data were down sampled to 300 Hz and filtered with a fourth-order dual pass 100 Hz Butterworth filter. This filter was selected based on the observed mean power frequency during simulated falls on the hip (Levine et al., 2013). Utilizing kinematic data of the impacting thigh, a femur coordinate system was defined (Figure 3.2). The long axis of the femur (Y) was defined by a line connecting the GT (origin) to the lateral epicondyle. The X axis of the femur was defined by a line perpendicular to Y, lying in the plane defined by the GT, lateral, and medial epicondyles. The Z axis of the femur was defined by a line perpendicular to the Y and X axes, pointing anteriorly. To account for anteversion of the femur (Cibulka, 2004), a 15-degree rotation about Y was applied to align X with the femoral neck axis.

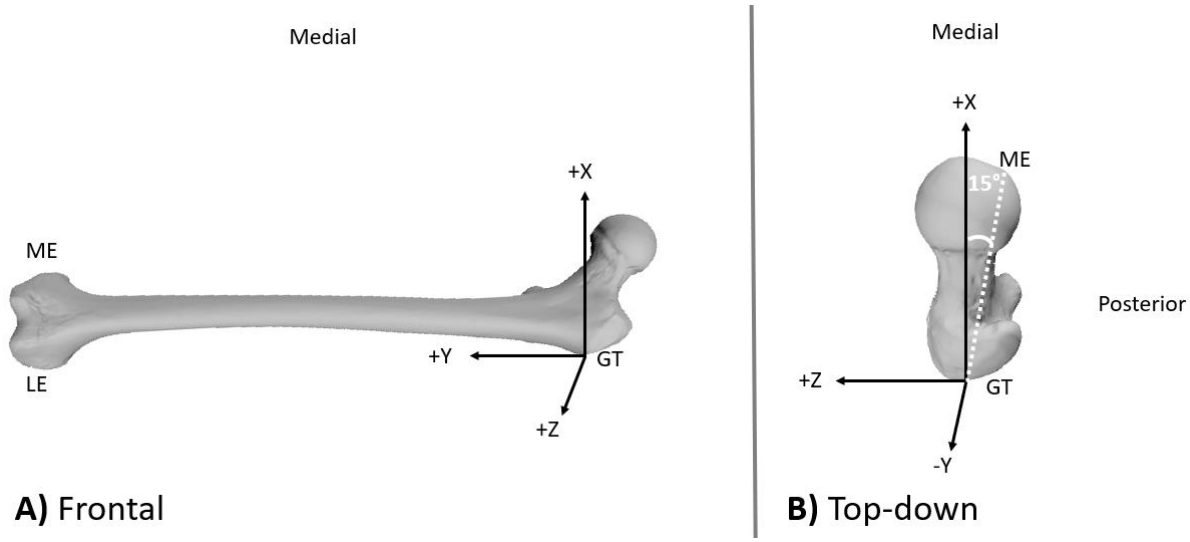

Figure 3.2: Femur co-ordinate system in the a) frontal and b) top-down view

Center of pressure (CoP) at F_{max} was calculated from kinetic data and expressed in the femur coordinate system. To assess the anatomical point of force application, the total distance between the

CoP and GT (*Dist*), as well as position of the CoP in the proximal-distal (CoP_{PD}) and anterior-posterior directions (CoP_{AP}) were calculated. F_{max} was subsequently decomposed and expressed in the femur coordinate system. The proportion of F_{max} directed through the femur Y (F_{Distal}), X (F_{Medial}), and Z ($F_{Anterior}$) axes were calculated to assess the orientation of the peak impact vector. To evaluate 'worst-case' scenarios, dependent variables for each paradigm were calculated as the average across the three trials with greatest F_{max}.

3.1.7 Statistical Analysis

Separate three-way mixed model analysis of variance (ANOVA) tests were performed to assess the influence of sex and TSTT-group (between subjects), as well as FSP (repeated measure), on F_{max}, F_{Distal}, F_{Medial}, $F_{Anterior}$, *Dist*, CoP_{PD}, and CoP_{AP}. Pairwise comparisons were performed when significant main effects of FSP or TSTT-group were observed. Tukey's post hoc tests were performed when significant interaction effects were observed. All statistical analysis was performed with a software package (SPSS version 21, Chicago, USA) using an α level of 0.05.

3.1.8 Results

3.1.9 Impact Force Magnitude

F_{max} was influenced by a significant FSP-sex interaction ($F_{2,70}$ = 8.5, p = 0.001); however, significant main effects of FSP were observed in both males ($F_{2,32}$ = 41.4, p < 0.001) and females ($F_{2,38}$ = 28.0, p < 0.001) (Figure 3.3). Pelvis release consistently elicited the lowest F_{max} (mean (SD) = 1540.9 (332.7) N) on average 58.7% lower than kneeling release (p < 0.001) and 50.5% lower than squat release (p < 0.001). F_{max} was not significantly different between kneeling and squat release (p = 0.111). The FSP-sex interaction was characterized by larger differences between paradigms in males than females. In males, F_{max} was on average 74.3% and 64.3% lower in pelvis release (mean (SD) = 1667.6 (228.1) N) compared to kneeling release (p < 0.001) and squat release (p < 0.001) respectively. In females, F_{max} was on average 47.5% and 36.7% lower in pelvis release (mean (SD) = 1431.5 (373.0) N) compared to kneeling (p < 0.001) and squat release (p < 0.001), respectively.

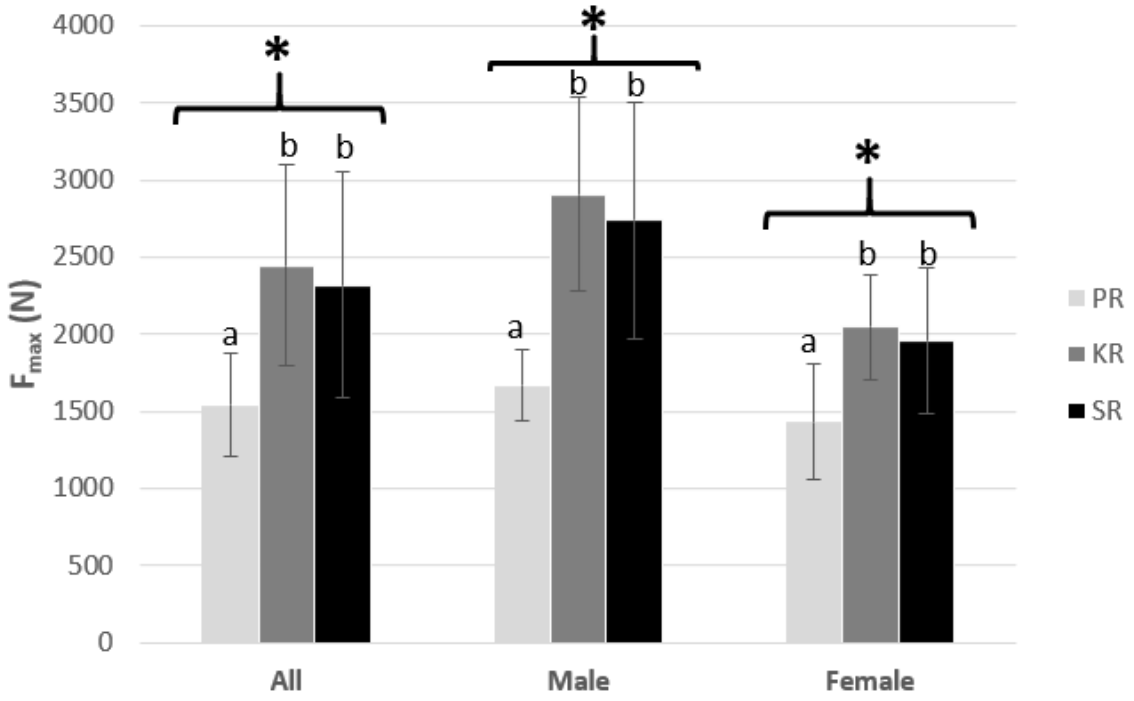

Figure 3.3: Influence of FSP (PR: pelvis; KR: kneeling; and SR: squat release) on F_{max}. A significant FSP-sex interaction was observed but main effects of FSP were observed in both males and females (* indicates significant ANOVA main effects; letters refer to significant differences between groups based on Tukey's post hoc tests at $\alpha = 0.05$).

A significant main effect of sex on F_{max} was observed overall ($F_{1,35} = 30.8$, $p < 0.001$), as well as in each FSP. On average, F_{max} was 34.5% lower in females (mean (SD) = 1812.63 (478.7) N) than males, ranging from 16.5% lower in pelvis release ($F_{1,35} = 6.3$, $p = 0.017$) to 41.8% lower in kneeling release ($F_{1,35} = 31.8$, $p < 0.001$). However, when normalized to participant body weight (BW) F_{max} was not significantly different between males (mean (SD) = 3.02 (0.86) BW) and females (mean (SD) = 2.80 (0.72) BW) ($F_{1,35} = 3.8$, $p = 0.059$) (Figure 3.4).

A significant main effect of TSTT-group on F_{max} was observed ($F_{2,35} = 4.3$, $p = 0.022$) (Figure 3.4). Post-hoc analysis revealed that F_{max} was 19.5% lower in the low-TSTT group (mean (SD) = 1904.9 (666.1) N) compared to the high-TSTT group (mean (SD) = 2276.5 (807.6) N) ($p = 0.007$). F_{max} in the mid-TSTT group (mean (SD) = 2138.0 (639.6) N) was not statistically different than the low-TSTT ($p = 0.057$) or high-TSTT groups ($p = 0.370$). When normalized to participant BW, this trend reverses ($F_{2,35}$

= 3.9, p = 0.049) such that F_{max} was 13.1% higher in the low-TSTT (mean (SD) = 3.06 (0.80) BW) compared to high-TSTT group (mean (SD) = 2.70 (0.79) BW) (p = 0.023).

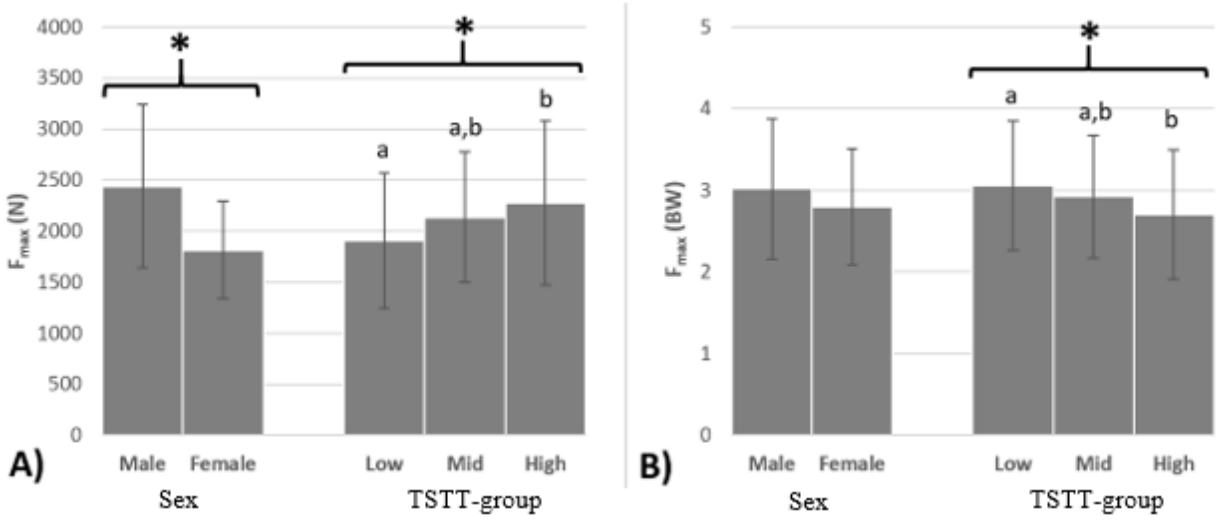

Figure 3.4: Influence of sex and TSTT-group on a) F_{max} and b) F_{max} normalized to BW (* indicates significant ANOVA main effects; letters refer to significant differences between groups based on Tukey's post hoc tests at α = 0.05).

3.1.10 Loading Vector Orientation

Significant main effects of FSP were observed on F_{Distal} ($F_{2,70}$ = 861.7, p < 0.001) and F_{Medial} ($F_{2,70}$ = 637.6, p < 0.001) (Figures 3.5a and 3.7). In this plane, the average loading vectors for all three releases were directed medially and distally towards the knee. With respect to the femoral shaft, kneeling release was associated with the most perpendicular loading vector, while squat release elicited the most distally directed vector (mean (SD) F_{Medial} = 0.901 (0.071), 0.538 (0.137), 0.0866 (0.085); and F_{Distal} = 0.0719 (0.069), 0.388 (0.145), 0.866 (0.110) for kneeling, pelvis, and squat release respectively; all p < 0.001). No differences in F_{Medial} or F_{Distal} were observed across sex or TSTT-group (p > 0.111).

$F_{Anterior}$ was influenced by a significant FSP-sex interaction ($F_{2,70}$ = 5.4, p = 0.007; Figure 3.5a and b); however, significant main effects of FSP were observed in both males ($F_{2,32}$ = 57.9, p < 0.001) and females ($F_{2,38}$ = 61.4, p < 0.001). In both males and females, pelvis release was associated with a posteriorly directed loading vector (mean (SD) $F_{Anterior}$ = -0.076 (0.046)) and was significantly different from the anteriorly directed kneeling ($F_{Anterior}$ = 0.024 (0.032)) and squat release ($F_{Anterior}$ = 0.049 (0.056))

(all p < 0.001) (Figure 3.5). In females, $F_{Anterior}$ during squat release ($F_{Anterior}$ = 0.066 (0.068)) was more anteriorly directed than kneeling release ($F_{Anterior}$ = 0.028 (0.040)) (p = 0.040); however, no differences between these paradigms on $F_{Anterior}$ were observed in males ($F_{Anterior}$ = 0.029 (0.025) vs. 0.019 (0.002) for squat and kneeling release respectively; p = 0.113). No differences in $F_{Anterior}$ were observed across TSTT groups ($F_{2,35}$ = 0.1, p = 0.910).

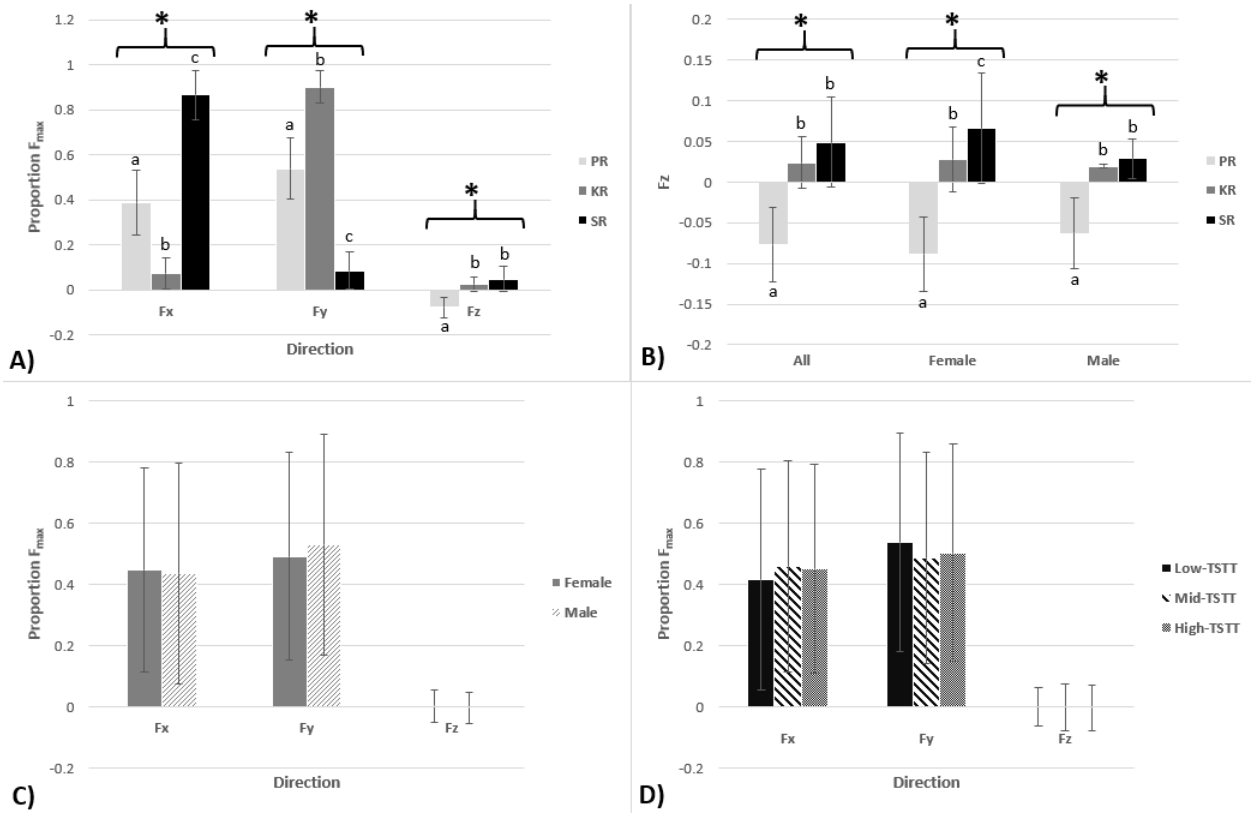

Figure 3.5: Influence of a) FSP (PR: pelvis; KR: kneeling; and SR: squat release), c) sex, and d) TSTT on proportion of force in the Fx (medial), Fy (distal), and Fz (anterior) directions. $F_{Anterior}$ was influenced by a FSP-sex interaction (b) (* indicates significant ANOVA main effects; letters refer to significant differences between groups based on Tukey's post hoc tests at α = 0.05).

3.1.11 Anatomical Point of Application

Significant main effects of FSP were observed on *Dist* ($F_{2,70}$ = 3.2, p = 0.045), CoP_{PD} ($F_{2,70}$ = 4.1, p = 0.022) and CoP_{AP} ($F_{2,70}$ = 5.4, p = 0.011) (Figure 3.6a). CoP in squat release was applied on average 29.5% further from the GT compared to pelvis release (mean (SD) *Dist* = 2.8 (1.7) vs. 2.1 (1.8)

cm, respectively) (p = 0.021); however, kneeling release (*Dist* = 2.5 (1.3) cm) was not statistically different from the other two paradigms (both $p > 0.165$). In all paradigms, the mean location of CoP was posterior and distal relative to the GT. CoP location during pelvis release (CoP_{PD} = 0.9 (1.7) cm; CoP_{AP} = -0.1 (1.3) cm) was more proximal and anterior than kneeling (CoP_{PD} = 1.7 (1.9) cm; CoP_{AP} = -1.1 (2.4) cm) and squat release (CoP_{PD} = 1.5 (1.5) cm; CoP_{AP} = -1.1 (1.6) cm) (all $p < 0.034$). CoP mean location ($CoP_{PD,}$ CoP_{AP}) was not significantly different between kneeling and squat release (all $p > 0.464$).

Significant main effects of sex were observed on *Dist* ($F_{1,35}$ = 13.1, $p < 0.001$) and CoP_{PD} ($F_{1,35}$ = 12.8, p = 0.001) (Figure 3.6b). On average, the point of application was 55.3% further from the GT in females (mean (SD) *Dist* = 3.0 (1.8) cm) compared to males (*Dist* = 1.9 (1.1) cm). Mean CoP location in females (CoP_{PD} = 1.9 (2.1) cm; CoP_{AP} = -0.7 (1.8) cm) was more distal than in males (CoP_{PD} = 0.7 (0.9) cm; CoP_{AP} = -0.8 (2.0) cm); however, no differences were observed across sex in the anterior-posterior direction ($F_{1,35} < 0.0$, p = 0.904).

Significant main effects of TSTT-group were observed on *Dist* ($F_{2,35}$ = 10.4, $p < 0.001$) and CoP_{PD} ($F_{2,35}$ = 5.2, p = 0.011) (Figure 3.6c). CoP was on average 79.6% and 59.8% further from the GT in high-TSTT (mean (SD) *Dist* = 3.5 (2.0) cm) compared to low-TSTT (*Dist* = 1.9 (1.2) cm) and mid-TSTT groups (*Dist* = 2.2 (1.2) cm) respectively (both $p < 0.002$). No statistical difference in *Dist* between low-TSTT and mid-TSTT groups were observed (p = 0504). The high-TSTT group mean CoP location (CoP_{PD} = 2.1 (2.3) cm; CoP_{AP} = -1.3 (2.8) cm) was more distal than low-TSTT (CoP_{PD} = 0.9 (1.0) cm; CoP_{AP} = -0.6 (1.2) cm) and mid-TSTT groups (CoP_{PD} = 1.1 (1.5) cm; CoP_{AP} = -0.4 (1.2) cm) (both $p <$ 0.004); however, no differences were observed across TSTT-group mean CoP location in the anterior-posterior direction ($F_{2,35}$ = 1.8, p = 0.182).

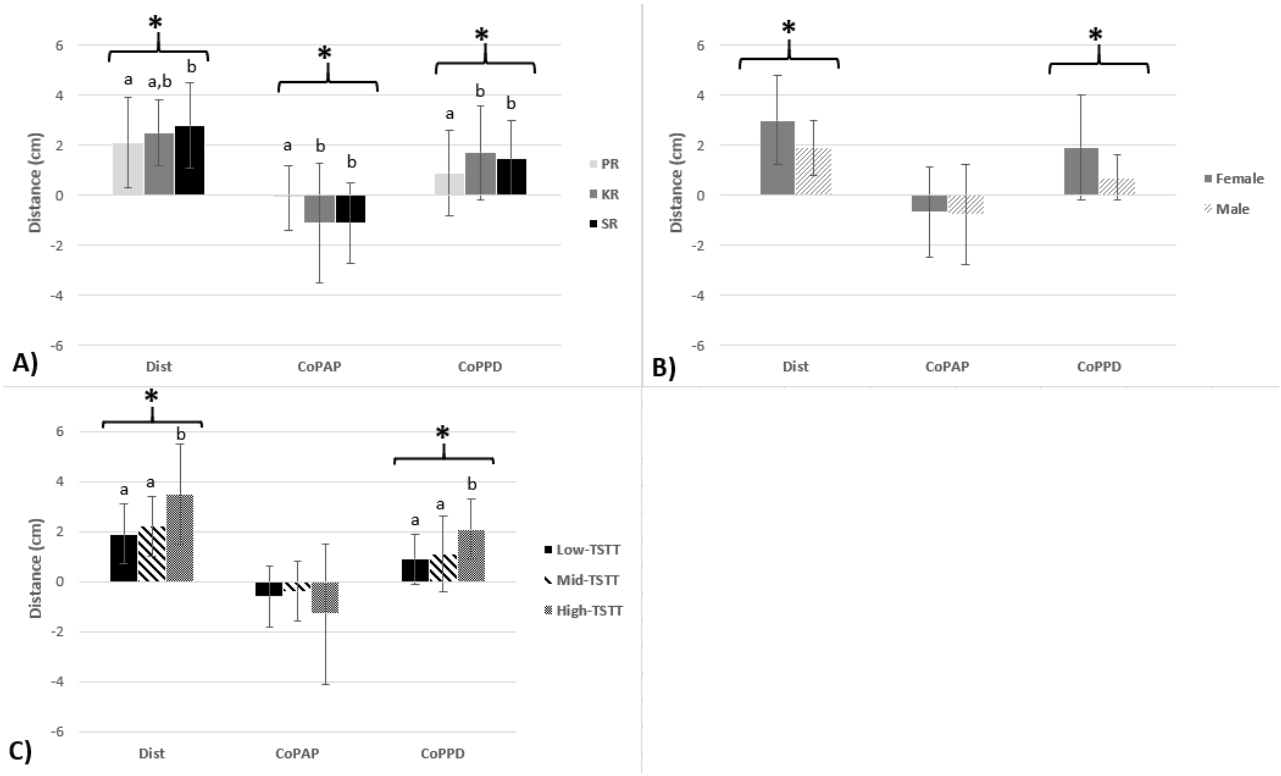

Figure 3.6: Influence of a) FSP (PR: pelvis; KR: kneeling; and SR: squat release), b) sex, and c) TSTT on *D*ist, as well as mean CoP_{AP} and CoP_{PD} (* indicates significant ANOVA main effects; letters refer to significant differences between groups based on Tukey's post hoc tests at $\alpha = 0.05$).

3.1.12 Discussion

The goal of this study was to evaluate the influence of FSP, sex, and TSTT on femoral loading conditions during lateral falls on the hip. In support of our first hypothesis pelvis release elicited the lowest F_{max} and was applied closest to the GT; however, *Dist* was not significantly different between pelvis and kneeling release. The loading vector orientation was significantly different in each FSP. In the A-P plane, pelvis release was directed posteriorly, while kneeling and squat release were directed anteriorly. In the neutral plane of the femur, the average loading vectors for all three releases were directed up-wards (medially) and distally towards the knee. With respect to the femoral shaft, kneeling release was associated with the most perpendicular loading vector, while squat release elicited the most distally directed vector. In contrast to our second hypothesis, females elicited lower F_{max} than males in all FSP. While no differences in loading vector orientation were observed across sex in the neutral plane of the femur, squat release was more anteriorly directed than kneeling release in females but not males. *Dist* was however, greater in females than males. In contrast to our third hypothesis, F_{max} was lower in

the low-TSTT compared to high-TSTT group. *Dist* was however, greater in the high-TSTT group compared to mid-TSTT and low TSST groups, and no differences in loading vector orientation were observed across TSTT groups. These data provide novel insights into factors influencing 3-D femoral loading conditions during falls and may serve as inputs into computational models examining tissue level loading and fracture risk.

Loading conditions were found to vary in terms of force magnitude, orientation, and point of application across FSP (Figure 3.7). The magnitude of differences in F_{max} across FSP, were dependent on sex. The increase in F_{max} in kneeling and squat release compared to pelvis release was greater in males than females. In squat and kneeling release, lateral impact velocity, as well as shear and vertical impact forces are increased compared to pelvis release; however, no differences in vertical impact velocity have been observed (Levine, 2017). The increase in vertical forces, independent of impact velocity, can be attributed to increases in effective mass, through increased inclination of the upper body during kneeling and squat release. Since males carry a greater proportion of their mass in their upper body (Ley et al., 1992), this increase in effective mass was likely greater in males than females, which in turn contributed to the observed sex-FSP interaction on F_{max}. In the neutral plane of the femur, the average loading vectors for all three releases were directed up-wards (medially) and distally towards the knee. With respect to the femoral shaft, kneeling release was associated with the most perpendicular loading vector, while squat release elicited the most distally directed vector. In the A-P plane, pelvis release was directed posteriorly, while kneeling and squat release were directed anteriorly. Combined, the observed differences in loading vector orientation will influence stress generation in the proximal femur; however, these relationships would be dependent on underlying femoral geometry (ex. contribution of force between axial and bending stresses in the femoral neck will depend on neck-shaft angle and degree of anteversion). In all paradigms, the mean location of CoP was posterior and distal relative to the GT. Pelvis release CoP location was more proximal and anterior (closer to GT) than kneeling and squat release. The greater *Dist* in kneeling and squat release could act to increase stress generation in the proximal femur through increases in internal bending moment arms. However, more distal CoP location may be indicative of shunting of impact energy away from the GT, which could reduce the amount of energy delivered to the proximal femur. Simulation of multiple FSP in clinical screening models could increase fracture prediction accuracy, as 'worst-case' loading conditions (eliciting minimum strength) have been found to vary across individuals, with minimum strength being the strongest predictor of fracture (Falcinelli et al., 2014).

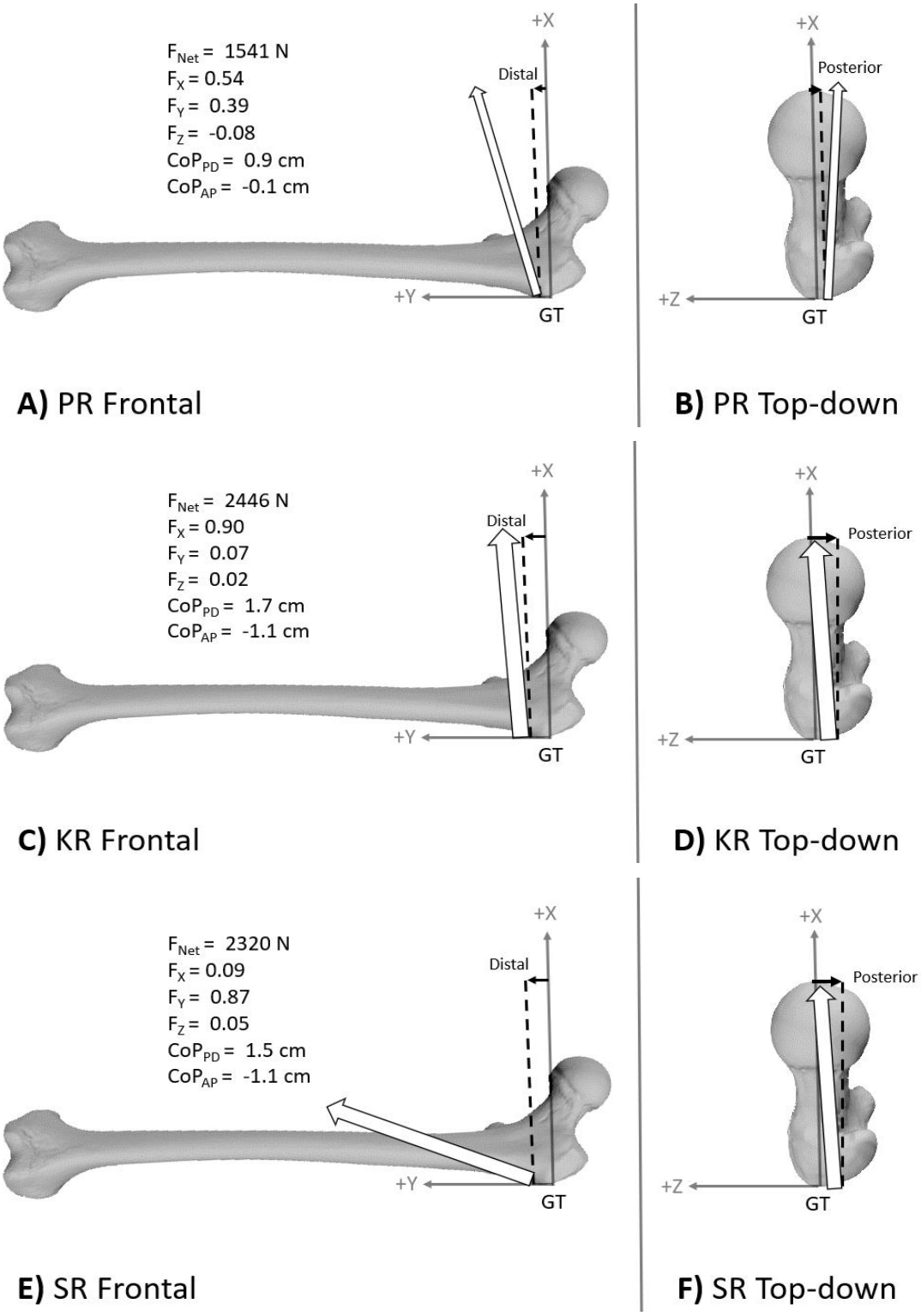

Figure 3.7: Comparison of mean impact characteristics during: a, b) pelvis (PR); c, d) kneeling (KR); and e, f) squat release (SR).

Sex-based differences in loading conditions were observed; however, they do not (in isolation) mechanistically support epidemiological findings. Compared to males, females elicited lower F_{max} and greater *Dist*. While local tissue composition differences (Ley et al., 1992) could act to reduce system stiffness in females, the observed differences in F_{max} appear to be driven by impact energy (when normalized to body mass, no differences in F_{max} were observed across sex; Figure 3.4). The more distal CoP location observed in females could theoretically increase bending stresses in the proximal femur (independent of force magnitude); however, when combined with previous reports that females exhibit more evenly distributed loads than males (Pretty et al., 2017), a more distal point of force application could reduce the amount of energy delivered to the proximal femur. Femoral geometry and strength differ across sex and age (Keaveny et al., 2010; Nissen et al., 2005) and will influence the translation of impact loading parameters to femoral stresses, as well as femoral strength and fracture risk. Tissue level models incorporating the present data, as well as anatomically aligned pressure distributions, are required to determine how the observed sex-based differences influence fracture risk.

The protective capacity of TSTT to reduce impact energy (Etheridge et al., 2005) is complicated by its association with body mass (Maitland, 1993). In contrast to epidemiological findings (Johansson et al., 2014), F_{max} was 19.5% lower in the low-TSTT compared to high-TSTT group. However, when normalized to body mass, this trend reverses such that F_{max} was 13.1% higher in the low-TSTT compared to high-TSTT group (Figure 3.4). While the current data suggest the associated increases in body mass outweigh the protective effects of TSTT with respect to impact energy, underlying differences in femur strength (associated with body mass and composition (Travison, Araujo, Esche, Beck, & Mckinlay, 2008) may support a net positive effect of TSTT on fracture risk. Beyond energy absorption, TSTT may additionally influence anatomical exposure during an impact (i.e. amount of energy transferred to the proximal femur; Chapter 4). Increased TSTT (through association with BMI) has previously been found to reduce localization of loads (more evenly distributed over a larger area) during pelvis release simulations (Pretty et al, 2017). Coupled with a more distal anatomical point of application observed in the current study, increased TSTT may shunt energy distally into the femoral shaft. However, a more distal anatomical point of application could also serve to increase stresses in the proximal femur through increases in internal bending moment arms. Additional analysis, including soft tissue and proximal femur models are required to gain a more comprehensive view of the role of TSTT on fracture risk.

There were several limitations associated with this study. First, as an essential safety precaution, only healthy young adults completed low-energy (yet clinically relevant) fall simulations. While the current results provide novel insight into loading conditions during these FSP, future work should aim

to characterize loading conditions during real falls in older adults from video recordings (Robinovitch et al., 2013b). Second, in this study soft tissues overlying the hip were characterized by thickness, neglecting material properties that influence energy absorption capacity. Stiffness of these tissues have been found to differ across age (Choi et al., 2015); however, future work is required to determine if these properties and by extension energy absorption capacity for a given TSTT, differ across sex and body composition. Third, we did not consider the role of underlying femoral geometry (Levine, Pretty, Nouri, Mourtzakis, & Laing, 2018) and its potential interaction with TSTT and FSP on impact dynamics. A femoral neck anteversion of 15-degrees was assumed in this study based on adult population means (Cibulka, 2004) and applicability to tissue level models (dual-energy X-ray absorptiometry scans of the hip are performed at 15-degrees internal rotation); however, anteversion is subject to individual variability, reduces over the life cycle, and is generally greater in females than males (Cibulka, 2004; Gulan, Matovinović, Nemec, Rubinić, & Ravlić-Gulan, 2000). Last, this study was limited to skin-surface impact dynamics, limiting the ability to draw conclusions about tissue level loading and fracture risk. Coupling of the current data with participant-specific proximal femur models would enable a comprehensive evaluation of the effect of FSP, sex, and TSTT on femoral stresses and fracture risk (Chapter 5).

In summary, this is the first study to evaluate the influence of FSP, sex, and TSTT on anatomically relevant loading conditions during lateral falls on the hip. The results suggest that loading conditions varied across FSP representing falls observed in older adults (Choi et al., 2015; Kangas et al., 2012; Robinovitch et al., 2013b). Due to the observed differences in loading conditions and potential interactions with individual femoral geometry, this study supports the simulation of multiple FSP in clinical screening models (Falcinelli et al., 2014). Sex and TSTT primarily influenced force magnitude and point of application. In both cases, differences in force magnitude should be interpreted with consideration of impact energy (complicated by associations with body mass). While the more distal point of application observed in kneeling and squat release, as well as among females and high-TSTT participants could be indicative of energy shunting away from the GT, increases in internal bending moments could act to increase stresses in the proximal femur. The current data should serve as inputs to computational models to evaluate tissue level stresses and fracture risk (Chapter 5).

Chapter 4

Pressure Distribution during Lateral Falls on the Hip: Implications of Participant Characteristics and Methodology

4.1.1 Introduction

From a mechanistic perspective, the risk of hip fracture is directly related to the loads applied to the proximal femur (Hayes et al., 1996). Towards the development of interventions aimed at hip fracture prevention and clinical screening, recent studies are advancing our understanding of pelvis/proximal femur system dynamics during lateral impacts (Choi & Robinovitch, 2018; Levine et al., 2018; Martel, Levine, Pretty, & Laing, 2018; Nasiri & Luo, 2016). However, limited literature is available on factors influencing the distribution of loads over the hip region during lateral falls. As anatomical exposure to loads is a key determinant of injury risk (Cummings & Nevitt, 1989), enhanced knowledge of pressure distribution over the hip could provide insights into injury mechanics, and potentially be incorporated as inputs into computational models of pelvic impacts.

Fall simulation studies investigating skin-surface pressure distributions have primarily focused on evaluating the energy-shunting capacity of hip protectors worn by females (Choi et al., 2010; Laing & Robinovitch, 2008); however, the majority of hip fractures occur in unpadded individuals (Yang et al., 2018). Utilizing a pressure measurement system, Choi and colleagues (2010) evaluated how the protective effect of soft shell hip protectors depends on fall direction (anterior-posterior) and body mass index (BMI). Hip protector use reduced peak pressure on average 70% (reduction twice as great in low- compared to high-BMI individuals); however, force overlying the femur was unaffected (shunted distally along the diaphysis). Pretty and colleagues (2017) evaluated the effects of sex, BMI, and local muscle activation on pressure distribution during unpadded trials. Males and low-BMI individuals exhibited more focal loading compared to females and high-BMI individuals, inferred through distribution of force in circular regions centered about peak pressure location. While these studies provide novel insight into factors influencing load distribution during lateral falls, they were limited to a single pelvis release fall simulation paradigm (FSP). It is unclear how pressure distribution varies across FSP that encompass the variability of lateral falls observed in older adults (Choi, Wakeling, & Robinovitch, 2015; Kangas et al., 2012; Robinovitch et al., 2013b) and if previously reported sex and body composition effects (Pretty et al., 2017) are generalizable across FSP. Beyond global loading parameters (Chapter 3), knowledge of factors influencing the localization of force over the greater trochanter (GT) could provide additional insight into femoral loading and fracture risk (Chapter 5) during lateral falls onto the hip.

In addition to fall type and individual characteristics, methodological approaches may influence metrics of force localization. Laing and Robinovitch (2008) performed repeated trials onto load cell supported circular plates of varying radius to perform ensemble analysis. A pressure measurement

system enabled Choi and colleagues (2010) to analyze pressure distribution of a single trial; however, the region definitions adopted were not sensitive to proximal-distal location along the femur (force directed over the GT and in the femoral diaphysis were summed equally). Pretty and colleagues (2017) utilized a pressure measurement system but adopted circular region definitions (Laing and Robinovitch, 2008) centered about peak pressure location due to a lack of anatomical kinematics. While the approach adopted in this study provides information on force localization, it is unclear if this force is localized over the GT. Previous reports question the validity of assuming peak pressure location corresponds with the GT, with peak pressure location on average 5.2 cm from the GT during unpadded pelvis release (Choi et al., 2010). It is unclear if factors including FSP, sex, and body composition influence the location of peak pressure and by extension the validity of this assumed GT location approach. Evaluating the influence of this approach across FSP and individual characteristics will inform interpretation of studies evaluating pressure distribution/ force localization when collection of anatomical kinematics is not feasible.

To address these gaps in the literature, this study had two objectives. The primary purpose of this study was to evaluate the influence of FSP, sex, and TSTT on skin-surface pressure distributions during lateral falls on the hip. It was hypothesized that 1) pelvis release, 2) males, and 3) low-TSTT individuals would illicit more focal loading over the GT than kneeling and squat release, females, and high-TSTT individuals respectively. The secondary objective of this study was to evaluate the use of peak pressure location as a surrogate for GT location during pressure distribution analysis. It was hypothesized that 4) use of peak pressure location would overestimate loading over the GT. The influence of FSP, sex, and TSTT on the magnitude of this overestimation and location of peak pressure were also evaluated. Consistent with hypotheses 1-3, it was hypothesized that peak pressure location would be closer to the GT and by extension the overestimation of loading over the GT would be minimized in 5) pelvis release, 6) males, and 7) low-TSTT individuals.

4.1.2 Materials and Methods

This analysis utilized the same participants and experimental protocol outlined in Chapter 3.

4.1.3 Participants

Forty-one healthy young-adults (<35 years old) consented to participate in this study, covering a wide range of body compositions (Table 4.1). Exclusion criteria included any history of pelvis, femur or spine fractures, history of easily invoked bruising, or any other health conditions that may have been

aggravated by the experimental protocol. Transverse-plane TSTT was measured via ultrasound (C60x, 2-5 MHz transducer, M-Turbo Ultrasound, SonoSite, Inc., Bothell, WA) in a side-lying position, similar to that expected during the impact phase of the fall simulations. Participants were grouped into low-, mid- and high-STT groups based the following criteria: males low <3 cm, mid 3.1-4 cm, high >4.1 cm; females low <3.5, mid 3.6-5, high >5 cm (Levine, 2017). All participants provided written informed consent. This study was approved by the Office of Research Ethics at the University of Waterloo.

Table 4.1: Mean (SD) participant anthropometric characteristics.

Sex	STT	N	Height (m)	Mass (kg)	BMI (kg/m^2)	TSTT (cm)
Females						
	Low	7	1.62 (0.04)	54.0 (6.1)	20.4 (1.7)	3.0 (0.4)
	Mid	8	1.67 (0.06)	68.3 (10.0)	24.5 (2.7)	4.3 (0.3)
	High	7	1.65 (0.07)	81.2 (25.0)	29.7 (9.2)	6.6 (1.7)
Males						
	Low	7	1.80 (0.07)	73.0 (12.4)	22.4 (2.5)	2.4 (0.4)
	Mid	6	1.81 (0.05)	83.3 (5.9)	25.5 (2.3)	3.5 (0.3)
	High	6	1.79 (0.07)	92.1 (8.4)	28.8 (1.9)	4.9 (1.1)

4.1.4 Instrumentation

Participants impacted a dual arrangement of a force plate (OR6-3, Advanced Medical Technology, Inc., Watertown, Massachusetts, USA) and rigid pressure plate (0.5 m Hi-End footscan, RSscan International, Olen, Belgium), sampled at 500 Hz. The RSscan plate was composed of 4096 resistive sensors arranged in a 64 by 64 matrix, each with a resolution of 2.58 kPa and a range of 0–2000 kPa. A three-dimensional motion capture system (Optotrak Certus, NDI, Waterloo, ON, Canada) and a rigid body cluster placed on the impacting (left) thigh were utilized to track the position of the GT and lateral epicondyle of the impacting femur at 300 Hz.

4.1.5 Experimental Protocol

Each participant completed six blocks of trials, each consisting of one pelvis, one kneeling and one squat release, in randomized order (Figure 4.1). These paradigms have previously been utilized to investigate impact dynamics during lateral falls (Levine 2017; Chapter 3), with good experimental

repeatability (Levine, 2017). In all trials, participants impacted their left hip on the RSscan plate. Participants wore form-fitting spandex shorts to ensure limited clothing contamination of the pressure distribution.

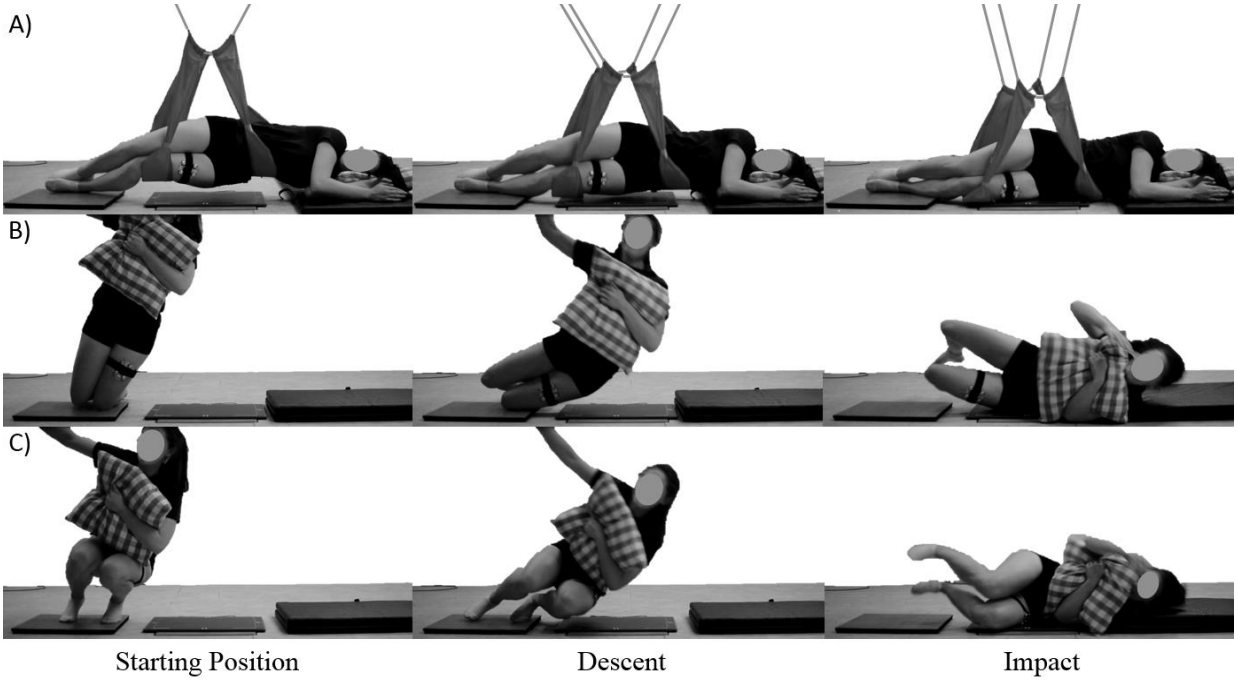

Figure 4.1: Phases of a) pelvis, b) kneeling, and c) squat release fall simulations (details available in Chapter 3).

4.1.6 Data Analysis

All data processing was performed using customized software routines (MATLAB version 7.10, Mathworks, Natick, MA, USA). Peak force (F_{max}) was determined from the vertical channel of the force platform. All subsequent analysis was performed at the time of F_{max}. Distance between peak pressure location and the GT ($Dist_{PP}$) was determined through spatial alignment of impacting thigh kinematics and the RSscan plate. Location of peak pressure with respect to the GT was determined in the anterior-posterior (PP_{AP}) and proximal-distal (PP_{PD}) directions relative to the femoral shaft (GT-lateral epicondyle). To assess the localization of impact force, a circular region (r = 5 cm) centered about the GT was defined (Figure 4.2a and b). Force in this region was integrated (spatially) and expressed as a percentage total force measured over the RSscan plate at the instant of F_{max} (F_{GT}). This analysis was

repeated utilizing methodology employed in a previous impact dynamics study lacking GT kinematics (Pretty et al., 2017), in which peak pressure location is utilized as a surrogate for GT location to calculate localized force (F_{PP}) (Figure 4.2c).

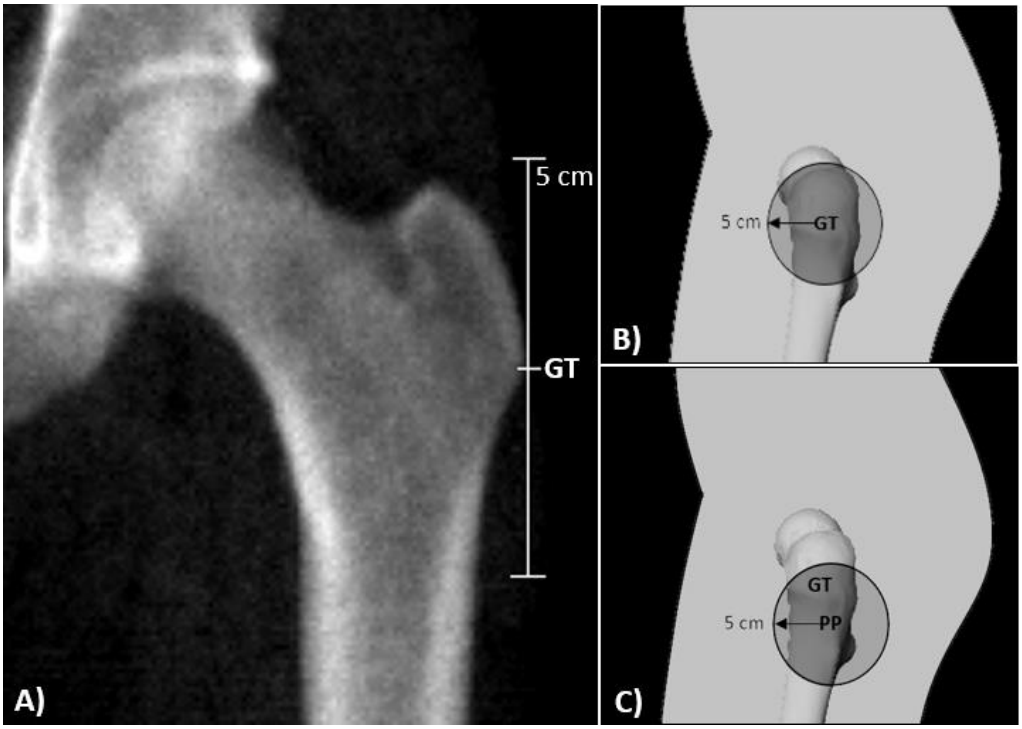

Figure 4.2: a) 5 cm radius in the frontal plane of a dual energy X-ray absorptiometry hip scan (Male: height = 1.79 m); b) F_{GT} was calculated through spatial integration of force in a 5cm radius circle centered about the GT; c) F_{PP} was calculated through spatial integration of force in a 5cm radius circle centered about the location of peak pressure (PP).

4.1.7 Statistical Analysis

All statistical analysis was performed with a software package (SPSS version 21, Chicago, USA) using an α level of 0.05. Regarding the first objective of this study, separate three-way mixed model analysis of variance (ANOVA) test were performed to assess the influence of sex and TSTT-group (between subjects), as well as FSP (repeated measure) on $F_{GT,}$ D_{PP}, PP_{AP} and PP_{PD}. To assess the use of peak pressure location as a surrogate for GT location during regional force integration (secondary objective), a four-way mixed model ANOVA test was performed. The influence of center location (repeated measure) on regional force (F_{GT} or F_{PP} for centered about GT or peak pressure location respectively) was assessed across FSP (repeated measure), as well as sex and TSTT-group (between

subjects). Pairwise comparisons were performed when significant main effects of FSP or TSTT-group were observed. Tukey's post hoc tests were performed when significant interaction effects were observed.

4.1.8 Results

4.1.9 Force Localization

F_{GT} was not influenced by significant interactions between independent variables. Main effects of FSP ($F_{2,70}$ = 9.2, p < 0.01), sex ($F_{1,35}$ = 19.6, p < 0.001), and TSTT ($F_{2,35}$ = 9.0, p = 0.001) on F_{GT} were observed (Figure 4.3). Pelvis release (mean (SD) F_{GT} = 76.4 (19.2) %) elicited more concentrated loading over the GT than kneeling (F_{GT} = 68.5 (20.1) %) and squat release (F_{GT} = 62.9 (18.3) %) (both p < 0.014). No differences in F_{GT} were observed between squat and kneeling release (p = 0.127). Males (F_{GT} = 77.4 (16.1) %) experienced more concentrated loading over the GT than females (F_{GT} = 62.7 (20.1) %). High-TSTT individuals (F_{GT} = 58.7 (20.9) %) experienced lower force concentration over the GT than mid-TSTT (F_{GT} = 71.5 (15.0) %) and low-TSTT individuals (F_{GT} = 77.2 (19.6) %) (both p < 0.003); however, no significant differences were observed between low- and mid-TSTT groups (p = 0.302).

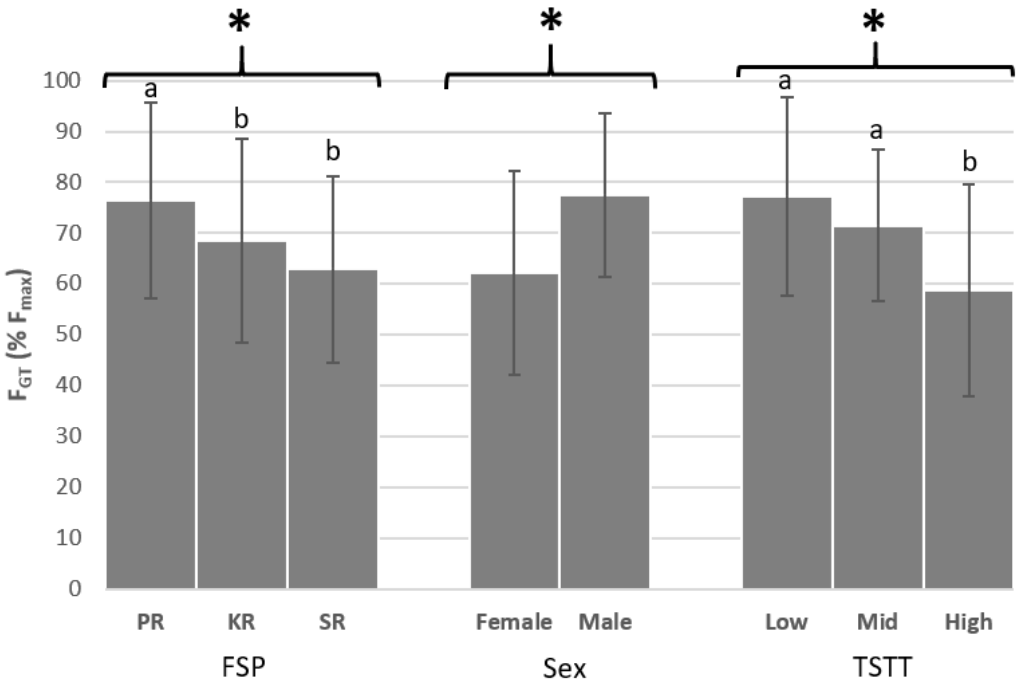

Figure 4.3: Influence of FSP (PR: pelvis; KR: kneeling; and SR: squat release), sex, and TSTT-group on F_{GT} (* indicates significant ANOVA main effects; letters refer to significant differences between groups based on Tukey's post hoc tests at α = 0.05).

4.1.10 Peak Pressure Location

A significant main effect of FSP on D_{PP} was observed ($F_{2,70}$ = 9.2, p < 0.001) (Figure 4.4a). Peak pressure location in pelvis release was on average closer to the GT (mean (SD) D_{PP} = 1.61 (1.24) cm) than in kneeling (D_{PP} = 2.65 (2.10) cm) and squat release (D_{PP} = 2.65 (1.49) cm) (both p < 0.001). In all FSP, average peak pressure location was posterior and distal to the GT. PP_{AP} was not significantly influenced by FSP ($F_{2,70}$ = 2.9, p = 0.060); however, PP_{DP} was influenced by a significant FSP-sex interaction ($F_{2,70}$ = 7.0, p = 0.002) (Figure 4.4b). In females, a main effect of FSP on PP_{DP} was observed ($F_{2,38}$ = 8.7, p = 0.001). Pelvis release elicited a more proximal mean peak pressure location (PP_{DP} = 0.32 (1.24) cm) than kneeling (PP_{DP} = 1.72 (2.08) cm) and squat release (PP_{DP} = 1.47 (1.83) cm) (both p < 0.004). PP_{DP} did not significantly differ between kneeling and squat release in females (p = 0.205). In males, no main effect of FSP was observed on PP_{DP} ($F_{2,32}$ = 2.0, p = 0.147).

D_{PP} ($F_{1,35}$ = 2.4, p = 0.134) and PP_{AP} ($F_{1,35}$ = 0.1, p = 0.750) did not significantly differ between males and females; however, a main effect of sex on PP_{PD} was observed ($F_{1,35}$ = 7.3, p = 0.010) (Figure 4.4c). Since PP_{PD} was influenced by a FSP-sex interaction, the effect of sex was evaluated in each FSP (Figure 4.4d). Females elicited a more distal location of peak pressure in kneeling ($F_{1,35}$ = 13.9, p = 0.001) and squat release ($F_{1,35}$ = 4.8, p = 0.034) compared to males; however, sex did not significantly influence PP_{PD} in pelvis release ($F_{1,35}$ = 0.0, p = 0.902).

A significant main effect of TSTT on D_{PP} was observed ($F_{2,35}$ = 5.3, p = 0.010) (Figure 4.4e). Peak pressure location in high-TSTT individuals was on average further from the GT (mean (SD) D_{PP} = 3.13 (2.18) cm) than in mid- (D_{PP} = 2.00 (1.06) cm) and low-TSTT (D_{PP} = 1.82 (1.50) cm) individuals (both p < 0.012) but no differences between low- and mid-TSST individuals were observed (p = 0.697). Mean peak pressure location was not influenced by TSTT in the anterior-posterior or proximal-distal directions ($F_{2,35}$ = 2.2, p = 0.128 and $F_{2,35}$ = 1.0, p = 0.363 for PP_{AP} and PP_{PD} respectively).

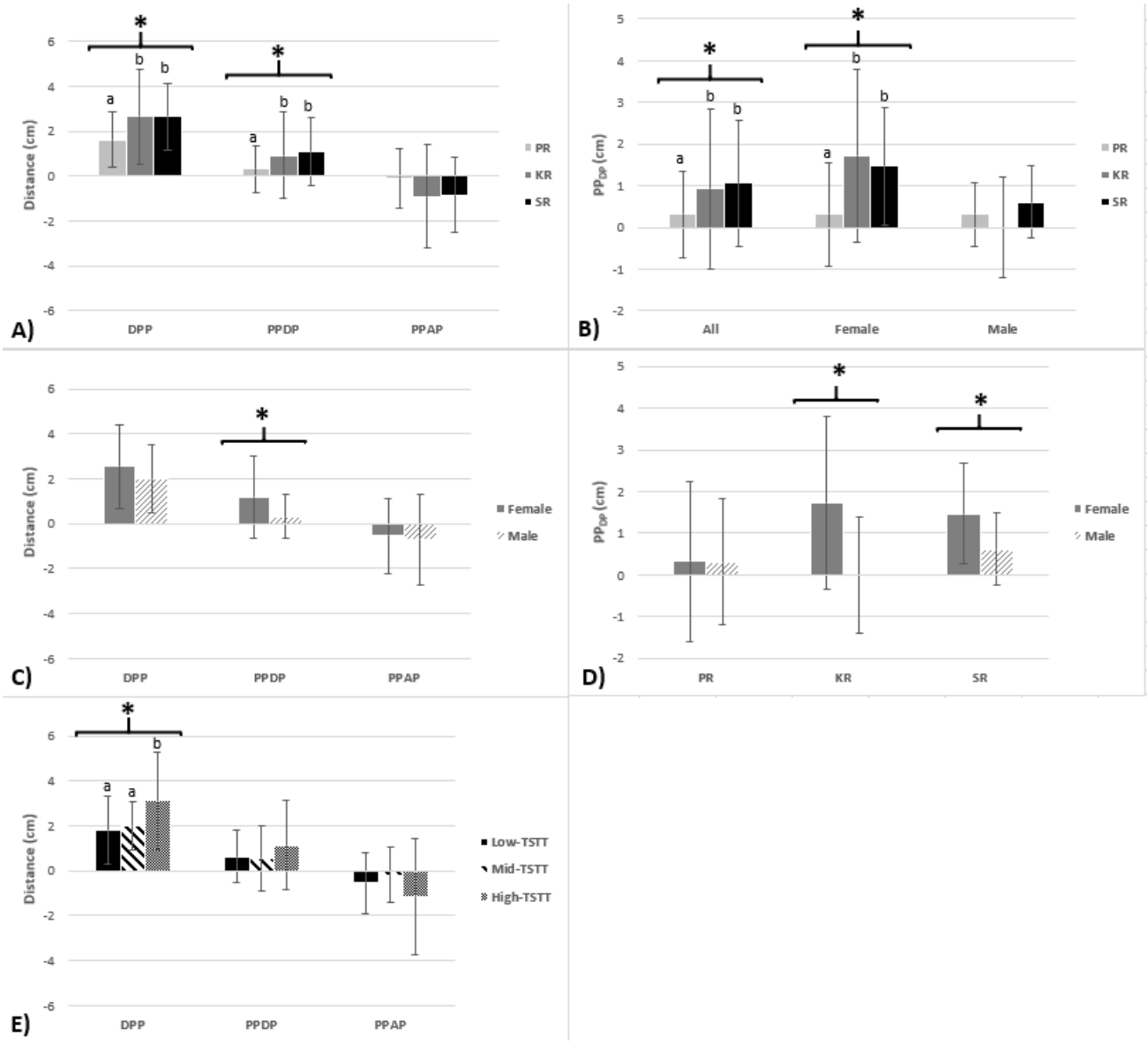

Figure 4.4: Influence of a) FSP (PR: pelvis; KR: kneeling; and SR: squat release), c) sex, and e) TSTT on peak pressure location relative to the GT (D_{PP}, PP_{PD}, and PP_{AP}). PP_{PD} was influenced by a FSP-sex interaction, which was evaluated across b) sex and d) FSP (* indicates significant ANOVA main effects; letters refer to significant differences between groups based on Tukey's post hoc tests at $\alpha = 0.05$).

4.1.11 Force Integration Center (GT vs PP)

Local force percentage (F_{GT} or F_{PP}) was influenced by center-FSP ($F_{2,70}$ = 11.1, p < 0.001) and center-sex ($F_{1,70}$ = 9.8, p = 0.004) interactions; however, a consistent main effect of center location was observed across sex and FSP ($F_{1,70}$ = 80.6, p < 0.001) (Figure 4.5). On average, F_{GT} (mean (SD) = 69.28 (19.84) %) was 16% lower than F_{PP} (80.39 (12.02) %). The center-FSP and center-sex interactions were characterized by differences in the magnitude of this overestimation. F_{PP} was 5.88, 15.4, and 20.3% greater than F_{GT} in pelvis ($F_{1,35}$ = 11.8, p = 0.002), kneeling ($F_{1,35}$ = 40.0, p < 0.001), and squat release ($F_{1,35}$ = 39.2, p < 0.001) respectively. In females, F_{PP} was 18.9% greater than F_{GT} ($F_{1,38}$ = 74.3, p < 0.001), compared to 8.5% in males ($F_{1,32}$ = 17.1, p = 0.001). No significant center-TSTT interaction was observed on local force percentage ($F_{2,70}$ = 1.7, p = 0.206).

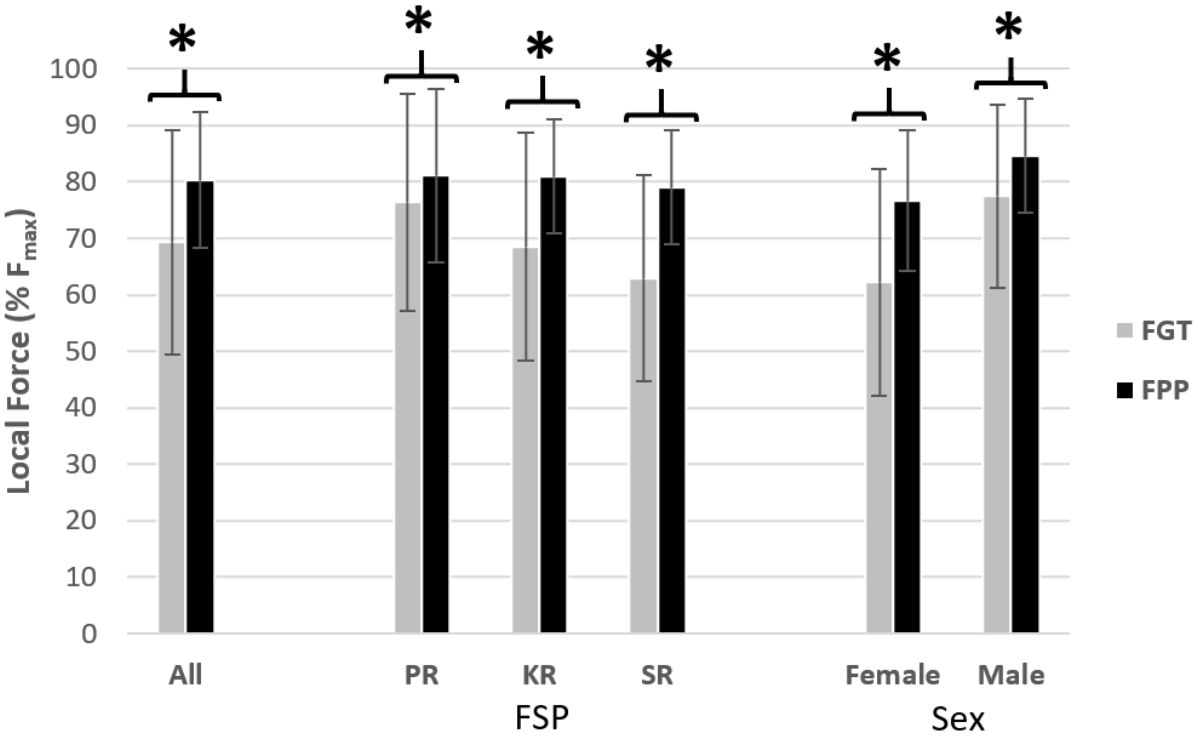

Figure 4.5: The influence of center location (GT vs PP) on the calculation of localized force (F_{GT} / F_{PP}) across FSP (PR: pelvis; KR: kneeling; and SR: squat release) and sex (* indicates significant ANOVA main effects; letters refer to significant differences between groups based on Tukey's post hoc tests at α = 0.05).

4.1.12 Discussion

The primary objective of this study was to evaluate the influence of FSP, sex, and TSTT on skin-surface pressure distributions during lateral falls on the hip. In support of hypotheses 1-3, pelvis release, males, and low/mid-TSTT individuals elicited greater F_{GT} than kneeling and squat release, females, and high-TSTT individuals respectively (Figure 4.3). The secondary objective of this study was to evaluate the use of peak pressure location as a surrogate for GT location during calculation of regional force percentages. In support of our fourth hypothesis, F_{PP} was consistently greater than F_{GT}, indicative of overestimation of force localization over the GT. In support of our fifth hypothesis, mean peak pressure location was closer to the GT and the F_{PP} overestimation was lower in pelvis than kneeling and squat release. In partial support of our sixth and seventh hypothesis, mean peak pressure location was more distal in females than males; however, no differences in average distance to the GT were observed across sex. Despite no observed sex differences in D_{PP}, F_{PP} overestimation was greater in females than males. In contrast, D_{PP} was greater in high-TSTT than mid- and low-TSTT individuals but no differences in F_{PP} overestimation were observed across TSTT. These data provide novel insights into factors influencing the percentage of total impact force localized over the GT, supplementing global loading parameters (Chapter 3) as inputs into computational models (Chapter 5) examining tissue level loading and fracture risk. Additionally, this study provides insight into the validity of utilizing peak pressure location as a surrogate for GT location during regional force calculations (Pretty et al., 2017) across FSP, sex and TSTT.

F_{GT} was found to be significantly different across FSP, sex, and TSTT-group. The most controlled release (pelvis release) was associated with more concentrated loads over the GT, equivalent to 7.9 and 13.5 % of F_{max} compared to kneeling and squat release respectively. However, kneeling and squat release have previously been found to illicit greater F_{max} (Chapter 3). While the increased forces in kneeling and squat release are disproportionately applied towards the periphery of the hip, kneeling release still elicited the greatest and pelvis release the lowest regional vertical force over the GT (mean (SD) = 1173.0 (376.6), 1713.0 (735.6), and 1405.2 (554.7) N for pelvis, kneeling, and squat release respectively) ($F_{2,70}$ = 15.6, $p < 0.001$; all pairwise $p < 0.010$). The current results do not (in isolation) mechanistically support the significantly higher rates of hip fracture observed in females compared to males (Bjorul et al., 2007; Chevalley et al., 2007). Males exhibit greater net impact forces (Chapter 3) and these forces were found to be more localized over the GT compared to females. On average, local force (N) over the GT was 66% greater in males than females ($F_{1,39}$ = 75.9, $p < 0.001$). The increased force directed over the proximal femur in males is likely driven by differences in impact energy (Chapter

3), as well as local body composition (Ley et al., 1992). Underlying differences in bone strength (Looker et al., 2001) and geometry (Nissen et al., 2005), as well as fall incidence and circumstances (Yang et al., 2018) likely drive sex-based fracture differences, despite the increased local loading observed in males in the current study. The current results support epidemiological findings linking increased TSTT to lower risk of hip fracture (Johansson et al., 2014). Although differences in impact energy increased F_{max} in high-TSTT individuals (Chapter 3), the current results suggest that these increased forces are applied peripherally away from the GT resulting in no differences in local forces (N) across TSTT ($F_{2,35}$ = 1.2, p = 0.309). Combined with previous reports positively correlating body mass with femur strength (Travison et al., 2008), these individuals would mechanistically be at a lower fracture risk (same local loading but greater femur strength with increasing TSTT). As anatomical exposure to loads is a key determinant of injury risk (Cummings & Nevitt, 1989), the current data should be incorporated in computational models (Chapter 5) to enable more comprehensive evaluation of the influence of FSP, sex, and TSTT on tissue level fracture risk.

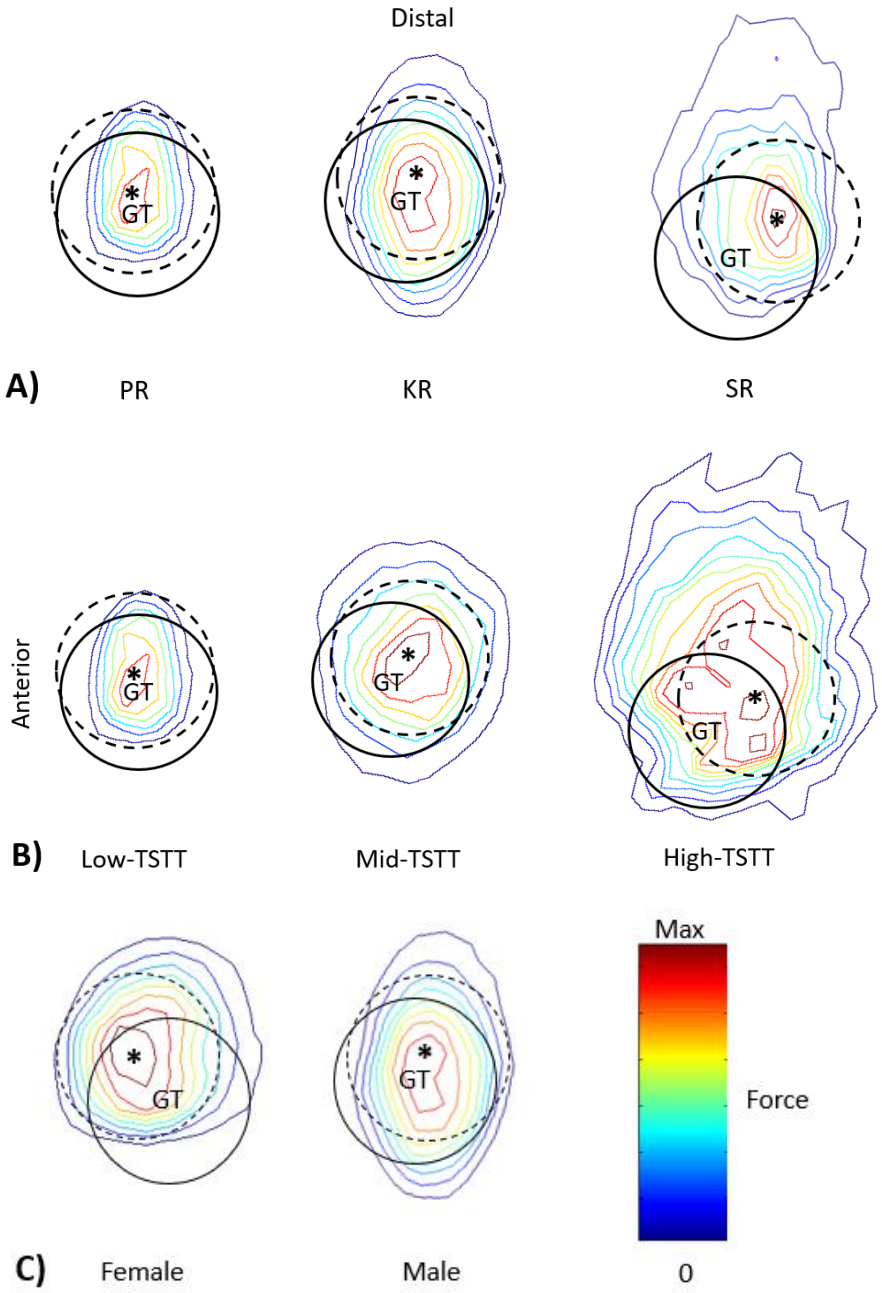

Figure 4.6: Sample pressure profiles across a) FSP (PR: pelvis; KR: kneeling; and SR: squat release; in a low-TSTT male); b) TSTT-group (during PR in male); and c) Sex (during KR in low-TSTT individuals). Rotation applied to vertically align femoral axis (GT-lateral epicondyle). F_{GT} was calculated through spatial integration of force in the solid circle centered about the GT. F_{PP} was calculated through spatial integration of force in the dashed circle centered about the location of peak pressure (*).

Location of peak pressure has previously been utilized as a surrogate for GT location during regional force analysis (Pretty et al., 2017); however, the validity of this approach is unclear. Choi and colleagues (2010) reported peak pressure location to be on average 5.2 cm from the GT during unpadded pelvis release. The current results suggest this discrepancy is lower on average, ranging from 1.61 cm in pelvis to 2.65 cm in kneeling and squat release. The discrepancy between these studies could be due to high (relative to other skeletal landmarks) inter-rater GT palpation discrepancy (Moriguchi et al., 2009), as well as methodological differences (Choi et al. (2010) utilized a modified pelvis release which could have resulted in a more distal point of impact). This approach overestimated local force over the GT on average 11.1% of F_{max}; however, the magnitude of this discrepancy was not consistent across sex or FSP. Overestimation was greater in females, as well as in kneeling and squat release compared to males and in pelvis release respectively. In both instances, the increased overestimation is likely driven by a more distal location of peak pressure relative to their comparators (Figure 4.4). Assuming similar load concentrations/profiles, a more distal peak pressure location would reduce the force over the GT and subsequently increase overestimation (Figure 4.6a and c). Studies evaluating sex- and FSP-based differences on regional forces should utilize GT kinematics, as centering about peak pressure location is insensitive to the observed distal shunting of force, which will decrease sensitivity to observing differences. Interestingly, despite high-TSTT individuals eliciting peak pressure locations further from the GT than mid- and low-TSTT individuals, the magnitude of local force overestimation did not significantly differ (ranging from 10.6 to 14.4 % F_{max} for low- and high-TSTT respectively). The pressure profile of high-TSTT individuals was less focal and more evenly distributed than in low-TSTT individuals, which likely acted to reduce the peak pressure location sensitivity of local force overestimation (Figure 4.6b).

There were several limitations associated with this study. First, as an essential safety precaution, only healthy young adults completed low-energy (yet clinically relevant) fall simulations. While the current results provide novel insight into pressure distributions during these FSP, it is unclear if these results are applicable to higher energy falls in older adults. Stiffness of soft tissues overlying the GT have been found to decrease with age (Choi, Russell, Tsai, Arzanpour, & Robinovitch, 2015). Coupled with higher energy falls, these tissues likely bottom out, which in turn would influence pressure distribution. Future work should investigate the relationship between TSTT and tissue stiffness on pressure distribution during lateral falls. High-speed ultrasonography may enable measurement of time-varying TSTT during lateral fall simulations, providing insight into potential bottoming-out effects on pressure distributions. Second, we selected a 5 cm radius circle centered about the GT as a metric force

localization to the proximal femur. While this analysis provides additional insight compared to global peak force, it is unclear how skin surface pressure distributions translate to forces on / in the proximal femur. Cadaveric and computational analysis is required to provide insight into how observed skin-surface differences translate to forces that can be utilized in tissue-level models. Additionally, the use of participant specific region definitions (ex. normalized to thigh circumference or length) may more accurately characterize local loading than absolute region definitions (ex. 5 cm utilized in this study). Third, due to equipment limitations (uniaxial pressure measurement system) only vertical impact force was considered in this analysis. Although the contribution of shear forces is small relative to the vertical force, it is uncertain how these shear forces are distributed spatially. Thus, application of the reported F_{GT} to net impact forces in computational pelvic impact models (Chapter 5) may introduce additional sources of error. Lastly, we did not consider the role of underlying femoral geometry and its potential interaction with TSTT on pressure distribution. Levine and colleagues (2018) identified several metrics of femoral geometry that influence impact dynamics through force localization during pelvis release; however, it is unclear if these relationships are consistent across FSP.

In summary, this is the first study to quantify force localization over the GT across FSP that encompass the variability of lateral falls observed in older adults, as well as across TSTT groups representative of the older adult population (Lafleur, 2016). The results suggest males and low-TSTT individuals experience more focal loading over the GT independent of FSP; however, tissue-level models (Chapter 5) are required to determine how the observed differences in skin-surface pressure distributions translate to femoral loading and fracture risk. Pelvis release elicits lower impact loads than kneeling and squat release (Chapter 3) but the current analysis suggests these loads are more concentrated over the GT. Use of peak pressure location as a surrogate for GT consistently over estimated localized loading. The magnitude of this overestimation varied across FSP and sex, suggesting this assumption is inappropriate in studies evaluating the effect of these factors on force localization. Insights gained in this study could serve to inform the development of protective devices, supplement global loading parameters as inputs in computation models of pelvic impacts and inform methodological approaches in pressure analysis of lateral falls on the hip.

Chapter 5

Participant-Specific Beam Modelling of the Proximal Femur: The Influence of Fall Simulation Paradigm, Sex, and Trochanteric Soft Tissue Thickness on Femoral Neck Stresses and Fracture Risk

5.1.1 Introduction

Due to the mechanical nature of hip fractures, biomechanical modelling offers an 'exact' method of fracture risk screening (Luo, 2017). The utility of such models are subject to accurate representation of impact dynamics during a fall, as well as the ability of the femur to resist fracture. While femoral strength is dependent on the loading conditions during a fall (Keyak et al., 2001), these factors are commonly investigated in isolation. Experimental fall simulation studies provide valuable insight into factors influencing skin surface impact dynamics including force magnitude, orientation, distribution, and anatomical point of application (Chapters 3 and 4). In isolation however, these impact characteristics offer limited insight into tissue level loading and fracture risk, which are dependent on underlying bone morphology. In contrast, computational tissue models enable detailed loading and fracture risk analysis but commonly utilize simplified loading conditions, which are insensitive to factors influencing whole body impact dynamics. As epidemiological factors associated with fracture risk could influence both skin surface and tissue level dynamics, coupling of these approaches could offer more comprehensive insights into the mechanical basis of epidemiological findings.

Impact configuration has been identified as a key determinant of injury risk (Cummings & Nevitt, 1989). In a comparison of fall simulation paradigms (FSP) that encompass the variability of lateral falls observed in older adults (Choi, Wakeling, & Robinovitch, 2015; Kangas et al., 2012; Robinovitch et al., 2013b), impact force magnitude and distribution, as well as orientation and point of application with respect to the femur, varied significantly (Chapters 3 and 4). As this analysis was limited to the skin surface, it is unclear how the observed differences translate to femoral stresses and fracture risk. Differences in impact vector orientation likely interact with underlying femoral geometry (ex. neck shaft angle) to influence the relative contribution of impact force to bending and axial stresses. Computational models and cadaveric testing have demonstrated the directional sensitivity of femur fracture tolerance (Keyak et al., 2001; Pinilla et al., 1996); however, these analyses did not simulate fall loading conditions observed experimentally (Chapters 3 and 4). Coupling of experimental loading conditions with tissue level models, may provide insight into differences in femoral stresses and fracture risk across FSP.

In contrast to epidemiological findings linking females with higher rates of hip fracture (Bjorul et al., 2007; Chevalley et al., 2007), males have been found to exhibit greater and more focal loading over the greater trochanter (GT) during simulated falls. Differences in impact energy (Chapter 3), pelvic stiffness (Levine et al., 2013) and local tissue composition (Ley et al., 1992) act to increase skin surface loading in males compared to females; however, these differences do not translate to fracture outcomes.

Underlying differences in femoral strength (Looker et al., 2001) and geometry (Nissen et el., 2005) may influence stress generation and enable males to withstand greater loading without fracture. Studies assessing sex-based differences in fracture risk often neglect sex differences in impact dynamics, which may overestimate the increased risk observed in females (Cummings et al., 2006; Keyak et al., 2011). Utilizing a multilevel subject specific modeling technique, Nasiri and Luo (2016) demonstrated that incorporating subject-specific impact parameters influenced the sex-fracture risk relationship. Among low-body mass index (BMI) individuals, females exhibited greater fracture risk however, this relationship reversed among high-BMI individuals. While this analysis attempted to account for sex differences in impact dynamics, it remains unclear if sex differences on fracture risk are present (or consistent) when experimental data (directly measured and incorporating metrics beyond impact force) are utilized during tissue level modelling.

Increased trochanteric soft tissues thickness (TSTT) has been linked to lower epidemiological risk of fracture (Johansson et al., 2014), primarily attributed to energy absorption during an impact (Etheridge et al., 2005). While associated increases in body mass and thus impact energy appear to outweigh the increased energy absorption (Chapter 3), increased TSTT also has been found to influence the distribution of force over the hip during a lateral fall (Chapter 4). In high TSTT individuals, the increased force was applied peripherally away from the hip, resulting in no differences in forces over the GT across TSTT. Assuming no net difference in energy delivered to the proximal femur, increased femoral strength (through association with body mass (Travison et al., 2008)) in high-TSTT individuals would result in lower fracture risk. Computational models often neglect the influence of TSTT on impact force or utilize a simplistic linear relationship (Robinovitch et al., 1995). In a finite element model of the pelvis system (including soft tissues) a protective effect of TSTT on fracture risk was demonstrated; however, this analysis did not account for associated increases in impact energy or femoral strength (Majumder et al., 2007, 2008). Coupling of experimental data and tissue level models could provide insight into the role of TSTT on fracture risk during lateral falls.

Thus, the purpose of this study was to evaluate the influence of FSP, sex, and TSTT on femoral stresses and fracture risk during lateral falls on the hip. Specifically, this study aimed to combine previously exclusive approaches – experimental fall simulations and computational tissue models – to enable a more comprehensive evaluation of these factors through subject-specific modelling. Our first hypothesis was that due to lower impact energy (Chapter 3), pelvis release would elicit lower stresses and fracture risk compared to kneeling and squat release. Similarly, it was hypothesized that due to increased impact energy (Chapter 3) and force localization (Chapter 4), males would elicit greater

stresses than females. These increased stresses were not hypothesized to translate to increases in fracture risk, due to higher bone strength in males than females (Keaveny et al., 2010). Our third hypothesis was that since no differences in force over the GT were observed across TSTT (Chapter 4), resultant femoral stresses would not significantly vary. In the absence of tissue loading differences, low TSTT individuals were hypothesized to elicit greater *FRI* than high TSTT individuals (through mass driven femoral strength differences (Travison et al., 2008)).

5.1.2 Materials and Methods

5.1.3 Participants

Thirty-three healthy young-adults (<35 years old) from a previously collected fall simulation study (Chapters 3 and 4) consented to participate in this study (Table 5.1). Exclusion criteria included any history of pelvis, femur or spine fractures, history of easily invoked bruising, or any other health conditions that may have been aggravated by the experimental protocol. Transverse-plane TSTT was measured via ultrasound (C60x, 2-5 MHz transducer, M-Turbo Ultrasound, SonoSite, Inc., Bothell, WA) in a side-lying position, similar to that expected during the impact phase of the fall simulations. Participants were grouped into low-, mid- and high-STT groups based the following criteria: males low <3 cm, mid 3.1-4 cm, high >4.1 cm; females low <3.5, mid 3.6-5, high >5 cm (Levine, 2017). All participants provided written informed consent. This study was approved by the Office of Research Ethics at the University of Waterloo.

Table 5.1: Mean (SD) participant anthropometric characteristics.

Sex	STT	N	Height (m)	Mass (kg)	BMI (kg/m^2)	TSTT (cm)
Females						
	Low	6	1.63 (0.04)	53.8 (6.6)	20.2 (1.7)	2.9 (0.3)
	Mid	5	1.66 (0.04)	66.5 (8.9)	24.2 (2.6)	4.1 (0.3)
	High	6	1.64 (0.07)	82.5 (27.1)	30.6 (9.8)	6.8 (1.8)
Males						
	Low	5	1.81 (0.08)	72.3 (14.4)	21.9 (2.6)	2.3 (0.5)
	Mid	5	1.80 (0.04)	85.0 (4.7)	26.4 (0.7)	3.6 (0.3)
	High	6	1.79 (0.07)	92.1 (8.4)	28.8 (1.9)	4.9 (1.1)

5.1.4 Fall Simulations

Data from a previously collected fall simulation protocol (Chapter 3, 4) were utilized in the current analysis for application to subject-specific beam models. Briefly, participants completed a series of pelvis, kneeling, and squat release fall simulation paradigms (FSP) (Figure 5.1). In each trial, the participant's left hip impacted a dual arrangement of a force plate (OR6-3, Advanced Medical Technology, Inc., Watertown, Massachusetts, USA) and rigid pressure plate (0.5 m Hi-End footscan, RSscan International, Olen, Belgium), sampled at 500 Hz. A three-dimensional motion capture system (Optotrak Certus, NDI, Waterloo, ON, Canada) and a rigid body cluster placed on the impacting (left) thigh were utilized to track the position of the GT and lateral epicondyle of the impacting femur at 300 Hz.

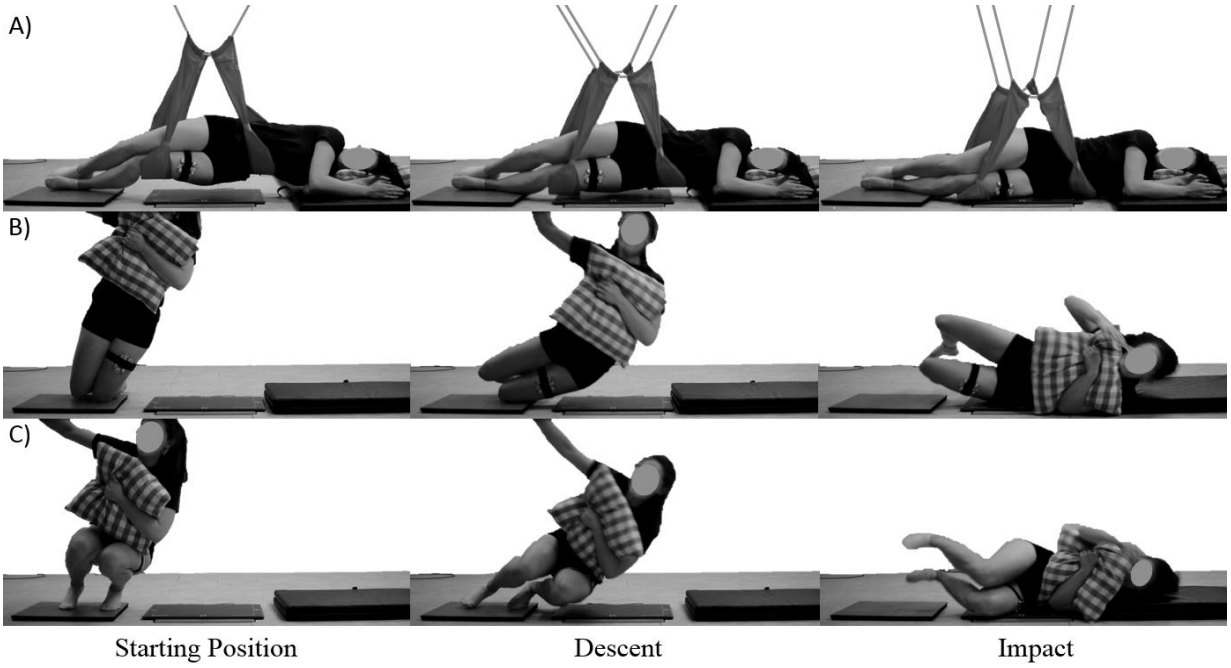

Figure 5.1: Phases of a) pelvis, b) kneeling, and c) squat release fall simulations.

Peak net force and center of pressure at peak force were extracted and expressed in previously defined femur co-ordinate system (Chapter 3; Figure 5.2). To account for localization of force over the GT, the proportion of force in a circular region (r = 5cm) centered about the GT was determined (Chapter 4). Local force (F_{GT}) was calculated as the product of this proportion and peak net force. The orientation and point of application of the net force vector in the frontal plane of the femur was expressed as the

angle (θ) to the long axis of the femur (Y) and the distance along this axis with respect to the GT (*Dist*). To assess 'worst-case' falls, the three trials of each FSP eliciting the greatest peak net force were included in this analysis (for each participant).

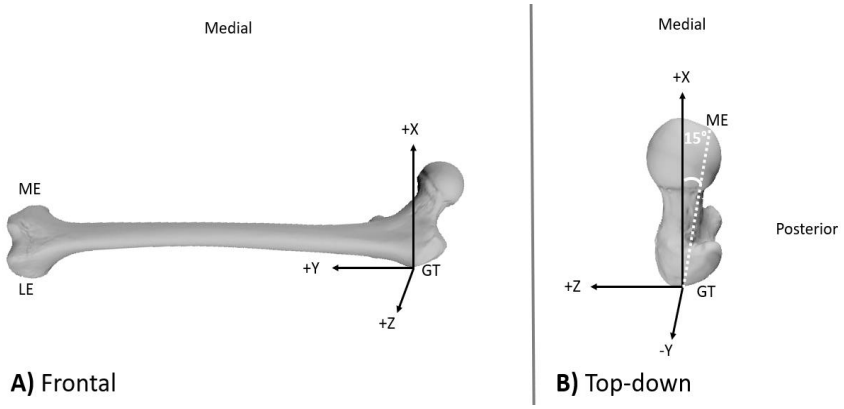

Figure 5.2: Femur co-ordinate system in the a) frontal and b) top-down view

5.1.5 Imaging and Beam Modelling

Left hip dual energy X-ray absorptiometry (DXA) images were conducted using the Hologic Discovery W fan-beam bone densitometer and digitized using Hologic APEX Software Version 3.2 (Hologic, Inc. Bedford, MA, USA). A certified Medical Radiation Technologist completed all imaging with hip internal rotation standardized to 15 degrees using a rigid positioning device. Images were exported in DICOM report format and all processing was completed using custom MATLAB routines (R2014b, Mathworks, Natick, Massachusetts, USA).

DXA images were converted to 8-bit grayscale format (Figure 5.3a) and underwent edge sharpening, dilating and interior filling. Femurs were semi-automatically segmented using an edge detection filter utilizing the Canny algorithm (Canny, 1986) with a threshold of 0.05 (Figure 5.3b). Due to overlapping bone, segmentation of the femoral head from the pelvis required user intervention. The femoral head was assumed to have a circular profile enabling extraction via manual scaling and positioning of a masking tool (Naylor, McCloskey, Eastell, & Yang, 2013). The segmented femur grayscale images were subsequently calibrated to produce areal bone mineral density (aBMD) maps. Briefly, this was accomplished assuming a linear relationship between grayscale intensity and aBMD (Yang, 2017). Scan-specific fourteen-point calibrations were performed using user defined regions of interest in the Hologic Apex software (aBMD) and MATLAB environment (grayscale intensity). This

approach produced calibration curves with a mean (SD) r^2 of 0.996 (0.01) and encompassed on average 98 (4) % of observed femur pixel intensities.

Following segmentation and calibration, femoral axes, regions of interest, and clinical geometry were defined (Figure 5.3c). The neutral femoral shaft axis (NFSA) was defined through linear fitting of femoral shaft cross-section centroid locations, equally spaced along the most distal 5 cm of the visible shaft. The femoral neck axis (FNA) was defined from the apex of the femoral head to the inferior aspect of the GT. The intersection of NFSA and FNA was taken as the neutral point of the proximal femur. The angle between these axes (neck shaft angle (NSA)) and femoral neck axis length (FNAL) were extracted due to their potential influence on femoral neck stress generation (Table 5.3). The narrow neck (NN) cross-section was defined by a line corresponding with the minimum neck width (NW) taken orthogonal to FNA (Khoo et al., 2005). This cross-section was selected for stress and fracture risk analysis due to its clinical importance – up to 61% of hip fractures occur in the femoral neck region (Bjørgul & Reikerås, 2007).

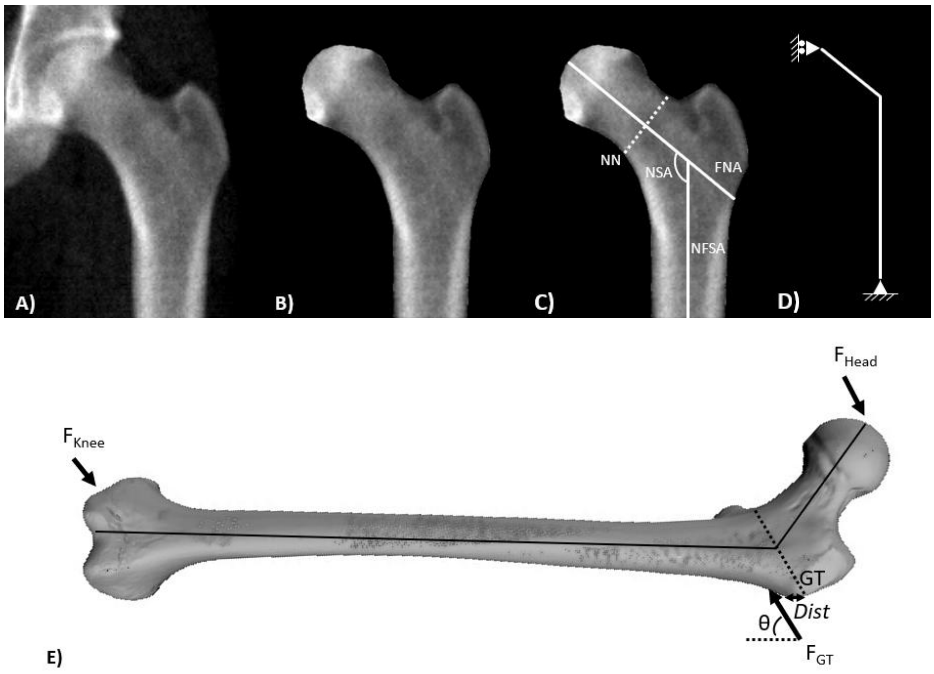

Figure 5.3: DXA image processing. a) Left hip DXA scan imported; b) Femur segmented from surrounding tissues; c) Neutral femoral shaft axis (NFSA), femoral neck axis (FNA), and narrow neck cross-section (NN) defined. The intersection of FNA and NFSA was taken as the neutral point of the femur and the angle between these axes was extracted (neck shaft angle (NSA)), d) Beam model boundary conditions; and e) Application of experimental data.

To enable stress analysis, subject-specific beam models were generated. The femur was modelled as two beams (NFSA and FNA) with a fixed connection supported by a roller joint at the femoral head and a pin joint at the knee (Figure 5.3d). Femoral shaft length (GT to lateral epicondyle) was manually palpated to determine NFSA beam length. All other spatial and mechanical properties were extracted from the DXA images. In order to spatially align experimental data for application in the beam models, two assumptions were required. First, the NFSA was assumed to run parallel to the kinematic long axis of the femur. Second, the kinematic GT location was assumed to correspond with the intersection of bone surface and a line passing through the neutral point of the femur and bisecting NSA.

Trial specific impact dynamics were simulated in the beam models. F_{GT} was applied to the proximal femur at an angle (θ) with respect to NFSA and at a distance (*Dist*) from the GT. Three-point bending was simulated with parallel resultant forces at the femoral head and knee satisfying static equilibrium (Figure 5.3e). Internal forces and bending moments in the plane of the image were calculated at the narrow neck cross-section.

Utilizing techniques developed by Mourtada and colleagues (1996) and subsequently implemented by Yang et al. (2009), mechanical properties of the femur were extracted from DXA images to allow the estimation of cross-section stresses. The anteroposterior thickness of the femur (in cm) at a pixel t_i was determined as:

$$t_i = aBMD_i/p_b \quad \text{(Equation 5.1)}$$

where $aBMD_i$ is the areal bone mineral density of the pixel and p_b is the bone mineral density of fully mineralized bone, which was assigned to 1.0 5g/cm^2. This value was calculated based on the work of Martin (1984), assuming the density of mineral is ~3 g/cm^2 and that mineral occupies ~35% of fully mineralized bone (1.05 g/cm^2 = 0.35 * 3 g/cm^2). For a given narrow neck cross-section composed of N pixels, the cross-sectional area (CSA), centroid location (y_c) and cross-sectional moment of inertia (CSMI) can be calculated:

$$CSA = \Delta L \sum_{i=1}^{i=N} t_i \quad \text{(Equation 5.2)}$$

$$y_c = \sum t_i \, y_i / CSA \quad \text{(Equation 5.3)}$$

$$CSMI = \Delta L \sum_{i=1}^{i=N} t_i (y_i - y_c)^2 \quad \text{(Equation 5.4)}$$

where ΔL is the spacing between pixels and y_i is the location of a pixel in the cross section. The normal stress in each pixel in the narrow neck cross-section (in 10^{-2} MPa) was calculated using the flexure formula as follows:

$$\sigma_i = \frac{Fa}{CSA} + \frac{M(y_i - y_c)}{CSMI} \quad \text{(Equation 5.5)}$$

where Fa is the axial force and M is the internal bending moment. The first term of this equation accounts for the axial stress produced in the cross-section due to non-orthogonal loading, which is algebraically summed with the bending stress at each pixel (second term). As the normal stress in a pixel is proportional to the distance from the centroid, peak stresses at the superior-lateral ($SL\sigma$) and inferior-medial ($IM\sigma$) edges of the narrow neck were extracted.

To assess fracture risk during each simulated fall (neglecting individual fall probability), a stress-based narrow neck fracture risk index (*FRI*) was defined as the mean ratio between pixel normal stress (σ_i) and corresponding yield stress based on the empirical functions derived by Morgan et al. (2001, 2003) ($Tensile/Compressive\ \sigma_{Yi}$):

$$FRI = \frac{\sum_{i=1}^{i=N} \frac{\sigma_i}{Tensile/Compressive\ \sigma_{Yi}}}{N} \quad \text{(Equation 5.6)}$$

$$Compressive\ \sigma_Y = \begin{cases} 85.5{p_{app}}^{2.26}, & p_{app} \leq 0.355\ g/cm^3 \\ 38.5{p_{app}}^{1.48}, & p_{app} > 0.355\ g/cm^3 \end{cases} \quad \text{(Equation 5.7)}$$

$$Tensile\ \sigma_Y = \begin{cases} 50.1{p_{app}}^{2.04}, & p_{app} \leq 0.355\ g/cm^3 \\ 22.6{p_{app}}^{1.26}, & p_{app} > 0.355\ g/cm^3 \end{cases} \quad \text{(Equation 5.8)}$$

where p_{app} is the apparent bone density calculated from volumetric bone mineral density (vBMD) according to Schileo et al. (2008) and vBMD is calculated according to the empirical function outlined by Luo (2018):

$$p_{app} = \frac{vBMD}{0.68172} \quad \text{(Equation 5.9)}$$

$$vBMD = 1.20 * \frac{aBMD}{NW} + 0.0242 \quad \text{(Equation 5.10)}$$

where NW is the width of the narrow neck cross section. Yield stresses were subsequently increased by a factor of 1.20 to account for the side artifact errors in biomechanical testing of cadaveric specimens when determining the density-material property relationships (Bevill, Easley, & Keaveny, 2008; Un, Bevill, & Keaveny, 2006).

5.1.6 Statistical Analysis

Separate three-way mixed model analysis of variance (ANOVA) tests were performed to assess the influence of sex and TSTT-group (between subjects), as well as FSP (repeated measure), on narrow neck $SL\sigma$, $IM\sigma$, and FRI. Pairwise comparisons were performed when significant main effects of FSP or TSTT-group were observed. Tukey's post hoc tests were performed when significant interaction effects were observed. All statistical analysis was performed with a software package (SPSS version 21, Chicago, USA) using an α level of 0.05.

5.1.7 Results

No significant interactions were observed, and main effects were interpreted throughout. FSP significantly influenced $SL\sigma$ ($F_{2,54} = 13.7$, $p < 0.001$), $IM\sigma$ ($F_{2,54} = 11.5$, $p < 0.001$), and FRI ($F_{2,54} = 7.7$, $p = 0.001$). Kneeling release elicited the greatest, and pelvis release the lowest compressive stresses in the superior-lateral narrow neck (mean (SD) $SL\sigma$ = 4418.4 (1921.6), 3901.6 (1971.8), and 3128.3 (1471.6) kPa for kneeling, squat and pelvis release respectively; all pairwise $p < 0.012$). In the inferior-medial narrow neck, squat release elicited the greatest, and pelvis release the lowest tensile stresses ($IM\sigma$ = 4008.5 (2438.7), 3388.6 (1588.1), and 2785.2 (1439.0) kPa for squat, kneeling, and pelvis release respectively; all pairwise $p < 0.032$) (Figure 5.4). The observed differences in femoral stresses across FSP influenced narrow neck FRI. FRI during squat (FRI = 0.1115 (0.0846)) and kneeling release (FRI = 0.1100 (0.0660)) were significantly greater than during pelvis release (FRI = 0.0845 (0.0564); both pairwise $p < 0.007$); however, no differences between squat and kneeling release were observed (p = 0.960) (Figure 5.5).

Sex did not significantly influence $SL\sigma$ ($F_{1,27} < 0.1$, $p = 0.854$), $IM\sigma$ ($F_{1,27} < 0.1$, $p = 0.882$), or FRI ($F_{1,27} = 0.5$, $p = 0.484$) (Figures 5.4 and 5.5).

TSTT-group significantly influenced $SL\sigma$ ($F_{2,27} = 3.4$, $p = 0.049$), $IM\sigma$ ($F_{2,27} = 3.5$, $p = 0.043$), and FRI ($F_{2,27} = 3.7$, $p = 0.037$). High TSTT-group individuals elicited lower compressive stresses at the superior-lateral narrow neck (p = 0.016) and lower tensile stresses at the inferior-medial narrow neck (p = 0.016) compared to low TSTT-group individuals (mean (SD) $SL\sigma$ = 3082.5 (1092.6), 4769.2 (2548.2)

kPa and *IM*σ = 2687.0 (1037.9), 4433.1 (2710.9) kPa for high and low TSTT-groups respectively). Narrow neck stresses were not significantly different (all pairwise p > 0.074) in mid TSTT-group individuals (*SL*σ = 3648.2 (1173.4) kPa and *IM*σ = 3099.6 (1064.4) kPa) compared to low and high TSTT-group individuals (Figure 5.4). *FRI* at the narrow neck was greater in low than high TSTT-group individuals (p = 0.011) but mid TSTT-group individuals were not significantly different from either of these groups (both p > 0.127; *FRI* = 0.1407 (0.1032), 0.0969 (0.0326), and 0.0707 (0.0286) for low, mid, and high TSTT-groups) (Figure 5.5).

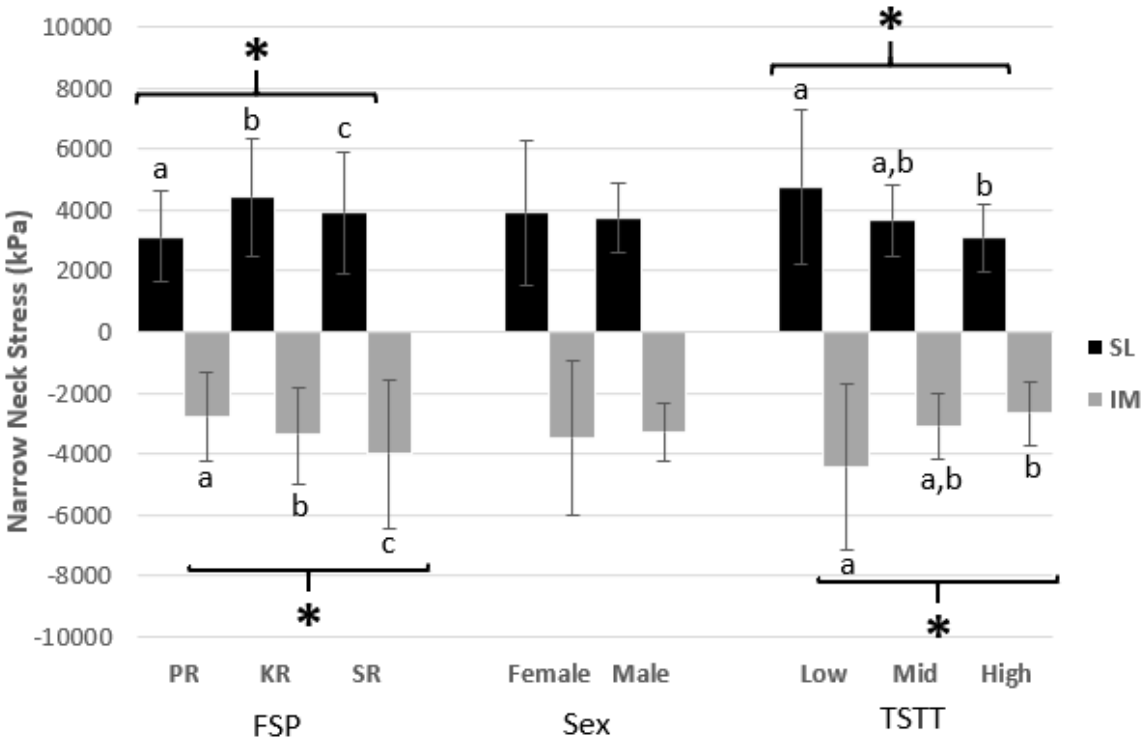

Figure 5.4: Stresses at the narrow neck superior-lateral (SL) and inferior-medial (IM) edges across FSP (PR: pelvis; KR: kneeling; and SR: squat release), sex, and TSTT. Compressive and tensile stresses are displayed as positive and negative respectively (* indicates significant ANOVA main effects; letters refer to significant differences between groups based on Tukey's post hoc tests at α = 0.05)

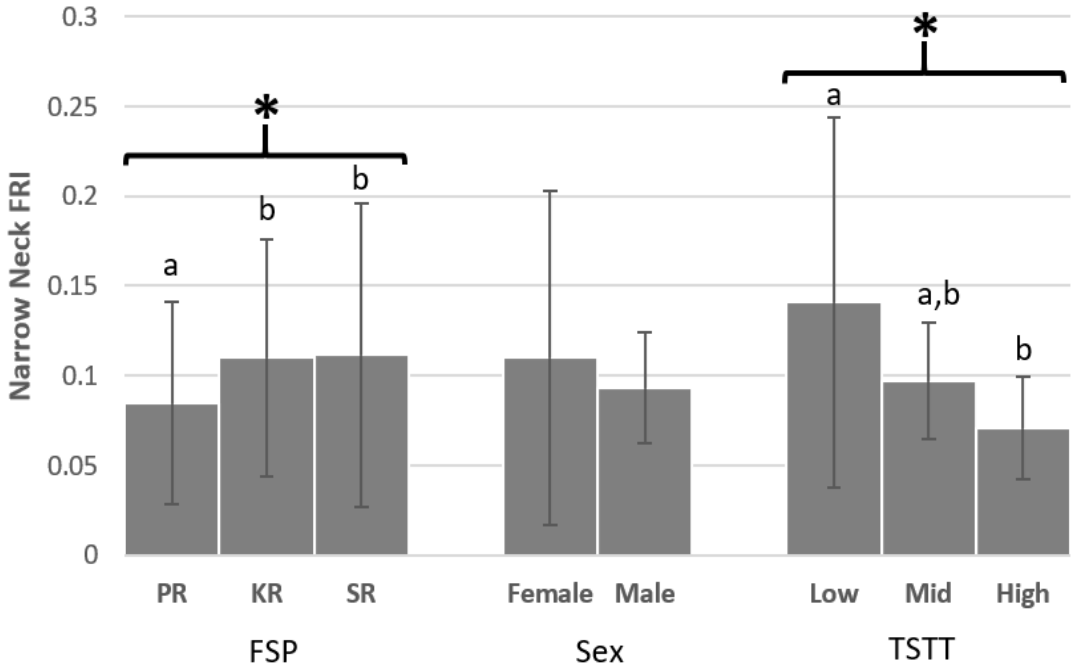

Figure 5.5: Mean narrow neck Fracture Index (FRI) across FSP (PR: pelvis; KR: kneeling; and SR: squat release), sex, and TSTT (* indicates significant ANOVA main effects; letters refer to significant differences between groups based on Tukey's post hoc tests at $\alpha = 0.05$at $\alpha = 0.05$).

5.1.8 Discussion

The objective of this study was to comprehensively evaluate the influence of FSP, sex, and TSTT on femoral stresses and fracture risk through subject-specific modelling. In support of our first hypothesis, pelvis release elicited lower *SL*σ, *IM*σ, and *FRI* compared to squat and kneeling release. In partial support of our second hypothesis, no sex differences were observed on *SL*σ, *IM*σ, or *FRI*. In contrast to our third hypothesis low TSTT individuals elicited greater *SL*σ and *IM*σ than high TSTT individuals, despite similar loading dynamics. As hypothesized low TSTT individuals exhibited greater *FRI* than high TSTT individuals. These data provide novel insights into factors influencing femoral stresses and fracture risk during simulated lateral falls.

Femoral neck stresses and *FRI* were found to vary across FSP. Pelvis release elicited the lowest *SL*σ, *IM*σ, and *FRI*, which can primarily be attributed to lower F_{GT} (Table 5.2). Squat and kneeling release did not significantly vary in *FRI*; however, kneeling release was associated with greater compressive stresses in the superior-lateral neck (*SL*σ), while squat release was associated with greater tensile stresses in the inferior-medial neck (*IM*σ). Differences in impact angle (θ) between these releases

appear to interact with underlying femur geometry (neck shaft angle) to influence stress generation (Table 5.2; Figure 5.6). Squat release was directed more parallel with the narrow neck cross section than kneeling release, which acts to minimize axial compression and maximize bending stresses. As these stresses are algebraically summed at each pixel, for similar F_{GT} squat release elicited greater tensile stresses in the inferior-medial and lower compressive stresses in the superolateral cortex. Despite no differences in *FRI* (a cross-sectional metric), the observed stress differences have implications toward local failure. Experimental fracture testing of the proximal femur with high speed video indicates that fall induced fractures are a result of a two-stage failure process, with fracture initiation in the superior-lateral cortex followed by failure in the inferior-medial neck (de Bakker et al., 2009). Combined with reports of differential bone loss in the superior-lateral cortex (Yoshikawa, Turner, Peacock, Slemenda, & Weaver, 1994; Mayhew et al., 2005) and considering the axial compression produced by muscles during a fall (Choi et al., 2018), fall orientations resembling kneeling release may represent a higher fracture risk.

Table 5.2: Mean (SD) experimental data inputs.

Factor		F_{GT} (N)	θ (deg)	Dist (cm)
FSP				
(Release)	Pelvis	1123.1 (351.6)	47.4 (11.6)	0.9 (1.9)
	Kneeling	1814.3 (586.7)	75.9 (7.0)	1.4 (1.3)
	Squat	1598.9 (616.6)	17.8 (8.6)	1.4 (1.4)
Sex				
	Female	1247.0 (488.4)	46.5 (25.1)	1.7 (1.9)
	Male	1793.8 (584.7)	47.7 (25.9)	0.7 (0.9)
TSTT				
	Low	1574.1 (568.6)	47.7 (26.4)	0.6 (1.0)
	Mid	1480.6 (483.7)	47.1 (25.0)	1.3 (1.4)
	High	1481.5 (718.5)	46.4 (25.5)	1.6 (1.9)

Table 5.3: Mean (SD) DXA characteristics.

Factor		Neck aBMD (g/cm^2)	NN Width (cm)	NN CSA (cm^2)	NN CSMI (cm^4)	NSA (deg)	FNAL (cm)
Sex							
	Female	0.86 (0.11)	2.63 (0.22)	2.47 (0.51)	1.51 (0.39)	128.4 (2.9)	8.63 (0.43)
	Male	1.01 (0.14)	3.18 (0.26)	3.38 (0.67)	2.91 (0.80)	129.2 (4.6)	9.83 (0.37)
TSTT							
	Low	0.90 (0.10)	2.85 (0.45)	2.60 (0.80)	1.81 (0.88)	127.8 (4.2)	9.09 (0.81)
	Mid	0.88 (0.12)	2.92 (0.33)	2.76 (0.51)	2.09 (0.76)	129.8 (4.1)	9.22 (0.71)
	High	1.01 (0.14)	2.93 (0.34)	3.31 (0.72)	2.63 (1.01)	128.8 (3.2)	9.34 (0.69)

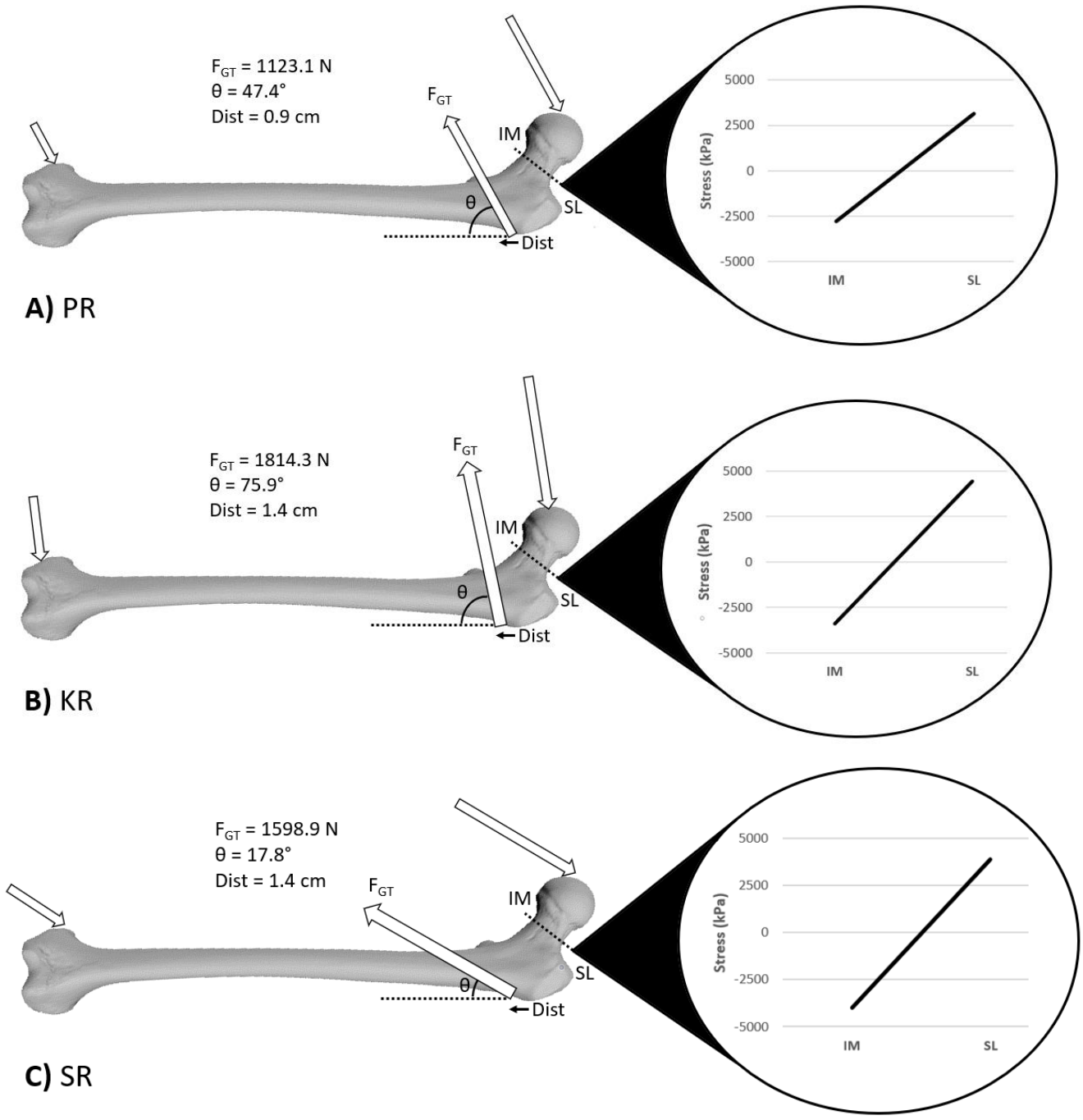

Figure 5.6: Stress generation in the superior-lateral (SL) and inferior-medial (IM) narrow neck during a) pelvis (PR), b) kneeling (KR), and c) squat release (SR). Compressive stresses are indicated as positive.

In contrast to skin surface impact dynamics, no sex differences were observed on femoral neck stresses or *FRI*. Despite increased energy delivered to the proximal femur in males (Table 5.2), differences in underlying structural parameters (Table 5.3) mitigated the translation of F_{GT} to *SL*σ and *IM*σ. Femoral neck aBMD and narrow neck width were significantly greater in males than females ($p < 0.001$). Consistent with previous reports (Nieves et al., 2005), these differences translated to increased CSA (resistance to axial compression), CSMI (resistance to bending) and mean yield stress (*FRI* denominator) in males ($p < 0.001$). While the current results do not (in isolation) support epidemiological findings, age related changes in femur morphology would act to increase stress generation and reduce femur strength in females. Compared to males, females lose an additional 16% of their femur strength over the life cycle and substantial declines in strength start a decade earlier than in males (Keaveny et al., 2010). Differential loss of bone in the superior-lateral cortex with advancing age has been shown to increase *SL*σ through an inferior-medial narrow neck centroid shift, and this effect is greater in females than males (Beck et al., 2006). These age-related changes likely act to increase *FRI* in females for a given fall; however, fall rates and circumstances (not included in the current analysis) would also influence fracture probability. While no differences in fall rates have been observed across sex (Yang et al., 2018), the circumstances of falls in females (ex. tripping during gait) are associated with greater hip fracture risk (Yang, Feldman, & Robinovitch, 2018; Yang et al., 2018). Thus, the increased hip fracture rates observed in females (Bjorul et al., 2007; Chevalley et al., 2007) are likely driven by an increased propensity for high energy falls and increased susceptibility to fracture (for a given fall) compared to males.

The current findings support epidemiological reports linking increased TSTT with reduced hip fracture risk (Johansson et al., 2014). Low TSTT individuals ellicited greater *SL*σ, *IM*σ, and *FRI* than high TSTT individuals. While similar energy was delivered to the proximal femur (Table 5.2), high TSTT individuals had greater resistance to stress generation (aBMD, CSA, and CSMI), as well as greater mean yield stress than low TSTT individuals (Table 5.3). The observed influence of TSTT was highly dependent on the inclusion of force localization as a model input. Global impact force was greater in high TSTT individuals (Chapter 3) than low TSTT individuals; however, this increased force was directed peripherally away from the hip resulting in no net difference in F_{GT} (Chapter 4). When global force was utilized in beam analysis, TSTT had no influence on *SL*σ ($F_{2,27} = 0.5$, $p = 0.621$), *IM*σ ($F_{2,27} = 0.4$, $p = 0.694$), or *FRI* ($F_{2,27} = 0.9$, $p = 0.418$). Due to the apparent importance of force localization, future work should focus on determining how skin surface pressure distributions influence transmission of impact energy to the proximal femur.

There were several limitations associated with this study. First, as an essential safety precaution, only healthy young adults completed low-energy (yet clinically relevant) fall simulations. Age related changes in femoral geometry and bone mineral distribution (Beck et al., 2006), as well as soft tissue properties (Choi et al., 2015) limit our ability to project the current results to the older adult population. Similarly, due to the nonlinear mechanical nature of the tissues comprising the pelvis system, the ability to extrapolate the current results to higher energy impacts is challenging. Second, the current 2D analysis does not account for out of plane bending and shear stresses. While lateral falls were simulated to limit out of plane loading (< 10% of peak force out of plane (Chapter 3)), future 3D analysis should evaluate falling configurations with varying levels of anterior-posterior rotation. Third, the current model utilizes simple beam mechanics rather than more computationally intense finite-element (FE) analysis. Application of time varying loading conditions in dynamic 3D FE models would more accurately characterize femoral loading. Fourth, we selected a 5 cm radius circle centered about the GT as a metric of force localization to the proximal femur. While this analysis enabled inclusion of spatial loading parameters, it is unclear how skin surface pressure distributions influence force transmission to the proximal femur. Cadaveric and computational analyses are required to enable mapping of skin surface impact dynamics to femoral loading for utilization in tissue-level models. Lastly, the contribution of local muscle activation was not included in the current study. Hip musculature would act to increase compressive stresses in the femoral neck (Choi et al., 2018); however, limited information is available on muscle activation during falls onto the hip. Future work should quantify muscle activation states during realistic fall scenarios for inclusion in femoral stress analysis.

In summary, this is the first study to couple experimental fall simulations with tissue level models to evaluate factors influencing femoral neck stresses and fracture risk. The results suggest that FSP not only influences the magnitude of stresses and fracture risk at the narrow neck, but also potential fracture mechanisms. Kneeling release was associated with greater compressive stresses in the superior-lateral neck, while squat release was associated with greater tensile stresses in the inferior-medial neck. Coupled with age related thinning of the superior cortex (Mayhew et al., 2005) and axial compression due to muscle activation (Choi et al., 2018), kneeling release may result in a higher risk of cortical buckling compared to tensile failure. Underlying differences in narrow neck mechanical properties were found to substantially influence stress generation and *FRI*, suggesting caution should be employed when interpreting differences in skin surface impact dynamics. The approaches adopted in the current study may be valuable in the evaluation of protective devices such as hip protectors and compliant flooring.

Chapter 6 Thesis Synthesis and Conclusions

6.1.1 Summary of Findings

The purpose of this thesis was to evaluate the influence of FSP, sex, and TSTT on impact characteristics during lateral falls on the hip and how the application of these loading conditions influence femoral neck stresses and fracture risk. By combining two previously exclusive approaches (experimental fall simulations and tissue level modelling), this thesis utilized a participant-specific approach, sensitive to both impact dynamics and underlying femoral geometry.

FSP significantly influenced skin surface loading conditions, as well as femoral neck stresses and fracture risk. Compared to kneeling and squat release, pelvis release elicited lower peak force magnitude; however, this force was applied closer to and was more concentrated over the greater trochanter. Despite the differences in force distribution, kneeling and squat release still elicited greater force directed over the proximal femur. Beyond force magnitude and distribution, these FSP varied significantly in impact vector orientation with respect to the femur. Kneeling release was associated with the most perpendicular loading vector, while squat release elicited the most distally directed vector in the frontal plane. In the anterior-posterior plane, pelvis release was directed posteriorly, while kneeling and squat release were directed anteriorly. Observed difference in skin surface loading conditions across FSP interacted with underlying femoral geometry to influence stress generation and fracture risk. Compressive stress at the superior-lateral femoral neck was greatest in kneeling release, while tensile stress at the inferior-medial femoral neck was greatest in squat release (driven by proportion of force resulting in axial compression vs. bending stress). While no differences in femoral neck fracture risk were observed between kneeling and squat release, kneeling release may elicit a greater risk of local compressive failure in the superior femoral neck.

At the skin surface, sex and TSTT significantly influenced impact dynamics; however, underlying differences in femur morphology influenced the translation of these loading conditions to femoral neck stresses and fracture risk. Compared to females, males exhibited greater impact force magnitude, which was applied closer to and was more concentrated over the greater trochanter of the proximal femur. This increased loading in males was mitigated by differences in femur morphology (greater resistance to bending and shear stress generation, as well as strength), resulting in no differences in femoral neck stresses or fracture risk. The increased risk of hip fracture in females may be explained by age related changes in femur morphology, as well as sex-differences in the circumstances of falls.

High-TSTT individuals exhibited greater impact force magnitude; however, these loads were applied further from and less focally over the greater trochanter compared to low-TSTT individuals. Combined, no differences were observed in the amount of force directed over the proximal femur across TSTT. Despite similar loading conditions, low-TSTT individuals elicited greater femoral neck stresses and fracture risk compared to their high-TSTT counterparts, driven by differences in underlying femur morphology (reduced resistance to bending and shear stress generation). The protective influence of TSTT to redistribute impact force peripherally away from the greater trochanter appears to play an important role in fracture risk. When global impact force was utilized instead of local force during modelling, no differences in femoral stresses or fracture risk were observed across TSTT.

6.1.2 Contributions

This thesis sought to address three gaps identified in the literature:

- *Literature Gap #1: Lack of detailed loading conditions during real falls (or simulated falls as a surrogate) for application in biomechanical models*
- *Literature Gap #2: The effect of loading condition variation between fall types, sex, and individual body compositions on femoral neck stresses and fracture risk is unknown*
- *Literature Gap #3: The effect of various factors on tissue level loading during a fall are not investigated during simulated fall studies due to their restriction to skin surface impact characteristics*

With respect to Literature Gap #1, mean loading conditions for three simulated falls, across sex and a wide range of body compositions were presented in Chapters 3 and 4. Compared to previous fall simulation studies (primarily focused on vertical force magnitude), this thesis more comprehensively evaluated impact dynamics (net force magnitude and localization, as well as orientation and point of application with respect to the femur) for application in biomechanical models. Towards more accurately representing impact dynamics, these loading conditions could be utilized as inputs to fracture screening models simulating multiple fall types. Literature Gap #2 was addressed at the skin surface level in Chapters 3 and 4, while Chapter 5 evaluated the influence of FSP, sex, and TSTT on femoral neck stresses and fracture risk. Through coupling of experimental loading conditions with participant-specific models, this analysis was sensitive to influences of these factors on both loading and underlying femur morphology. Insights gained into the mechanistic basis of these factors on fracture risk have several applications. First, the influence of sex and TSTT on force distribution could be incorporated in the

design of subject-specific hip protectors, with the objective to maximize efficacy through energy shunting. Second, the mechanistic nature of these clinical risk factors could be incorporated into deterministic fracture screening methods. Understanding the mechanism driving observed fracture rates could increase the sensitivity and specificity of fracture screening compared to statistical approaches. The adopted participant-specific approach could not feasibly, nor safely be implemented to identify clinically high-risk individuals. Alternatively, this thesis highlights the importance of considering loading conditions during fracture risk assessment and provides a framework for translating skin-surface impact dynamics to femoral neck stresses and fracture risk (Literature Gap #3). This approach could subsequently be applied to fall simulation studies evaluating factors such as protective device design or the influence of underlying femoral geometry (which have been linked to fracture risk).

While valuable, the current findings must be interpreted within the context of the methodology used. As an essential safety precaution, young healthy adults completed low energy fall simulations. Age related changes in femoral geometry and bone mineral distribution (Beck et al., 2006), as well as soft tissue properties (Choi et al., 2015) limit our ability to project the current results to the older adult population. Similarly, due to the nonlinear mechanical nature of the tissues comprising the pelvis system, the ability to extrapolate the current results to higher energy impacts is challenging.

6.1.3 Future Directions

Two important avenues for future work were identified in this thesis. First, the role of local muscle activation during a fall was not included in the current analysis. Previous reports have demonstrated the influence of muscle activation on skin surface impact dynamics (Martel et al., 2018; Pretty et al., 2017) and femoral neck stresses in mechanical testing systems (Choi et al., 2014; Choi & Robinovitch, 2018). Inclusion of muscle forces in tissue level analysis would more accurately characterize femoral stresses during an impact (increase axial compression). However, limited information is available on muscle activation and forces during falls onto the hip. Future work should quantify muscle activation states during realistic fall scenarios for inclusion in femoral stress analysis. Second, TSTT has previously been identified as a protective factor against hip fracture (Johansson et al., 2014). The current analysis mechanistically supports these findings; however, our results suggest force localization was a key determinant of TSTT's protective effect. Future work should evaluate how TSTT influences transmission of skin-surface impact loads to the proximal femur. Such analysis could enable more accurate translation of pressure distribution data to femoral forces for use in tissue level analysis.

Beyond thickness, future work should evaluate the influence of soft tissue mechanical properties (which change with age (Choi et al., 2015)) on fracture risk.

Bibliography

Ariza, O., Gilchrist, S., Widmer, R. P., Guy, P., Ferguson, S. J., Cripton, P. a., & Helgason, B. (2015). Comparison of explicit finite element and mechanical simulation of the proximal femur during dynamic drop-tower testing. *Journal of Biomechanics*, *48*(2), 224–232. https://doi.org/10.1016/j.jbiomech.2014.11.042

Åstrand, J., Nilsson, J., & Thorngren, K. (2012). Screening for osteoporosis reduced new fracture incidence by almost half Screening for osteoporosis reduced new fracture incidence by almost half. *Acta Orthopaedica ISSN:*, *83*(6), 661–665. https://doi.org/10.3109/17453674.2012.747922

Autier, P., Haentjens, P., Bentin, J., Baillon, J. M., Grivegne, A. R., Closon, M. C., & Boonen, S. (2000). International Original Article Costs Induced by Hip Fractures : A Prospective Controlled Study in, 373–380.

Backman, S. (1957). The proximal end of the femur. Investigations with special reference to the etiology of femoral neck fractures. Anatomical studies. Roentgen projections. Theoretical stress calculations. Experimental production of fractures. *Acta Radiologica Supplementum*, *146*, 1–160.

Beck, T. J. (2007). Extending DXA beyond bone mineral density: Understanding hip structure analysis. *Current Osteoporosis Reports*, *5*(2), 49–55. https://doi.org/10.1007/s11914-007-0002-4

Beck, T. J., Looker, A. C., Mourtada, F., Daphtary, M. M., & Ruff, C. B. (2006). Age trends in femur stresses from a simulated fall on the hip among men and women: evidence of homeostatic adaptation underlying the decline in hip BMD. *Journal of Bone and Mineral Research : The Official Journal of the American Society for Bone and Mineral Research*, *21*(9), 1425–1432. https://doi.org/10.1359/jbmr.060617

Beck, T. J., Mourtada, F. a., Ruff, C. B., Scott W.W., J., & Kao, G. (1998). Experimental testing of a DEXA-derived curved beam model of the proximal femur. *Journal of Orthopaedic Research*, *16*(3), 394–398. https://doi.org/10.1002/jor.1100160317

Beck, T. J., Ruff, C. B., & Bissessur, K. (1993). Age-Related Changes in Female Femoral Neck Geometry : Implications for Bone Strength. *Calcif Tissue Int*, *53*(Suppl 1), S41–S46.

Bevill, G., Easley, S. K., & Keaveny, T. M. (2008). Side-artifact errors in yield strength and elastic modulus for human trabecular bone and their dependence on bone volume fraction and anatomic

site. *Journal of Biomechanics*, *40*(15), 3381–3388.

Bhan, S., Levine, I. C., & Laing, A. C. (2014). Energy absorption during impact on the proximal femur is affected by body mass index and flooring surface. *Journal of Biomechanics*, *47*(10), 2391–2397. https://doi.org/10.1016/j.jbiomech.2014.04.026

Bjørgul, K., & Reikerås, O. (2007). Incidence of hip fracture in southeastern Norway: A study of 1,730 cervical and trochanteric fractures. *International Orthopaedics*, *31*(5), 665–669. https://doi.org/10.1007/s00264-006-0251-3

Bonewald, L. (2007). Osteocytes as Dynamic Multifunctional Cells. *ANNALS OF THE NEW YORK ACADEMY OF SCIENCES*, *1116*, 281–290. https://doi.org/10.1196/annals.1402.018

Bouxsein, M. L., & Seeman, E. (2009). Quantifying the material and structural determinants of bone strength. *Best Practice & Research Clinical Rheumatology*, *23*(6), 741–753. https://doi.org/10.1016/j.berh.2009.09.008

Bouxsein, M. L., Szulc, P., Munoz, F., Thrall, E., Sornay-Rendu, E., & Delmas, P. D. (2007). Contribution of trochanteric soft tissues to fall force estimates, the factor of risk, and prediction of hip fracture risk. *Journal of Bone and Mineral Research : The Official Journal of the American Society for Bone and Mineral Research*, *22*(6), 825–831. https://doi.org/10.1359/jbmr.070309

Brekelmans, W. A. M., Poort, H. W., & Slooff, T. J. J. H. (1972). A New Method to Analyse the Mechanical Behaviour of Skeletal Parts. *Acta Orthopaedica Scandinavica*, *43*(5), 301–317. https://doi.org/10.3109/17453677208998949

Broy, S. B., Cauley, J. A., Lewiecki, M. E., Schousboe, J. T., Shepherd, J. A., & Leslie, W. D. (2015). Fracture Risk Prediction by Non-BMD DXA Measures: The 2015 ISCD Official Positions Part 1: Hip Geometry. *Journal of Clinical Densitometry*, *18*(3), 287–308. https://doi.org/10.1016/j.jocd.2015.06.005

Canadian Institute for Health Information. (2010). Seniors and falls: Fall-related hospitalizations.

Canny, J. F. (1986). A Computational Approach to Edge Detection. *TPAMI*, *8*(6), 679–698. https://doi.org/http://doi.acm.org/10.1145/11274.11275

Carpenter, R. D., Beaupré, G. S., Lang, T. F., Orwoll, E. S., & Carter, D. R. (2005). New QCT analysis approach shows the importance of fall orientation on femoral neck strength. *Journal of*

Bone and Mineral Research : The Official Journal of the American Society for Bone and Mineral Research, *20*(9), 1533–1542. https://doi.org/10.1359/JBMR.050510

Chan, M., Estève, D., Fourniols, J., Escriba, C., & Campo, E. (2012). Smart wearable systems : Current status and future challenges. *Artificial Intelligence In Medicine*, *56*(3), 137–156. https://doi.org/10.1016/j.artmed.2012.09.003

Chevalley, T., Guilley, E., Herrmann, F. R., Hoffmeyer, P., Rapin, C. H., & Rizzoli, R. (2007). Incidence of hip fracture over a 10-year period (1991-2000): Reversal of a secular trend. *Bone*, *40*(5), 1284–1289. https://doi.org/10.1016/j.bone.2006.12.063

Choi, W. J., Cripton, P. A., & Robinovitch, S. N. (2014). Effects of hip abductor muscle forces and knee boundary conditions on femoral neck stresses during simulated falls. *Osteoporosis International*, *26*(1), 291–301. https://doi.org/10.1007/s00198-014-2812-4

Choi, W. J., Hoffer, J. a., & Robinovitch, S. N. (2010). Effect of hip protectors, falling angle and body mass index on pressure distribution over the hip during simulated falls. *Clinical Biomechanics*, *25*(1), 63–69. https://doi.org/10.1016/j.clinbiomech.2009.08.009

Choi, W. J., & Robinovitch, S. N. (2018). Effect of pelvis impact angle on stresses at the femoral neck during falls. *Journal of Biomechanics*, *74*, 41–49. https://doi.org/10.1016/j.jbiomech.2018.04.015

Choi, W. J., Russell, C. M., Tsai, C. M., Arzanpour, S., & Robinovitch, S. N. (2015). Age-related changes in dynamic compressive properties of trochanteric soft tissues over the hip. *Journal of Biomechanics*, *48*(4), 695–700. https://doi.org/10.1016/j.jbiomech.2014.12.026

Choi, W. J., Wakeling, J. M., & Robinovitch, S. N. (2015). Kinematic analysis of video-captured falls experienced by older adults in long-term care. *Journal of Biomechanics*, *48*(6), 911–920. https://doi.org/10.1016/j.jbiomech.2015.02.025

Cibulka, M. (2004). Determination and Significance of Femoral Neck Anteversion. *Physical Therapy*, *84*(6). https://doi.org/10.1093/ptj/84.6.550

Cooper, C., Campion, G., & Melton, L. J. (1992). Hip Fractures in the Elderly : A World-Wide Projection. *Osteoporosis International*, *2*, 285–289.

Cordey, J., & Gautier, E. (1999). Strain gauges used in the mechanical testing of bones Part 1: Theoretical and technical aspects. *Injury*, *30*, SA7-SA13.

Cree, M., Soskolne, C. L., Belseck, E., Mcelhaney, J. E., & Brant, R. (2000). Mortality and Institutionalization Following Hip Fracture, 283–288.

Cummings, S., Black, D., Nevitt, M. C., Browner, W., Cauley, J., Ensrud, K., … Vogt, T. (1993). Bone density at various sites for fractures prediction of hip. *The Lancet*, *341*, 72–75.

Cummings, S. R., Cawthon, P. M., Ensrud, K. E., Cauley, J. A., Fink, H. A., & Orwoll, E. S. (2006). BMD and risk of hip and nonvertebral fractures in older men: A prospective study and comparison with older women. *Journal of Bone and Mineral Research*, *21*(10), 1550–1556. https://doi.org/10.1359/jbmr.060708

Cummings, S. R., & Melton, L. J. (Iii). (2002). Epidemiology and outcomes of osteoporotic fractures. *The Lancet*, *359*, 1761–1767. https://doi.org/10.1016/S0140-6736(02)08657-9

Currey, J. D. (1986). Power law models for the mechanical properties of cancellous bone. *Engineering in Medicine*, *15*(3), 153–154.

Danielson, M. E., Beck, T. J., Karlamangla, A. S., Greendale, A., Atkinson, E. J., Lian, Y., … Ruppert, K. (2014). A comparison of DXA and CT based methods for estimating the strength of the femoral neck in post-menopausal women. *Osteoporosis International*, *24*(4), 1379–1388. https://doi.org/10.1007/s00198-012-2066-y.A

de Bakker, P. M., Manske, S. L., Ebacher, V., Oxland, T. R., Cripton, P. a., & Guy, P. (2009). During sideways falls proximal femur fractures initiate in the superolateral cortex: Evidence from high-speed video of simulated fractures. *Journal of Biomechanics*, *42*(12), 1917–1925. https://doi.org/10.1016/j.jbiomech.2009.05.001

Duan, Y., Beck, T., Wang, X., & Seeman, E. (2003). Structural and Biomechanical Basis of Sexual Dimorphism in Femoral Neck Fragility Has Its Origins in Growth and Aging. *Journal of Bone and Mineral Research*, *18*(10), 1766–1774.

Duboeuf, F., Hans, D., Schott, a M., Kotzki, P. O., Favier, F., Marcelli, C., … Delmas, P. D. (1997). Different morphometric and densitometric parameters predict cervical and trochanteric hip fracture: the EPIDOS Study. *Journal of Bone and Mineral Research : The Official Journal of the American Society for Bone and Mineral Research*, *12*(11), 1895–1902. https://doi.org/10.1359/jbmr.1997.12.11.1895

Dufour, a. B., Roberts, B., Broe, K. E., Kiel, D. P., Bouxsein, M. L., & Hannan, M. T. (2012). The

factor-of-risk biomechanical approach predicts hip fracture in men and women: The Framingham Study. *Osteoporosis International*, *23*(2), 513–520. https://doi.org/10.1007/s00198-011-1569-2

Eberle, S., Göttlinger, M., & Augat, P. (2013). An investigation to determine if a single validated density-elasticity relationship can be used for subject specific finite element analyses of human long bones. *Medical Engineering and Physics*, *35*(7), 875–883. https://doi.org/10.1016/j.medengphy.2012.08.022

Enns-bray, W. S., Bahaloo, H., Fleps, I., Ariza, O., Gilchrist, S., Widmer, R., & Guy, P. (2018). Journal of the Mechanical Behavior of Biomedical Materials Material mapping strategy to improve the predicted response of the proximal femur to a sideways fall impact. *Journal of the Mechanical Behavior of Biomedical Materials*, *78*, 196–205. https://doi.org/10.1016/j.jmbbm.2017.10.033

Etheridge, B. S., Beason, D. P., Lopez, R. R., Alonso, J. E., McGwin, G., & Eberhardt, A. W. (2005). Effects of trochanteric soft tissues and bone density on fracture of the female pelvis in experimental side impacts. *Annals of Biomedical Engineering*, *33*(2), 248–254. https://doi.org/10.1007/s10439-005-8984-5

Falcinelli, C., Schileo, E., Balistreri, L., Baruffaldi, F., Bordini, B., Viceconti, M., … Taddei, F. (2014). Multiple loading conditions analysis can improve the association between finite element bone strength estimates and proximal femur fractures: A preliminary study in elderly women. *Bone*, *67*, 71–80. https://doi.org/10.1016/j.bone.2014.06.038

Faulkner, K., Wacker, W., Barden, H., Simonelli, C., Burke, P., Ragi, S., & Del Rio, L. (2006). Femur strength index predicts hip fracture independent of bone density and hip axis length. *Osteoporosis International*, *17*, 593–599. https://doi.org/10.1007/s00198-005-0019-4

Ford, C., Keaveny, T., & Hayes, W. (1996). The Effect of Impact Direction on the Structural Capacity of the Proximal Femur During Falls. *Journal of Bone and Mineral Research*, *11*(3), 377–383.

Goh, J. C., Ang, E. J., & Bose, K. (1989). Effect of preservation medium on the mechanical properties of cat bones. *Acta Orthopaedica Scandinavica*, *60*(4), 465–467. https://doi.org/10.3109/17453678909149321

Grassi, L., Schileo, E., Taddei, F., Zani, L., Juszczyk, M., Cristofolini, L., & Viceconti, M. (2012). Accuracy of finite element predictions in sideways load configurations for the proximal human femur. *Journal of Biomechanics*, *45*(2), 394–399. https://doi.org/10.1016/j.jbiomech.2011.10.019

Grassi, L., Väänänen, S. P., Ristinmaa, M., Jurvelin, J. S., & Isaksson, H. (2017). Prediction of femoral strength using 3D finite element models reconstructed from DXA images : validation against experiments. *Biomechanics and Modeling in Mechanobiology*, *16*(3), 989–1000. https://doi.org/10.1007/s10237-016-0866-2

Grisso, J., Kelsey, J., Strom, B., Chiu, G., Maislin, G., O'Brien, L., … Kaplan, F. (1991). Risk factors for falls as a cause of hip fracture in women. The Northeast Hip Fracture Study Group. *New England Journal of Medicine*, (324), 1326–1331.

Gulan, G., Matovinović, D., Nemec, B., Rubinić, D., & Ravlić-Gulan, J. (2000). Femoral neck anteversion: Values, development, measurement, common problems. *Collegium Antropologicum*, *24*(2), 521–527. Retrieved from http://www.scopus.com/inward/record.url?eid=2-s2.0-0034576206&partnerID=40&md5=a420722254b4042abcd490c37024a201

Haentjens, P., Magaziner, J., Colón-Emeric, C. S., Vanderschueren, D., Milisen, K., Velkeniers, B., & Boonen, S. (2010). Meta-analysis: Excess Mortality After Hip Fracture Among Older Women and Men. *Annals of Internal Medicine*, *152*(6), 380–390. https://doi.org/10.1059/0003-4819-152-6-201003160-00008.Meta-analysis

Haider, I. T., Speirs, A. D., & Frei, H. (2013). Effect of boundary conditions, impact loading and hydraulic stiffening on femoral fracture strength. *Journal of Biomechanics*, *46*(13), 2115–2121. https://doi.org/10.1016/j.jbiomech.2013.07.004

Hannan, M. T., Broe, K. E., Cupples, L. A., Dufour, A. B., Rockwell, M., & Kiel, D. P. (2012). Height loss predicts subsequent hip fracture in men and women of the Framingham Study. *Journal of Bone and Mineral Research*, *27*(1), 146–152. https://doi.org/10.1002/jbmr.557

Hayes, W. C., Myers, E. R., Morris, J. N., Gerhart, T. N., Yett, H. S., & Lipsitz, L. a. (1993). Impact near the hip dominates fracture risk in elderly nursing home residents who fall. *Calcified Tissue International*, *52*(3), 192–198. https://doi.org/10.1007/BF00298717

Hayes, W. C., Myers, E. R., Robinovitch, S. N., Van Den Kroonenberg, a., Courtney, a. C., & McMahon, T. a. (1996). Etiology and prevention of age-related hip fractures. *Bone*, *18*(1), S77–S86. https://doi.org/10.1016/8756-3282(95)00383-5

Helgason, B., Perilli, E., Schileo, E., Taddei, F., Brynjólfsson, S., & Viceconti, M. (2008). Mathematical relationships between bone density and mechanical properties: A literature review. *Clinical Biomechanics*, *23*(2), 135–146. https://doi.org/10.1016/j.clinbiomech.2007.08.024

Hillier, T. A., Cauley, J. A., Rizzo, J. H., Pedula, K. L., Ensrud, K. E., Bauer, D. C., … Cummings, S. R. (2011). WHO Absolute Fracture Risk Models (FRAX): Do Clinical Risk Factors Improve Fracture Prediction in Older Women Without Osteoporosis ? *JBMR*, *26*(8), 1774–1782. https://doi.org/10.1002/jbmr.372

Hopkins, R. B., Burke, N., Von Keyserlingk, C., Leslie, W. D., Morin, S. N., Adachi, J. D., … Tarride, J. (2016). The current economic burden of illness of osteoporosis in Canada. *Osteoporosis International*, *27*(10), 3023–3032. https://doi.org/10.1007/s00198-016-3631-6

Hopkins, R., Pullenayegum, E., Goeree, R., Adachi, J., Papaioannou, A., Leslie, W., … Thabane, L. (2016). Estimation of the lifetime risk of hip fracture for women and men in Canada. *Osteoporosis International*, *23*(3), 921–927. https://doi.org/10.1007/s00198-011-1652-8.Estimation

Hui, S. L., Slemenda, C. W., & Johnston, C. C. (1989). Baseline Measurement of Bone Mass Predicts Fracture in White Women. *American College of Physicians*, *111*(5), 355–361.

Huiskes, R., & Chao, E. Y. S. (1983). A survey of finite element analysis in orthopedic biomechanics: The first decade. *Journal of Biomechanics*, *16*(6), 385–409. https://doi.org/10.1016/0021-9290(83)90072-6

Johannesdottir, F., Aspelund, T., Reeve, J., Poole, K. E., Sigurdsson, S., Harris, T. B., … Sigurdsson, G. (2013). Similarities and Differences Between Sexes in Regional Loss of Cortical and Trabecular Bone in the Mid - Femoral Neck : The AGES - Reykjavik Longitudinal Study. *Journal of Bone and Mineral Research*, *28*(10), 2165–2176. https://doi.org/10.1002/jbmr.1960

Johannesdottir, F., Thrall, E., Muller, J., Keaveny, T. M., Kopperdahl, D. L., & Bouxsein, M. L. (2017). Comparison of non-invasive assessments of strength of the proximal femur. *Bone*, *105*,

93–102. https://doi.org/10.1016/j.bone.2017.07.023

Johansson, H., Kanis, J. a., Od??n, A., McCloskey, E., Chapurlat, R. D., Christiansen, C., … Carola Zillikens, M. (2014). A meta-analysis of the association of fracture risk and body mass index in women. *Journal of Bone and Mineral Research*, *29*(1), 223–233. https://doi.org/10.1002/jbmr.2017

Jordan, K. M., & Cooper, C. (2002). Epidemiology of osteoporosis. *Best Pract Res Clin Rheumatol.*, *16*(5), 795–806. https://doi.org/10.1053/berh.2002.0264

Kangas, M., Vikman, I., Nyberg, L., Korpelainen, R., Lindblom, J., & Jämsä, T. (2012). Comparison of real-life accidental falls in older people with experimental falls in middle-aged test subjects. *Gait and Posture*, *35*(3), 500–505. https://doi.org/10.1016/j.gaitpost.2011.11.016

Kanis, J. A., Johnell, O., Oden, A., & Johansson, H. (2008). FRAX ™ and the assessment of fracture probability in men and women from the UK. *Osteoporosis International*, *19*, 385–397. https://doi.org/10.1007/s00198-007-0543-5

Kannegaard, P. N., van der Mark, S., Eiken, P., & Abrahamsen, B. (2010). Excess mortality in men compared with women following a hip fracture. National analysis of comedications, comorbidity and survival. *Age and Ageing*, *39*(2), 203–209. https://doi.org/10.1093/ageing/afp221

Kannus, P., Parkkari, J., Niemi, S., Palvanen, M., & States, U. (1996). Epidemiology of Osteoporotic Ankle Fractures in Elderly Persons in Finland. *Ann Intern Med.*, *125*(12), 975–978.

Kaptoge, S., Beck, T. J., Reeve, J., Stone, K. L., Hillier, T. A., Cauley, J. A., & Cummings, S. R. (2008). Prediction of Incident Hip Fracture Risk by Femur Geometry Variables Measured by Hip Structural Analysis in the Study of Osteoporotic Fractures. *Journal of Bone and Mineral Research*, *23*(12), 1892–1904. https://doi.org/10.1359/jbmr.080802

Kaptoge, S., Dalzell, N., Loveridge, N., Beck, T. J., Khaw, K., & Reeve, J. (2003). Effects of gender, anthropometric variables, and aging on the evolution of hip strength in men and women aged over 65. *Bone*, *32*, 561–570. https://doi.org/10.1016/S8756-3282(03)00055-3

Keaveny, T. M., Kopperdahl, D. L., Melton, L. J., Hoffmann, P. F., Amin, S., Riggs, B. L., & Khosla, S. (2010). Age-dependence of femoral strength in white women and men. *Journal of Bone and Mineral Research*, *25*(5), 994–1001. https://doi.org/10.1002/jbmr.091033

Keyak, J. H., & Rossi, S. a. (2000). Prediction of femoral fracture load using finite element models: An examination of stress- and strain-based failure theories. *Journal of Biomechanics*, *33*(2), 209–214. https://doi.org/10.1016/S0021-9290(99)00152-9

Keyak, J. H., Rossi, S. a., Jones, K. a., Les, C. M., & Skinner, H. B. (2001). Prediction of fracture location in the proximal femur using finite element models. *Medical Engineering and Physics*, *23*(9), 657–664. https://doi.org/10.1016/S1350-4533(01)00094-7

Keyak, J. H., Sigurdsson, S., Karlsdottir, G., Oskarsdottir, D., Sigmarsdottir, A., Zhao, S., … Lang, T. F. (2011). Male-female differences in the association between incident hip fracture and proximal femoral strength: A finite element analysis study. *Bone*, *48*(6), 1239–1245. https://doi.org/10.1016/j.bone.2011.03.682

Keyak, J. H., Sigurdsson, S., Karlsdottir, G. S., Oskarsdottir, D., Sigmarsdottir, A., Kornak, J., … Lang, T. F. (2013). Effect of finite element model loading condition on fracture risk assessment in men and women: The AGES-Reykjavik study. *Bone*, *57*(1), 18–29. https://doi.org/10.1016/j.bone.2013.07.028

Keyak, J. H., Skinner, H. B., & Fleming, J. a. (2001). Effect of force direction on femoral fracture load for two types of loading conditions. *Journal of Orthopaedic Research*, *19*(4), 539–544. https://doi.org/10.1016/S0736-0266(00)00046-2

Kheirollahi, H., & Luo, Y. (2015). Assessment of Hip Fracture Risk Using Cross-Section Strain Energy Determined by QCT-Based Finite Element Modeling. *BioMed Research International*, *2015*.

Khoo, B. C. C., Beck, T. J., Qiao, Q. H., Parakh, P., Semanick, L., Prince, R. L., … Price, R. I. (2005). In vivo short-term precision of hip structure analysis variables in comparison with bone mineral density using paired dual-energy X-ray absorptiometry scans from multi-center clinical trials. *Bone*, *37*(1), 112–121. https://doi.org/10.1016/j.bone.2005.03.007

Kiebzak, G. M., Beinart, G. A., Perser, K., Ambrose, C. G., Siff, S. J., & Heggeness, M. H. (2002). Undertreatment of Osteoporosis in Men With Hip Fracture. *Arch Intern Med*, *162*, 2217–2222.

Koch, J. C. (1917). The Laws of Bone Architecture. *The American Journal of Anatomy*, *21*(2).

Kopperdahl, D. L., Aspelund, T., Hoffmann, P. F., Siggeirsdottir, K., Harris, T. B., & Keaveny, T. M. (2015). Assessment of Incident Spine and Hip Fractures in Women and Men using Finite

Element Analysis of CT Scans. *J Bone Miner Res*, *29*(3), 570–580. https://doi.org/10.1002/jbmr.2069.Assessment

Krege, J. H., Wan, X., Lentle, B. C., Berger, C., Langsetmo, L., Adachi, J. D., … Kreiger, N. (2013). Fracture risk prediction : importance of age , BMD and spine fracture status. *BoneKEy Reports*, *2*(February), 1–7. https://doi.org/10.1038/bonekey.2013.138

Lachance, C. C., Jurkowski, M. P., Dymarz, A. C., Robinovitch, N., Feldman, F., Laing, A. C., & Mackey, D. C. (2017). Compliant flooring to prevent fall-related injuries in older adults : A scoping review of biomechanical efficacy , clinical effectiveness , cost-effectiveness , and workplace safety. *PLoS ONE*, *12*(2), 1–23. https://doi.org/10.1371/journal.pone.0171652

Lafleur, B. (2016). Factors Influencing Measures of Trochanteric Soft Tissue Thickness by.

Laing, a. C., & Robinovitch, S. N. (2008). Effect of soft shell hip protectors on pressure distribution to the hip during sideways falls. *Osteoporosis International*, *19*(7), 1067–1075. https://doi.org/10.1007/s00198-008-0571-9

Laing, a C., & Robinovitch, S. N. (2008). The force attenuation provided by hip protectors depends on impact velocity, pelvic size, and soft tissue stiffness. *J Biomech Eng*, *130*(6), 61005. https://doi.org/10.1115/1.2979867

Laing, A. C., & Robinovitch, S. N. (2010). Characterizing the effective stiffness of the pelvis during sideways falls on the hip. *Journal of Biomechanics*, *43*(10), 1898–1904. https://doi.org/10.1016/j.jbiomech.2010.03.025

Lee, D.-H., Jung, K. Y., Hong, a R., Kim, J. H., Kim, K. M., Shin, C. S., … Kim, G. (2016). Femoral geometry, bone mineral density, and the risk of hip fracture in premenopausal women: a case control study. *BMC Musculoskeletal Disorders*, *17*(1), 42. https://doi.org/10.1186/s12891-016-0893-2

Leibson, C., Tosteson, A., Gabriel, S., Ransom, J., & Melton, L. (2002). Mortality , Disability , and Nursing Home Use for Persons with and without Hip Fracture: A Population-Based Study. *Journal of American Geriatrics Society*, *50*, 1644–1650.

Leslie, W. D., Donnell, S. O., Jean, S., Walsh, P., Bancej, C., & Hanley, D. A. (2009). Trends in Hip Fracture Rates in Canada, *302*(8), 883–889.

Leslie, W. D., Morin, S., Lix, L. M., Johansson, H., Oden, a, McCloskey, E., & Kanis, J. a. (2012).

Fracture risk assessment without bone density measurement in routine clinical practice. *Osteoporosis International : A Journal Established as Result of Cooperation between the European Foundation for Osteoporosis and the National Osteoporosis Foundation of the USA*, *23*(1), 75–85. https://doi.org/10.1007/s00198-011-1747-2

Levine, I. C. (2017). The effects of body composition and body configuration on impact dynamics during lateral falls : insights from in-vivo , in-vitro , and in- silico approaches by.

Levine, I. C., Bhan, S., & Laing, A. C. (2013). The effects of body mass index and sex on impact force and effective pelvic stiffness during simulated lateral falls. *Clinical Biomechanics*, *28*(9–10), 1026–1033. https://doi.org/10.1016/j.clinbiomech.2013.10.002

Levine, I. C., Pretty, S. P., Nouri, P. K., Mourtzakis, M., & Laing, A. C. (2018). Pelvis and femur geometry: Relationships with impact characteristics during sideways falls on the hip. *Journal of Biomechanics*, *80*, 72–78. https://doi.org/10.1016/j.jbiomech.2018.08.029

Ley, Lees, & Stevenson. (1992). Sex- and menopause-associated in body-fat distribution. *AM J Clin Nutr*, *55*, 950–954.

Lo, J., & Ashton-Miller, J. (2008). Effect of Pre-Impact Movement Strategies on the Impact Forces Resulting From a Lateral Fall. *Journal of Biomechanics*, *41*(9), 1969–1977. https://doi.org/10.1016/j.jbiomech.2008.03.022.Effect

Lochmüller, E. M. M., Groll, O., Kuhn, V., & Eckstein, F. (2002). Mechanical strength of the proximal femur as predicted from geometric and densitometric bone properties at the lower limb versus the distal radius. *Bone*, *30*(1), 207–216. https://doi.org/10.1016/S8756-3282(01)00621-4

Long, Y., Leslie, W. D., & Luo, Y. (2015). Study of DXA-derived lateral-medial cortical bone thickness in assessing hip fracture risk. *Bone Reports*, *2*, 44–51. https://doi.org/10.1016/j.bonr.2015.02.003

Looker, A. C., Beck, T. J., & Orwoll, E. S. (2001). Does body size account for gender differences in femur bone density and geometry? *Journal of Bone and Mineral Research*, *16*(7), 1291–1299. https://doi.org/10.1359/jbmr.2001.16.7.1291

Lovejoy, C. (1988). Evolution of Human Walking. *Scientific American*, *295*(5), 118–125.

Luo, Y. (2016). A biomechanical sorting of clinical risk factors affecting osteoporotic hip fracture. *Osteoporosis International*, *27*(2), 423–439. https://doi.org/10.1007/s00198-015-3316-6

Luo, Y. (2017). *Image-Based Multilevel Biomechanical Modeling for Fall-Induced Hip Fracture*. https://doi.org/10.1007/978-3-319-51671-4

Luo, Y. (2018). Empirical Functions for Conversion of Femur Areal and Volumetric Bone Mineral Density. *Journal of Medical and Biological Engineering*, (0123456789). https://doi.org/10.1007/s40846-018-0394-x

Luo, Y., Ferdous, Z., & Leslie, W. D. (2011). A preliminary dual-energy X-ray absorptiometry-based finite element model for assessing osteoporotic hip fracture risk. *Proceedings of the Institution of Mechanical Engineers, Part H: Journal of Engineering in Medicine*, *225*(12), 1188–1195. https://doi.org/10.1177/0954411911424975

Magaziner, J., Simonsick, E. M., Kashner, T. M., Hebel, J. R., & Kenzora, J. E. (1990). Predictors of Functional Recovery One Year Following Hospital Discharge for Hip Fracture : A Prospective Study. *Journal of Gerontology*, *45*(3), 101–107.

Maitland, L. a, Myers, E. R., Hipp, J. a, Hayes, W. C., & Greenspan, S. L. (1993). Read my hips: measuring trochanteric soft tissue thickness. *Calcified Tissue International*, *52*(2), 85–89. https://doi.org/10.1007/BF00308313

Majumder, S., Roychowdhury, A., & Pal, S. (2007). Simulation of hip fracture in sideways fall using a 3D finite element model of pelvis-femur-soft tissue complex with simplified representation of whole body. *Medical Engineering and Physics*, *29*(10), 1167–1178. https://doi.org/10.1016/j.medengphy.2006.11.001

Majumder, S., Roychowdhury, A., & Pal, S. (2008). Effects of trochanteric soft tissue thickness and hip impact velocity on hip fracture in sideways fall through 3D finite element simulations. *Journal of Biomechanics*, *41*(13), 2834–2842. https://doi.org/10.1016/j.jbiomech.2008.07.001

Majumder, S., Roychowdhury, A., & Pal, S. (2009). Effects of body configuration on pelvic injury in backward fall simulation using 3D finite element models of pelvis-femur-soft tissue complex. *Journal of Biomechanics*, *42*(10), 1475–1482. https://doi.org/10.1016/j.jbiomech.2009.03.044

Majumder, S., Roychowdhury, A., & Pal, S. (2013). Hip fracture and anthropometric variations: dominance among trochanteric soft tissue thickness, body height and body weight during sideways fall. *Clinical Biomechanics (Bristol, Avon)*, *28*(9–10), 1034–1040. https://doi.org/10.1016/j.clinbiomech.2013.09.008

Martel, D. R., Levine, I. C., Pretty, S. P., & Laing, A. C. (2017). The influence of muscle activation on impact dynamics during lateral falls on the hip. *Journal of Biomechanics*. https://doi.org/10.1016/j.jbiomech.2017.11.002

Martel, D. R., Levine, I. C., Pretty, S. P., & Laing, A. C. (2018). The influence of muscle activation on impact dynamics during lateral falls on the hip. *Journal of Biomechanics*, *66*, 111–118. https://doi.org/10.1007/s10439-017-1928-z

Martin, R. (1984). Porosity and specific surface of bone. *Crit Rev Biomed Eng*, *10*(3), 179–222.

Mayhew, P. M., Thomas, C. D., Clement, J. G., Loveridge, N., Beck, T. J., Bonfield, W., … Reeve, J. (2005). Relation between age, femoral neck cortical stability, and hip fracture risk. *Lancet*, *366*(9480), 129–135. https://doi.org/10.1016/S0140-6736(05)66870-5

McClung, M. R. (2005). The Relationship between Bone Mineral Density and Fracture Risk. *Current Osteoporosis Reports*, *3*, 57–63.

Melton, L., Atkinson, E., O'Fallon, W., Wahner, H., & Riggs, B. (1993). Long-Term Fracture Prediction by Bone Mineral Assessed at Different Skeletal Sites. *Journal of Bone and Mineral Research*, *8*(10), 1227–1233.

Milovanovic, P., Zimmermann, E. A., Riedel, C., Herzog, L., Krause, M., Djonic, D., … Ritchie, R. O. (2015). Biomaterials Multi-level characterization of human femoral cortices and their underlying osteocyte network reveal trends in quality of young , aged , osteoporotic and antiresorptive-treated bone. *Biomaterials*, *45*, 46–55. https://doi.org/10.1016/j.biomaterials.2014.12.024

Morgan, E. F., Bayraktar, H. H., & Keaveny, T. M. (2003). Trabecular bone modulus – density relationships depend on anatomic site. *Journal of Biomechanics*, *36*, 897–904. https://doi.org/10.1016/S0021-9290(03)00071-X

Morgan, E. F., & Keaveny, T. M. (2001). Dependence of yield strain of human trabecular bone on anatomic site. *Journal of Biomechanics*, *34*, 569–577.

Moriguchi, C. S., Carnaz, L., Silva, L. C. C. B., Salasar, L. E. B., Carregaro, R. L., Sato, T. de O., & Coury, H. J. C. G. (2009). Reliability of intra- and inter-rater palpation discrepancy and estimation of its effects on joint angle measurements. *Manual Therapy*, *14*(3), 299–305. https://doi.org/10.1016/j.math.2008.04.002

Mourtada, F. a., Beck, T. J., Hauser, D. L., Ruff, C. B., & Bao, G. (1996). Curved beam model of the proximal femur for estimating stress using dual- energy x-ray absorptiometry derived structural geometry. *Journal of Orthopaedic Research*, *14*(3), 483–492. https://doi.org/10.1002/jor.1100140319

Nankaku, M., Kanzaki, H., Tsuboyama, T., & Nakamura, T. (2005). Evaluation of hip fracture risk in relation to fall direction. *Osteoporosis International*, *16*(11), 1315–1320. https://doi.org/10.1007/s00198-005-1843-2

Nasiri, M., & Luo, Y. (2016). Study of sex differences in the association between hip fracture risk and body parameters by DXA-based biomechanical modeling. *Bone*, *90*, 90–98. https://doi.org/10.1016/j.bone.2016.06.006

National Institutes of Health. (2001). Osteoporosis Prevention, Diagnosis, and Therapy. *JAMA*, *285*(6).

Naylor, K. E., McCloskey, E. V., Eastell, R., & Yang, L. (2013). Use of DXA-based finite element analysis of the proximal femur in a longitudinal study of hip fracture. *Journal of Bone and Mineral Research*, *28*(5), 1014–1021. https://doi.org/10.1002/jbmr.1856

Nguyen, T., Center, J., & Eisman, J. (2004). Osteoporosis : underrated , underdiagnosed and undertreated. *MJA*, *180*, S18-22.

Nieves, J. W., Formica, C., Ruffing, J., Zion, M., Garrett, P., Lindsay, R., & Cosman, F. (2005). Males have larger skeletal size and bone mass than females, despite comparable body size. *Journal of Bone and Mineral Research*, *20*(3), 529–535. https://doi.org/10.1359/JBMR.041005

Nikitovic, M., Wodchis, W. P., Krahn, M. D., & Cadarette, S. M. (2013). Direct health-care costs attributed to hip fractures among seniors: A matched cohort study. *Osteoporosis International*, *24*(2), 659–669. https://doi.org/10.1007/s00198-012-2034-6

Nissen, N., Hauge, E. M., Abrahamsen, B., Jensen, J. E. B., Mosekilde, L., & Brixen, K. (2005). Geometry of the proximal femur in relation to age and sex: A cross-sectional study in healthy adult danes. *Acta Radiologica*, *46*(5), 514–518. https://doi.org/10.1080/02841850510021562

Omsland, T. K., Emaus, N., Tell, G. S., Magnus, J. H., Awad, L., Holvik, K., … Meyer, H. E. (2014). Mortality following the fi rst hip fracture in Norwegian women and men (1999 – 2008). A NOREPOS study ☆. *Bone*, *63*, 81–86. https://doi.org/10.1016/j.bone.2014.02.016

Op Den Buijs, J., & Dragomir-Daescu, D. (2011). Validated finite element models of the proximal femur using two-dimensional projected geometry and bone density. *Computer Methods and Programs in Biomedicine*, *104*(2), 168–174. https://doi.org/10.1016/j.cmpb.2010.11.008

Orwoll, E. S., Marshall, L. M., Nielson, C. M., Cummings, S. R., Lapidus, J., Cauley, J. a, … Keaveny, T. M. (2009). Finite Element Analysis of the Proximal Femur and Hip Fracture Risk in Older Men. *JOURNAL OF BONE AND MINERAL RESEARCH J Bone Miner Res*, *2424*(3), 475–483. https://doi.org/10.1359/JBMR.081201

Pagani, S., Veronesi, F., Salamanna, F., Cepollaro, S., & Fini, M. (2018). An advanced tri-culture model to evaluate the dynamic interplay among osteoblasts, osteoclasts, and endothelial cells. *Journal of Cellular Physiology*, *233*, 291–301. https://doi.org/10.1002/jcp.25875

Palermo, A., Tuccinardi, D., Defeudis, G., Watanabe, M., & Manfrini, S. (2016). BMI and BMD : The Potential Interplay between Obesity and Bone Fragility. *International Journal of Environmental Research and Public Health*, *13*(544). https://doi.org/10.3390/ijerph13060544

Palvanen, M., Kannus, P., Piirtola, M., Niemi, S., Parkkari, J., & Ja, M. (2014). Effectiveness of the Chaos Falls Clinic in preventing falls and injuries of home-dwelling older adults : A randomised controlled trial §. *Injury*, *45*, 265–271. https://doi.org/10.1016/j.injury.2013.03.010

Papadimitropoulos, E. A., Coyte, P. C., Josse, R. G., & Greenwood, C. E. (1997). Current and projected rates of hip fracture in Canada.

Papapoulos, S. E., Quandt, S., Libeman, U., Hochberg, M., & Thompson, D. (2005). Meta-analysis of the efficacy of alendronate for the prevention of hip fractures in postmenopausal women. *Osteoporosis International*, *16*, 468–474. https://doi.org/10.1007/s00198-004-1725-z

Parachute. (2015). The Cost of Injury in Canada, 164.

Parkkari, J., Kannus, P., Palvanen, M., Natri, A., Vainio, J., Aho, H., … Ja, M. (1999). Majority of Hip Fractures Occur as a Result of a Fall and Impact on the Greater Trochanter of the Femur: A Prospective Controlled Hip Fracture Study with 206 Consecutive Patients. *Calcified Tissue International*, *65*, 183–187.

Pinilla, T. P., Boardman, K. C., Bouxsein, M. L., Myers, E. R., & Hayes, W. C. (1996). Impact direction from a fall influences the failure load of the proximal femur as much as age-related bone loss. *Calcified Tissue International*, *58*(4), 231–235.

https://doi.org/10.1007/s002239900040

Power, J., Loveridge, N., Lyon, A., Rushton, N., Parker, M., & Reeve, J. (2003). Bone Remodeling at the Endocortical Surface of the Human Femoral Neck: A Mechanism for Regional Cortical Thinning in Cases of Hip Fracture. *Journal of Bone and Mineral Research*, *18*(10), 1775–1780.

Pretty, S., Martel, D., & Laing, A. (2017). The Influence of Body Mass Index, Sex, & Muscle Activation on Pressure Distribution During Lateral Falls on the Hip. *Annals of Biomedical Engineering*, *45*(12), 2775–2783. https://doi.org/10.1007/s10439-017-1928-z

Public Health Agency of Canada. (2014). *Seniors ' falls in Canada: second report*.

Pulkkinen, P., Eckstein, F., Lochmüller, E.-M., Kuhn, V., & Jämsä, T. (2006). Association of geometric factors and failure load level with the distribution of cervical vs. trochanteric hip fractures. *Journal of Bone and Mineral Research : The Official Journal of the American Society for Bone and Mineral Research*, *21*(6), 895–901. https://doi.org/10.1359/JBMR.060305

Pulkkinen, P., Jämsä, T., Lochmüller, E. M., Kuhn, V., Nieminen, M. T., & Eckstein, F. (2008). Experimental hip fracture load can be predicted from plain radiography by combined analysis of trabecular bone structure and bone geometry. *Osteoporosis International*, *19*(4), 547–558. https://doi.org/10.1007/s00198-007-0479-9

Reeve, J., & Loveridge, N. (2014). The fragile elderly hip: Mechanisms associated with age-related loss of strength and toughness. *Bone*, *61*, 138–148. https://doi.org/10.1016/j.bone.2013.12.034

Reginster, J., Gillet, P., Sedrine, W. Ben, Brands, G., Ethgen, O., Froidmont, C. De, & Gosset, C. (1999). Direct Costs of Hip Fractures in Patients Over 60 Years of Age in Belgium. *Pharmacoeconomic*, *15*(5), 507–514.

Rezaei, A., & Dragomir-Daescu, D. (2015). Femoral Strength Changes Faster with Age Than BMD in Both Women and Men: A Biomechanical Study. *Journal of Bone and Mineral Research*, *30*(12), 2200–2206. https://doi.org/10.1002/jbmr.2572

Riggs, B. L., & Melton, L. J. (1995). The worldwide problem of osteoporosis: Insights afforded by epidemiology. *Bone*, *17*(5 SUPPL. 1). https://doi.org/10.1016/8756-3282(95)00258-4

Robinovitch, S. N., Feldman, F., Yang, Y., Schonnop, R., Leung, P. M., Sarraf, T., … Loughi, M. (2013a). Video capture of the circumstances of falls in elderly people residing in long-term care: An observational study. *The Lancet*, *381*(9860), 47–54. https://doi.org/10.1016/S0140-

6736(12)61263-X

Robinovitch, S. N., Feldman, F., Yang, Y., Schonnop, R., Leung, P. M., Sarraf, T., … Loughi, M. (2013b). Video capture of the circumstances of falls in elderly people residing in long-term care: An observational study. *The Lancet*, *381*(9860), 47–54. https://doi.org/10.1016/S0140-6736(12)61263-X

Robinovitch, S. N., Hayes, W. C., & McMahon, T. a. (1997). Distribution of contact force during impact to the hip. *Annals of Biomedical Engineering*, *25*(3), 499–508. https://doi.org/10.1007/BF02684190

Robinovitch, S. N., Hayes, W. C., & McMahon, T. a. (1991). Prediction of femoral impact forces in falls on the hip. *Journal of Biomechanical Engineering*, *113*(December 1991), 366–374. https://doi.org/10.1115/1.2895414

Robinovitch, S. N., McMahon, T. a., & Hayes, W. C. (1995). Force attenuation in trochanteric soft tissues during impact from a fall. *Journal of Orthopaedic Research*, *13*(6), 956–962. https://doi.org/10.1002/jor.1100130621

Rossman, T., Kushvaha, V., & Dragomir-daescu, D. (2016). Computer Methods in Biomechanics and Biomedical Engineering QCT / FEA predictions of femoral stiffness are strongly affected by boundary condition modeling. *Computer Methods in Biomechanics and Biomedical Engineering*, *19*(2), 208–216. https://doi.org/10.1080/10255842.2015.1006209

Rubenstein, L. Z. (2006). Falls in older people: Epidemiology, risk factors and strategies for prevention. *Age and Ageing*, *35*(SUPPL.2), 37–41. https://doi.org/10.1093/ageing/afl084

Rudman, K. E., Aspden, R. M., & Meakin, J. R. (2006). Compression or tension? The stress distribution in the proximal femur. *Biomedical Engineering Online*, *5*, 12. https://doi.org/10.1186/1475-925X-5-12

Ruff, C. B., & Hayes, W. C. (1988). Sex Differences in Age-Related Remodeling of the Femur and Tibia. *Journal of Orthopaedic Research*, *1977*(36), 886–896.

Santesso, N., Carrasco-Labra, A., & Brignardello-Petersen, R. (2014). Hip protectors for preventing hip fractures in older people. *Cochrane Database of Systematic Reviews*, (3). https://doi.org/10.1002/14651858.CD001255.pub5.www.cochranelibrary.com

Sarvi, M. N., & Luo, Y. (2015). A two-level subject-specific biomechanical model for improving

prediction of hip fracture risk. *Clinical Biomechanics*, *30*(8), 881–887. https://doi.org/10.1016/j.clinbiomech.2015.05.013

Sarvi, M. N., & Luo, Y. (2017). Sideways fall-induced impact force and its effect on hip fracture risk: a review. *Osteoporosis International*, *27*(6). https://doi.org/10.1007/s00198-017-4138-5

Schileo, E., Dall'Ara, E., Taddei, F., Malandrino, A., Schotkamp, T., Baleani, M., & Viceconti, M. (2008). An accurate estimation of bone density improves the accuracy of subject-specific finite element models. *Journal of Biomechanics*, *41*(11), 2483–2491. https://doi.org/10.1016/j.jbiomech.2008.05.017

Scott, V., Wagar, L., & Elliott, S. (2011). Falls & Related Injuries among Older Canadians: Fall-related Hospitalizations & Prevention Initiatives. *Division of Aging and Seniors, Public Health Agency of Canada*, 1–43.

Seeman, E. (2003). Physiology of Aging Invited Review : Pathogenesis of osteoporosis. *Journal of Applied Physiology*, *95*, 2142–2151.

Seeman, E. (2009). Bone Modeling and Remodeling. *Critical Reviews in Eukaryotic Gene Expression*, *19*(3).

Siris, E. S., Chen, Y.-T., Abbott, T. a, Barrett-Connor, E., Miller, P. D., Wehren, L. E., & Berger, M. L. (2004). Bone Mineral Density Thresholds for Pharmacological Intervention to Prevent Fractures. *Archives of Internal Medicine*, *164*(10), 1108–1112. https://doi.org/10.1001/archinte.164.10.1108

Statistics Canada. (2010). Canadian Community Health Survey - Healthy Aging (CCHS): Detailed information for 2008-2009. *Ottawa: Statistics Canada*, (Report No.: 5146).

Statistics Canada. (2011). Census of population. *Ottawa: Statistics Canada*.

Stolee, P., Poss, J., Cook, R. J., Byrne, K., & Hirdes, J. P. (2009). Risk factors for hip fracture in older home care clients. *Journals of Gerontology - Series A Biological Sciences and Medical Sciences*, *64*(3), 403–410. https://doi.org/10.1093/gerona/gln035

Travison, T. G., Araujo, A. B., Esche, G. R., Beck, T. J., & Mckinlay, J. B. (2008). Lean Mass and Not Fat Mass Is Associated With Male Proximal Femur Strength. *J Bone Miner Res*, *23*(2), 189–198. https://doi.org/10.1359/JBMR.071016

Turner, C. (2006). Bone Strength : Current Concepts. *Annals New York Academy of Sciences*, *1068*,

429–446. https://doi.org/10.1196/annals.1346.039

Turner, C. H. (1989). Yield Behavior of Bovine Cancellous Bone. *Transactions of the ASME, 111*, 256–260.

Un, K., Bevill, G., & Keaveny, T. M. (2006). The effects of side-artifacts on the elastic modulus of trabecular bone. *Journal of Biomechanics, 39*, 1955–1963. https://doi.org/10.1016/j.jbiomech.2006.05.012

van den Kroonenberg, A., Hayes, W. C., & Mcmahon, T. A. (1995). Dynamic Models for Sideways Falls From Standing Height. *Journal of Biomechanical Engineering*, *117*, 309–318.

Van Den Kroonenberg, A. J., Hayes, W. C., & McMahon, T. a. (1996). Hip impact velocities and body configurations for voluntary falls from standing height. *Journal of Biomechanics*, *29*(6), 807–811. https://doi.org/10.1016/0021-9290(95)00134-4

van der Zijden, a. M., Groen, B. E., Tanck, E., Nienhuis, B., Verdonschot, N., & Weerdesteyn, V. (2012). Can martial arts techniques reduce fall severity? An in vivo study of femoral loading configurations in sideways falls. *Journal of Biomechanics*, *45*(9), 1650–1655. https://doi.org/10.1016/j.jbiomech.2012.03.024

van Geel, T. A. C. M., van den Bergh, J. P. W., Dinant, G., & Geusens, P. P. (2010). Individualizing fracture risk prediction. *Maturitas*, *65*, 143–148. https://doi.org/10.1016/j.maturitas.2009.12.007

Varga, P., Schwiedrzik, J., Zysset, P. K., Fliri-hofmann, L., Widmer, D., Gueorguiev, B., … Windolf, M. (2016). Nonlinear quasi-static fi nite element simulations predict in vitro strength of human proximal femora assessed in a dynamic sideways fall setup. *Journal of the Mechanical Behavior of Biomedical Materials*, *57*, 116–127. https://doi.org/10.1016/j.jmbbm.2015.11.026

Wei, T., Hu, C., Wang, S., & Hwang, K. (2001). Fall Characterictics , Functional Mobility and Bone Mineral Density as Risk Factors of Hip Fracture in the Community-Dwelling Ambulatory Elderly. *Osteoporosis International*, *12*, 1050–1055.

Wolinsky, F. D., Bentler, S. E., Liu, L., Obrizan, M., Cook, E. A., Wright, K. B., … Wallace, R. B. (2009). Recent Hospitalization and the Risk of Hip Fracture Among Older Americans, *64*(2), 249–255. https://doi.org/10.1093/gerona/gln027

Wolinsky, F. D., Fitzgerald, J. F., & Stump, T. E. (1997). The effect of HIP fracture on mortality, hospitalization, and functional status: A prospective study. *American Journal of Public Health*,

87(3), 398–403. https://doi.org/10.2105/AJPH.87.3.398

World Health Organization. (1994). Assessment of fracture risk and its application to screening for postmenopausal osteoporosis. *Technical Report Series*.

Wu, T., Yu, S., Chen, D., & Wang, Y. (2017). Bionic Design, Materials and Performance of Bone Tissue Scaffolds. *Materials*, *10*(1187). https://doi.org/10.3390/ma10101187

Yang, H. (2017). Development of Image-Based Beam Model for Assessment of Osteoporotic Hip Fracture Risk By, (March).

Yang, L., Peel, N., Clowes, J. a, McCloskey, E. V, & Eastell, R. (2009). Use of DXA-based structural engineering models of the proximal femur to discriminate hip fracture. *Journal of Bone and Mineral Research : The Official Journal of the American Society for Bone and Mineral Research*, *24*(1), 33–42. https://doi.org/10.1359/jbmr.080906

Yang, Y., Feldman, F., & Robinovitch, S. (2018). BIOMECHANICAL DETERMINANTS OF HIP FRACTURE IN OLDER ADULTS: EVIDENCE FROM VIDEO CAPTURE OF FALLS IN LONG-TERM CARE. *Injury Prevention*, *24*(Suppl 1), A224.

Yang, Y., Schonnop, R., Feldman, F., & Robinovitch, S. N. (2013). Development and validation of a questionnaire for analyzing real-life falls in long-term care captured on video. *BMC Geriatrics*, *13*(40), 1–11.

Yang, Y., van Schooten, K. S., Sims-Gould, J., McKay, H. A., Feldman, F., & Robinovitch, S. N. (2018). Sex Differences in the Circumstances Leading to Falls: Evidence From Real-Life Falls Captured on Video in Long-Term Care. *Journal of the American Medical Directors Association*, *19*(2), 110–116. https://doi.org/10.1016/j.jamda.2017.08.011

Yoshikawa, T., Turner, C. H., Peacock, M., Slemenda, C. W., & Weaver, C. M. (1994). Geometric Structure of the Femoral Neck Measured Using Dual-Energy X-ray Absorptiometry T. *Journal of Bone and Mineral Research*, *9*(7), 1053–1064.

Yoshikawa, T., Turner, C. H., Peacock, M., Slemenda, C. W., Weaver, C. M., Teegarden, D., … Burr, D. B. (1994). Geometric structure of the femoral neck measured using dual???energy X???ray absorptiometry. *Journal of Bone and Mineral Research*, *9*(7), 1053–1064. https://doi.org/10.1002/jbmr.5650090713

Zani, L., Erani, P., Grassi, L., Taddei, F., & Cristofolini, L. (2015). Strain distribution in the proximal

Human femur during in vitro simulated sideways fall. *Journal of Biomechanics*, *48*(10), 2130–2143. https://doi.org/10.1016/j.jbiomech.2015.02.022